UNIVERSITY OF OKLAHOMA

GRADUATE COLLEGE

EXPERIMENTAL STUDY OF FLOW AND RHEOLOGY OF WATER-IN-CRUDE OIL EMULSIONS

A THESIS

SUBMITTED TO THE GRADUATE FACULTY

in partial fulfillment of the requirements for the

Degree of

MASTER OF SCIENCE

By

GNALY MARIE HELENE KOBEA
Norman, Oklahoma
2019

EXPERIMENTAL STUDY OF FLOW AND RHEOLOGY OF WATER-IN-CRUDE OIL EMULSIONS

A THESIS APPROVED FOR THE
MEWBOURNE SCHOOL OF PETROLEUM AND GEOLOGICAL ENGINEERING

BY

Dr. Mashhad Fahes, Chair

Dr. Zulfiquar Reza

Dr. Catalin Teodoriu

To my family, fiancé and friends

Acknowledgements

I would like to express my deepest gratitude to the Fulbright scholarship program for giving the opportunity to obtain this degree.

I owe my deepest gratitude to my advisor, Dr Fahs Mashhad, the best advisor any student can possibly have. Her continuous optimism towards this work, enthusiasm, support, encouragement and her unlimited patience made this work possible.

I am deeply grateful to Dr Catalin Teodoriu and Dr Zulfiquar Reza to have accepted to serve in my committee.

This thesis would not have been possible without Gary Stowe who helped me to figure out my way into the laboratory and I am beyond grateful. I would like to thank all my colleagues in the PERL lab for their guidance and assistance.

I humbly thank all my friends and everyone who supported me academically and emotionally in the completion of this work.

Table of Contents

List of Tables

List of Figures

Abstract

The formation of water-in-crude oil emulsion is one of the main causes of flow assurance issues in petroleum production systems. These mixture exhibit changes in their flow behavior, and the rheological models used to describe them. Minor changes in these properties are the cause of major drawbacks imposed on the production system. It is therefore important to understand the complex behavior of emulsions and identify the properties that create such changes. Most water-in-oil emulsions exhibit a shear thinning behavior. This behavior is obtained through the measurement of the shear rate and shear stress of the emulsion through a rheometer. The power law model is commonly used to characterize the viscosity of shear thinning Non-Newtonian emulsions.

The present work is an investigation of the rheology of water-in-oil emulsions during their flow in pipes. For this purpose, flow experiments were conducted with a 30% water cut water-in-oil emulsion, stabilized by a mixture of two surfactants: 3.5% TX 100 and 3.4% Span 80.The emulsion was circulated in a laboratory scale loop consisting primarily of two stainless steel pipes having outside diameter of 1/4” and 3/8”.The pressure drop, mass flow rate, and viscosity of the emulsion were recorded during the flow of the emulsion. The capillary viscometer was used to measure the viscosity before and after flow. These parameters along with the pipe characteristics were used to estimate the amount of shear exerted during the flow of the emulsions. The shear rate and shear stress derived experimentally showed that at 30% water cut the emulsion was exhibiting a non-Newtonian behavior. The rheology of the emulsion was then characterized using a rheometer. Data from the rheometer showed that the emulsion was exhibiting a Non-Newtonian behavior as well. The shear rate and shear stress from flow and rheometer data were compared and it was observed that the data follow the same trend, however, it was clear that the behavior does not follow the power law model. The effect of these differences on pressure drop estimates in a

field scale case was determined. Accordingly, the results were analyzed towards a protocol for the recommended way to characterize similar emulsions.

Chapter I: Introduction

Petroleum fluids during production encounter several flow issues that are of great interest to petroleum engineers. It is possible for the produced crude oil to mix with water thus forming a mixture called emulsion. The most common emulsion encountered during production in the oil industry is the water-in-oil (W/O) emulsion. The occurrence of such emulsion is attributed to the presence of surfactants in the oil and the shear force imposed on the fluids as they migrate in production lines. The emulsion is subjected to shear forces through pumps and other mechanical devices present along the production path. One of the major drawbacks of emulsion formation is the significant increase in their viscosity that creates a negative impact on the system. In addition to the viscosity, the pressure drop increase is correlated to the increase in water fraction. The accurate determination of the rheological characteristics of emulsions and the pressure drop in the emulsion during flow is very important. The rheology of emulsions is complex, and researchers are still investigating their behavior. This behavior is dictated by the rheology, and the knowledge derived from the studies will be of prime importance and a step forward in the understanding of emulsions.

Even though a platitude of studies can be found on emulsions, they are mainly focused on O/W emulsions and some aspects of W/O emulsions, thus creating a need for further work on the topic. The existing literature mainly derives the viscosity from measurements, and mostly expresses it as a function of the water phase and the oil phase as a relative viscosity. As far as experimental results are concerned, different oils having different characteristics are used, thus the results from studies are not always uniform and can be challenging to interpret and integrate into generalized conclusions. This led to discrepancies and divergence, thus the need to propose a

recommended protocol to be able to compare the studies on similar grounds. In the studies encountered, there was no mention of a capillary viscometer used in the measurement of the emulsion viscosity, the studies all used either a rotational viscometer or a rheometer to characterize the viscosity of the emulsion. Our interactions with industry professionals revealed that the use of capillary viscometers is a common practice to characterize emulsions in the field. Translating the results from one instrument to the next and understanding its relevance to the characteristics of emulsion flow in pipes is needed so that consistent studies can be performed.

1. Research Objective

On a broad scale, the study's aim is to investigate the flow behavior and the rheological behavior of Water-in-oil emulsions, towards an integrated workflow. In particular, the goal is to attempt answering the following questions: what would be the best method to characterize emulsion viscosity that would be relevant to flow characteristics in terms of the pressure-rate relationship? In other words, is the Power Law model a good fit for the rheological behavior of Water-in-oil emulsions?

2. Organization of the work

The present work is divided into 5 chapters including the current introduction. The next chapter establishes a review of the literature on the work and findings regarding emulsions, it's characteristics for stability and rheology, as well as its flow behavior. Chapter III describes the experimental procedure followed in our investigation. Chapter IV explains the results obtained and the findings. Finally, the conclusions from this work are presented in Chapter V, followed by recommendations for future work.

Chapter II: Literature Review

In oil and gas industry, it often occurs that crude oil is produced simultaneously with water. Oil and water are immiscible liquid phases, but due to several factors, they can form a complex mixture called an emulsion. By definition, a W/O emulsion is a dispersion of water droplets in crude oil. The formation of such a mixture is the most encountered problem in the oil and gas industry. Emulsion formation causes operational problems and is difficult to treat. Emulsions can form inside the reservoirs and migrate through the equipment till the storage facilities. For an emulsion to be formed, a surfactant and some agitation (mixing) are required. Turbulence occurs downhole, at the surface chokes, valves, pumps, and pipes yielding the undesirable creation of a crude oil emulsion (Lim et al., 2015). Emulsions have a negative impact because of the following:

- Emulsions can cause corrosion to the piping and transport systems and/or contaminate any chemicals used during upstream or downstream processes (Lim et al., 2015).
- They affect the flow regimes, causing a delay in transition from laminar to turbulent regime, as well as the general flow behavior of the fluid (Pal, 1987; Omer and Pal, 2013). Emulsions also cause a significant increase in pressure drop value (Pal, 1993; Russell et al., 1959; Naddler and Mewes, 1997).
- Emulsions can significantly impair flow assurance in addition to increasing operation expenditures. Boukadi et al. (2012) showed that when the emulsion viscosity is taken into consideration, there is an increase in the retention time from 3-20 min to 8-53min for the base case. He demonstrated that by calculating the separator size using modified Arnold-Stewart's method. This augmentation in retention time directly imply the need for a larger separator size and a larger footprint area necessary to accommodate the separator.

- The apparition of emulsions reduces the quality of crude oil. Basic Sediment and Water (BS&W, BSW or Watercut) is a measurement of impurities in liquid which includes free water, sediment, and oil emulsion as a volume percentage. BS&W can be determined using ASTM D4007, Standard Test Method for Water and Sediment in Crude Oil by the Centrifuge Method and typically limits vary from 0.5 - 2 wt% BS&W (Engineering Toolbox, 2017). If a crude oil does not meet the required crude oil quality, its price might be lowered leading to a possible economic loss.

Due to the factors listed above, emulsions are not desirable, but the formation of emulsions appears to be unavoidable. Therefore, it is essential to improve our understanding of their flow behavior. Several studies have discussed the flow of emulsions in pipelines, but more work needs to be done to fully understand their complexity.

1. Emulsion Formation

An emulsion is defined as a system in which two immiscible liquids are present: one liquid (the dispersed phase) is dispersed in in the form of droplets in the other liquid (the continuous phase). According to Schubert and Armbruster (1992), for an emulsion to form three main criteria are mandatory:

1. Presence of two immiscible liquids
2. Presence of a surface-active component which constitute the emulsifying agent
3. Presence of intense agitation or mixing to permit the dispersion of one liquid into another in the form of droplets.

In addition to the criteria mentioned above, a rule of thumb determines the type of emulsion formed for a given oil and water phase (Scharmm, 1992; Schubert and Armbruster,1992).

As two phases are present, one will have a small volume fraction and the other phase will have a larger volume fraction .The rule is that the phase having the larger volume fraction will form the continuous phase and the other will form the dispersed phase. It is important to note that in case both phases approximately have the same magnitude of phase to volume ratio, the type of emulsion created will be dependent on other factors.

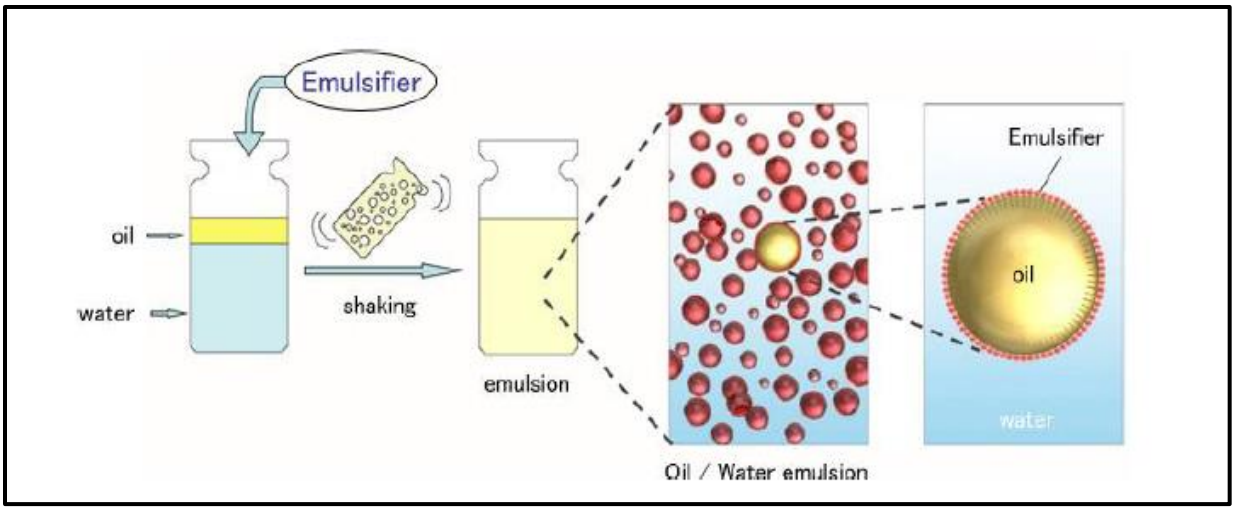

Fig. 1— Process of forming an Emulsion: water, oil, emulsifier and mixing are needed (After Oluwatosin, 2016)

2. Types of emulsions

Oil emulsion can be broadly classified into 3 categories (**Fig. 2**):

- Water-in-oil (W/O) emulsions, water is the dispersed phase and oil is the continuous phase
- Oil-in-Water (O/W) emulsions, oil is the dispersed phase and oil is the continuous phase
- Multiple or complex emulsions such as water-in-oil-in-water (W/O/W) emulsions water droplets are trapped in larger oil droplets which are in turn entrapped in a continuous water phase.

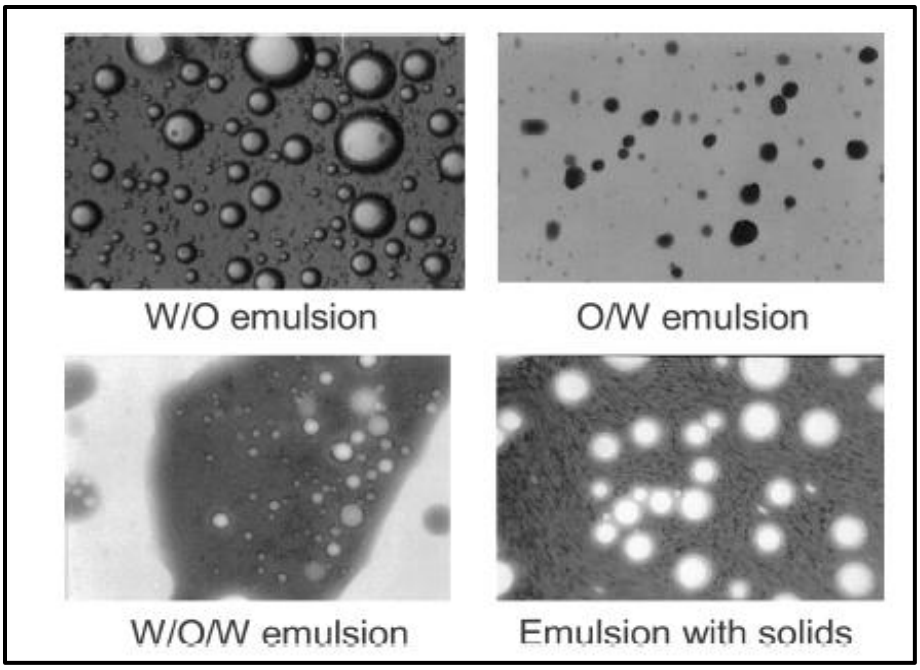

Fig. 2— Photomicrographs of emulsions showing different types of complex emulsions. (Kokal, 2005).

Even though emulsions can generate several operational problems, not all emulsions are undesirable. Schramm (1992) explained that there are desirable and undesirable emulsions in the petroleum industry. These emulsions are showed in **Table 1.**

3. Importance of Surface-active agent: Surfactant

The role of surfactant in the emulsification process is undeniable (**Fig.1**). In the absence of suitable surfactant, the emulsion will easily separate into an oil layer and a water layer. This is due to the fact that emulsions possess a minimal thermodynamic stability. The addition of a surface-active agent tends to lower the interfacial tension. The surface-active agent acts by accumulating at the oil-water interface and preventing coalescence of the droplets into bigger droplets (Sjöblom, 2006).

In fact, Becher (1957) claimed that agitation energy can be reduced by a factor of 10 or more if a surfactant film coats the droplets.

Table 1— Examples of emulsions in the petroleum industry (Schramm, 1992)

Occurrence	Usual types
Undesirable emulsions	
Well-head emulsions	W/O
Fuel oil emulsions (marine)	W/O
Oil sand floatation process, froth	W/O or O/W
Oil sand floatation process, diluted froth	O/W/O
Oil spill mousse emulsions	W/O
Tanker bilge emulsions	O/W
Desirable emulsions	
Heavy oil pipeline emulsions	O/W
Oil sand floatation process, slurry	O/W
Emulsion drilling fluid, oil-emulsion mud	O/W
Emulsion drilling fluid, oil-base mud	W/O
Asphalt emulsion	O/W
Enhanced oil recovery in situ emulsions	O/W

Emulsifiers or surfactants work by forming a mechanical barrier that keep droplets from coalescing: they generate the reduction of the interfacial tension and establishment of repulsive forces among oil droplets thus making the formation of smaller droplets easier. Surfactants partially provide a kinematic stability to the emulsion. They are natural emulsifiers present in crude oil such as asphaltenes, waxes, clays, sands (Isaacs and Chow, 1992).

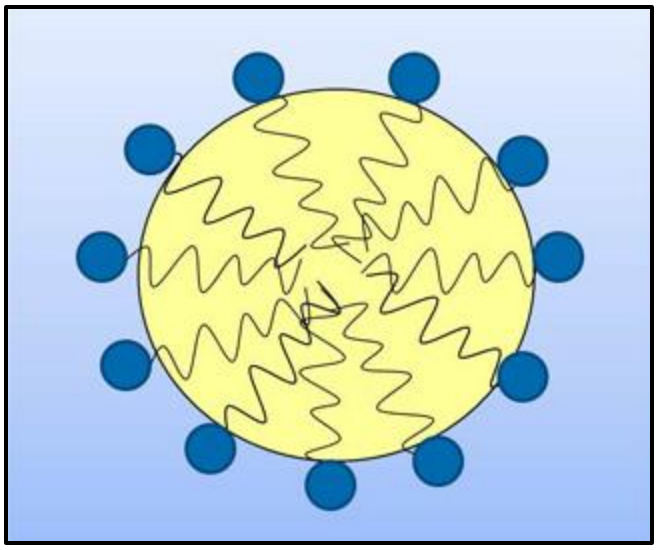

Fig. 3— Molecular structure of a surface-active emulsifier (aocs.org, 2014)

Surfactants own their blocking character to their chemical structure. A molecule of an emulsifying agent is composed of two parts: a hydrophilic head (water-loving, or polar) and a hydrophobic tail (oil-loving, or nonpolar). Because of their amphiphilic nature, the emulsifiers surround the oil droplet with their nonpolar tails extending into the oil, and their polar head groups facing the water. This organized aggregate is called micelle as shown in **Fig. 3**. An interfacial layer is created by trapping water droplets adsorbed by solid particles or surface-active materials. Interfacial films are categorized into two categories based on their mobilities (Jones et al., 1978; Strassner, 1968):

- **Rigid, or Solid, Films**: They are characterized by very-high interfacial viscosity.

They are possibly formed by polar fractions of the oil. They disturb the droplet-coalescence process by creating a structural barrier and increase emulsion stability

- **Mobile, or Liquid, Films**: They are characterized by low interfacial viscosities. They are less stable thus promotes the coalescence of water droplets.

Surfactants can be classified based on the nature of the polar (hydrophilic) part of the molecule (Shramm, 1992), that is their dissociation in water (Schubert, 1992):

- Anionic surfactants, they have a positive water-soluble group
- Nonionic surfactant, they have an uncharged water-soluble group
- Cationic surfactant, they have a negative water-soluble group
- Amphoteric or Zwitterionic surfactant, they have both positive and negative water-soluble group

Table 2 present the types of surfactants.

Table 2— Surfactant classifications

Class	**Example**
Anionic	Na stearate Na dodecyl sulfate Na dodecyl benzene sulfonate
Nonionic	Polyoxyethylene alcohol Alkylphenol ethoxylate
Cationic	Laurylamine hydrochloride Cetyl trimethylammonium bromide
Zwitterionic	Lauramidopropyl betaine Cocoamido-2-hydroxypropyl sulfobetaine

3.1. **Hydrophilic Lipophilic balance HLB**

Hydrophilic Lipophilic balance was introduced in the late 1940's by William griffin. Emulsifiers have an amphiphilic molecule i.e. they possess a hydrophilic head (water-loving, or polar) and a lipophilic tail (oil-loving, or nonpolar). Thus, the balance of the size and the strength of the polar portion relative to the non-polar portion of the emulsifier molecule is the HLB (**Fig.4**). The lipophilic group is generally composed of a fatty acid or fatty alcohol and the hydrophilic group comprise of water-soluble functional group. The HLB system assigns a numerical value to the

emulsifier and the liquid or system to be emulsified must match that same number. Griffin (1949) provided a formula to calculate the HLB value of esters:

$$HLB = 20\ (1 - \ S/A) \tag{1}$$

Where,

S= saponification number of the ester

A= acid number of the acid

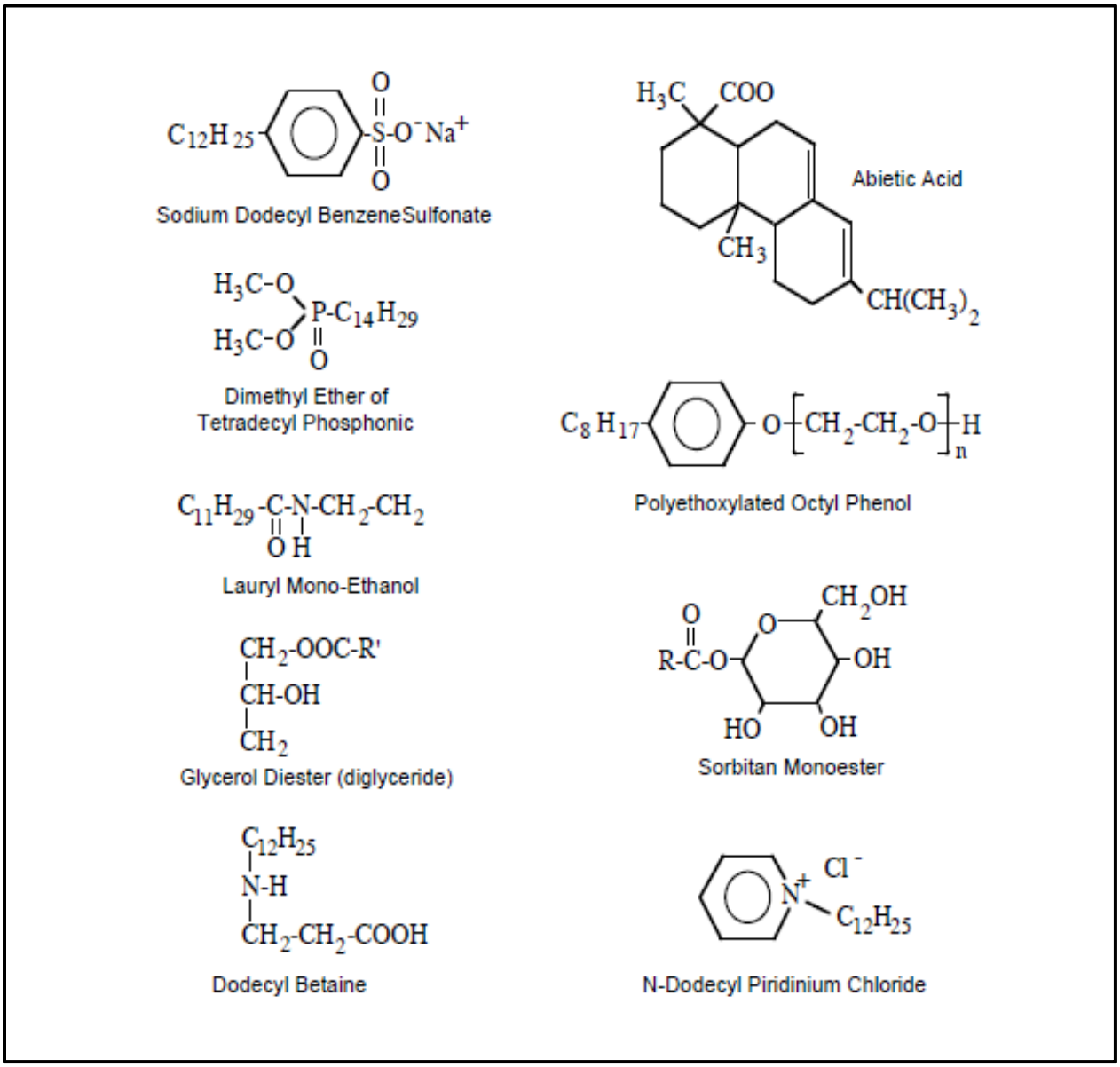

Fig. 4— Examples of surfactant structure. (Schramm, 1992)

HLB values typically varies between 0 and 20+. The higher the HLB number (above 11) the more hydrophilic and the lower the HLB number (below 9) the more lipophilic (ICI, 1980). This concept is strictly applicable to non-ionic surfactants (Hawkins watts). Therefore, the scalar scale that the HLB system provides enable a systematic way of selecting the appropriate emulsifiers to yield a stable emulsion. The application of the surfactants can be determined by their HLB value. Griffin (1948) presented the application of non-ionic surfactants based on a range of HLB value as follow:

- 0 to 3 corresponds to an anti-foaming agent
- 4 to 6 corresponds to a W/O emulsifier
- 7 to 9 corresponds to a wetting agent
- 8 to 18 corresponds to an O/W emulsifier
- 13 to 15 typically corresponds to detergents
- 10 to 18 corresponds to a solubilizer

Emulsifiers can be mixed to give a required HLB number. The HLB of the blend can be calculated using the following formula:

$$HLB = x_1 HLB_1 + x_2 HLB_2 \quad (2)$$

Where,

x_1 & x_2 are the weight percentage of surfactant 1 and 2 respectively

HLB_1 & HLB_2 are the HLB value of surfactant 1 and 2 respectively

In addition to finding the adequate HLB number that matches that of the oil, it is important to carefully choose the ideal chemical type possessing the right HLB (ICI, 1980). Oil emulsions can be O/W or W/O based on their HLB number. When considering the same oil, the required HLB for an O/W emulsion is higher than the required HLB value for W/O emulsion.

3.2. **Stability of emulsions**

Stability is an important characteristic of emulsions. An emulsion is labelled as unstable when the distinct oil and water phase separate easily or readily after some time without the action of an element to break them. Stability results from the presence of the interfacial film on the droplets in the emulsion and the small size of droplet. A stable emulsion has both detrimental and beneficial effects and is more difficult to separate. Bhardwaj and Hartland (1998) found that it is possible for the stability of an emulsion to vary from few minutes up to several years. Kinetic stability is a consequence of a small droplet size and the presence of an interfacial film around the water drop. The stability dependents on the structure and the rigidity of the emulsion droplets' interfacial films. This leads to the classification of emulsions into the following groups:

- Loose emulsions. They separate in a few minutes.
- Medium emulsions. Their separation occurs in ten minutes or more.
- Tight emulsions. They will separate within hours or days. They can sometimes show a partial separation only.

The stability of emulsions is also affected by the presence of solids such as asphaltenes, resins and waxes, the presence of fine solid particles, temperature, Ph and droplet size. Opawale et al. (2013) found out through experimental trials that an increase in water fraction, asphaltene content and shearing energy forms a tight emulsion. Abdurahman et al. (2008) and Henríquez (2009) showed that the higher the surfactant concentration the higher the stability. A very strong correlation between emulsion stability and viscosity was observed by Silset (2008). The researcher correlated the increase in stability to an increase in viscosity. Ashrafizadeh et al. (2012) and Ostubo et Prud'homme (1994) confirmed that the higher the surfactant concentration, the higher the viscosity because of the small size of the dispersed droplets that make the interaction energy stronger

between them. Mohammed (2009) reported from his experimental studies that the most stable emulsions was encountered at 60% water cut. He also observed that the viscosity of the emulsion increased by two orders of magnitude at high aqueous phase cut.

4. Rheology of emulsion

Emulsions are very complex systems at different levels. Their complexity arises from the changes in their physical properties that incur a negative impact. Flow assurance issues caused by emulsion result from minimal changes in its behavior and composition. For instance, the viscosity of an emulsion is predicted to increase as the water cut increases (Kokal, 2005). Therefore, measuring, adjusting and predicting these physical attributes of emulsions is very important. Rheology is the study of the flow characteristics and deformations of any type of fluid or solid. Deformation is generated by applying a force to a material thus causing it to deform and/or flow. The magnitude of the induced deformation and/or flow is then linked with a physicochemical property of the material (Tatar et al., 2017). Force is applied in the form of strain and stress and their relationship with time and temperature is recorded. There are five types of rheological models that may be exhibited by fluids. Each model has a typical flow curve as shown in **Fig. 5**. Each type of curve has a different relation between shear stress and rate. An emulsion can be categorized as Newtonian or non-Newtonian based on its composition (Becker, 1997). For Newtonian fluids, the shear stress is linearly proportional to the shear rate. This implies that the viscosity is independent of shear rate.

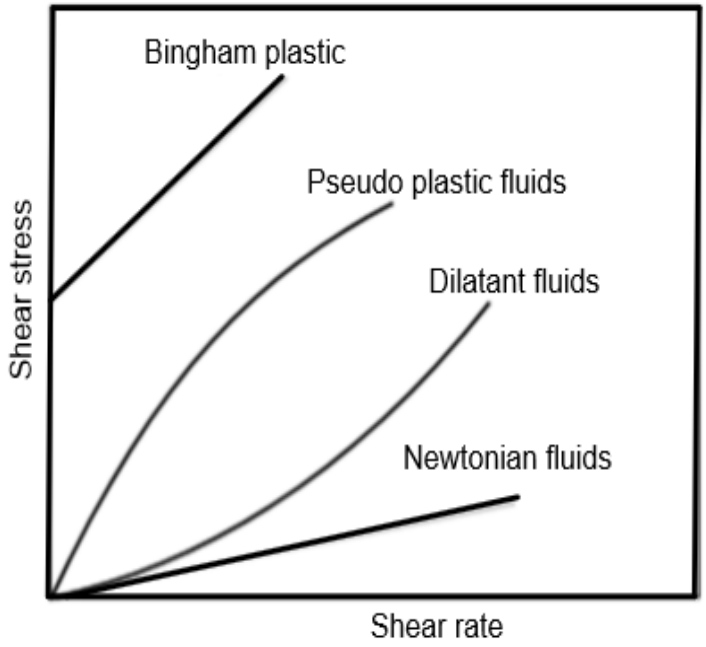

Fig. 5— Shear stress and shear rate of Newtonian and non-Newtonian (Omer,2009)

Newtonian fluids obey Newton law of viscosity given by:

$$\boldsymbol{\tau} = \mu\boldsymbol{\gamma} \tag{3}$$

Where,

τ = shear stress (Pa or N/m^2)

μ = fluid viscosity (kg/m.s or Pa.s)

γ = shear rate applied on the fluid (s^{-1})

For Non-Newtonian fluids, the viscosity depends on the variation of shear rate and they can be classified as pseudoplastic, dilatant, rheopectic, and thixotropic. For pseudoplastic fluids, their viscosity decreases as the shear rate increases and such fluids have “shear-thinning” flow. Dilatant fluid viscosity increases with an increase in shear rate and such fluids have “shear thickening” flow. Thixotropic and rheopectic fluids have a dependency on time. A thixotropic fluid experiences

a decrease in viscosity with time when a constant shear rate is being applied. A rheopectic fluid has its viscosity increasing over time with an increase in shear rate as shown in **Fig.6**.

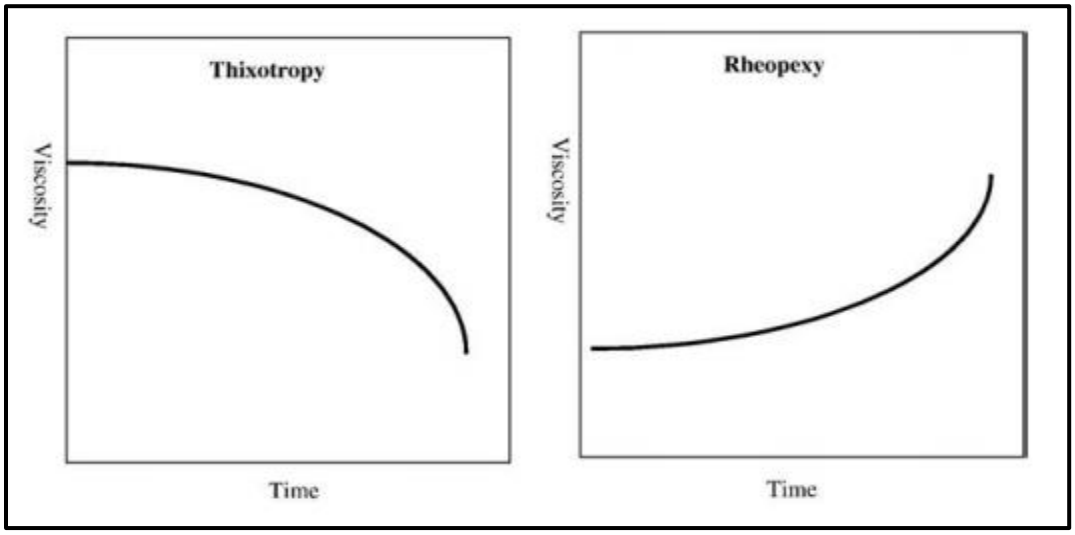

Fig. 6— Thixotropy and rheopexy profiles (viscosity vs time) (Souto and Muller, 2006; Leone et al.,2008)

Emulsions' rheological behavior is subjected to change. Emulsions usually exhibit a Newtonian behavior except at high water content, where they change into Non-Newtonian behavior.

Non-Newtonian fluids do not obey Newton law of viscosity, unlike Newtonian fluids. Some follow the Power law or Ostwald De Waele model given by:

$$\boldsymbol{\tau = K\,(\gamma)^{n}} \tag{4}$$

K = flow consistency index ($Pa.s^n$)

n= flow behavior index (dimensionless)

For pseudoplastic fluid, n is less than 1 (n<1). For Newtonian fluid, n is equal to 1 (n=1) and for dilatant fluid n is more than 1 (n>1).

4.1. **Factors affecting rheology**

The viscosity of emulsions is the most studied rheological parameter of emulsions. Due to this facts, the factors that have an impact on the rheology of an emulsion are: water volume fraction (ϕ), the viscosity of the continuous phase, temperature, shear rate, mean droplet size and size distribution of the droplets, viscosity of the dispersed phase, nature and concentration of the emulsifying agents as well as the presence of solids in addition to the dispersed phase (Johnsen et Rønningsen, 2003). In addition to these, there is: the chemical components of the continuous phase, the degree of mixing, etc.…

4.1.1 **Effect of water volume fraction**

Ronningsen (1995) studied the connection between the viscosity and the water cut of eight different crude oils. He found that there is a linear relationship between viscosity and low water fractions but at higher water fraction, the viscosity increases exponentially. He reported that during his investigation, the emulsions were Non-Newtonian at high water cut. Emulsions will exhibit a Newtonian behavior if the concentration of the dispersed phase is low to moderate. But if the concentration of the dispersed phase is high, the emulsion will behave as pseudoplastic or thixotropic. A comparison between emulsion viscosity measured experimentally and field data including flow rate, pressure drop, and temperature was made by Tjoeng and Loro (2016). They observed that the viscosity obtained with their empirical model matched the viscosity value obtained from the experiment for water cuts lower than 35%. But when water cut was above 35%, it was observed that the viscosity of the emulsions was over predicted by the model.

4.1.2 **Effect of droplet size**

It is very challenging to accurately predict droplet size and size distributions of emulsions theoretically and experimentally. Nevertheless, droplets having diameter size between 0.2 and 100 µm form stable emulsions and the size distribution is polydisperesed (Urdahl et al., 1997). At identical water cut, Calabrese et al. (1986) found that an emulsion will have a high viscosity if its size distribution is dominated by small droplets when compared to emulsions having a high mean droplet size. They have also demonstrated that the narrower the size distribution the higher the viscosity. At low concentrations of emulsion droplets, the emulsion will likely behave as a Newtonian fluid. However, an increase in the concentration of droplets changes the emulsion behavior to Non-Newtonian. Tadros (1994) demonstrated that shear-thinning Non-Newtonian behavior of emulsion result from the close packing of dispersed droplets when their concentration is high. Gomez (2018) showed that the centrifuge test increase the droplet size.

Over the years, several correlations were implemented in order to estimate the maximum diameter droplet size d_{max}.

The most commonly used model was developed by Hinze (1955):

$$\frac{d_{max}}{D} = 0.55 \left(\frac{\rho_C \mu_C^2 D}{\sigma}\right)^{-0.6} f^{-0.4} \tag{5}$$

Where, ρ_C is the continuous phase density, μ_c is the continuous phase velocity, σ is the interfacial tension and D is the pipe diameter and f is the friction factor.

Kubie and Gardner (1977) explained that d_{max} would decrease as the velocity of the continuous phase increases. They proposed a model that gives the maximum drop size diameter according to the pipe diameter and the continuous phases as follow:

$$\left[\frac{\rho_C \mu_C^2 \, d_{max}}{\sigma}\right] \left[f \, \frac{d_{max}}{D}\right]^{2/3} = 0.369 \tag{6}$$

Hesketh et al. (1987) found a new correlation described as follow:

$$d_{max} = 1.38\,(We_{cr})^{0.6}\left(\frac{\sigma^{0.6}}{\rho_c^{0.5}\mu_c^{0.1}}\right)\left(\frac{\rho_C}{\rho_d}\right)^{0.2}\left(\frac{D^{0.5}}{U^{1.1}}\right) \quad (7)$$

Where, We_{cr} is the critical Weber number $We_{cr} = \frac{\tau\, d_{max}\left(\frac{\rho_d}{\rho_c}\right)^{1/3}}{\sigma}$, τ is the stress on the droplet due to turbulent fluctuating eddies in the continuous phase , μ_c is the viscosity of the continuous phase and U is the average velocity.

Angeli (2001) revealed using videography that an increase of the velocity of the continuous phase corresponds to a decrease in d_{max} and proposed a new equation as described below:

$$d_{max}\, U_C^{1.8} = 4.2 * 10^{-2} * f^{-3.13} \quad (8)$$

Brauner and Ullmann (2002) proposed another model that includes a tunable constant and the dispersed phase concentration:

$$d_{max} = 2.22\, C_H D\left(\frac{\rho_c \mu_c^2 D}{\sigma}\right)^{-0.6}\left(\frac{\rho_m}{\rho_c(1-\phi_d)}\, f\right)^{-0.4}\left(\frac{\phi_d}{1-\phi_d}\right)^{0.6} \quad (9)$$

Where C_H is a tunable constant, ϕ_d is the dispersed phase concentration, ρ_m is the mixture density, and ρ_c is the continuous phase density.

4.1.3 **Effect of temperature**

Based on his experimental studies conducted on factors that affect the viscosity of surfactant-stabilize emulsions, Zaki (1997) declared that the dynamic viscosity of emulsions will decrease due to an increase in the crude oil fraction, an increase in temperature, and a decrease in the speed of mixing. The increase in temperature reduces the emulsions viscosity and break it. Grace (1992) revealed that emulsions will be completely destabilized if temperatures go beyond 50°C-65°C. An increase in temperature of emulsion increases raises the thermal energy of the droplets thus

increasing the frequency of droplet collision. Furthermore, increased temperature impacts the interfacial film by destabilizing it.

5. Phase inversion

One of the issues associated with water-in-crude oil emulsions is that their effective viscosity increases towards the phase inversion point thus creating a significant reduction in the produced rates. Phase inversion can be described as a swap between the dispersed phase and the continuous phase. In other words, the phase inversion point is a point at which a sudden change from a W/O emulsion to an O/W emulsion occurs or vice versa **(Fig.7)**.

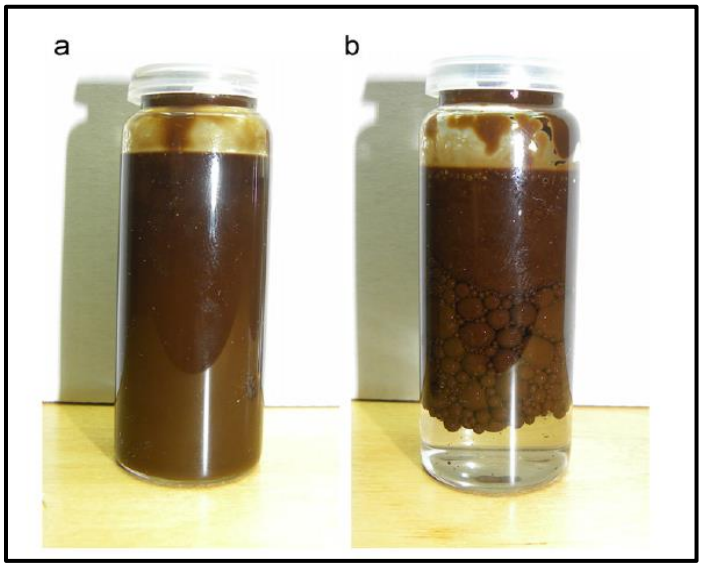

Fig. 7— W/O emulsion (a) and O/W emulsion (b) (After Placensia et al., 2013)

Phase inversion can also occur if an emulsion is overmixed or if the water cut becomes to large when compared to the continuous phase (Lunde, 2017).

Inversion point is usually found at water cuts between 60 and 90% (Urdahl et al., 1996). Plasencia et al. (2013) declared that an emulsion may remain Newtonian for a wide range of water fractions, but a Non-Newtonian behavior might be observed at relatively high water fraction. In their study,

Plasencia et al. (2013) investigated the inversion point of six different crude oils: A, B, C, D, E, and F. The emulsions made from crude oil A, B, and D, respectively, experienced inversion at 45% 55% and 58% while emulsions for crude C, E, and F did not invert. For higher water phase, he observed that the droplets were increasing in size and therefore linked this occurrence to the triggering of the inversion process. From his work he found that the phase inversion results from the combination of effects other than the viscosity of the continuous phase which they assumed plays a less important role in this process. Pal (1993) explained that the inversion point can be detected measuring the electrical conductance of emulsions. A sudden change in the conductance corresponds to a phase inversion point. Omer (2009) confirmed the same by showing that water-in-oil emulsions have a very low conductance in contrast to oil-in-water emulsions that exhibit higher conductance value as presented in **Fig. 8**.

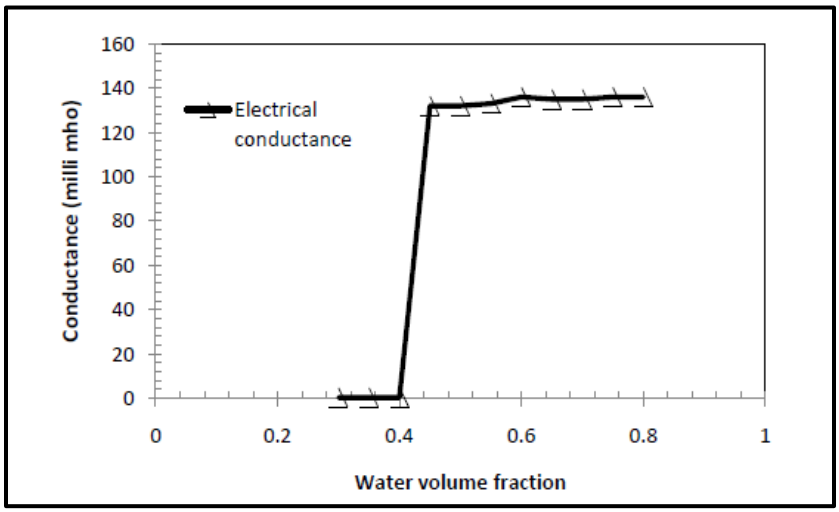

Fig. 8— Electrical conductance vs. water volume fraction (Omer ,2009)

There are two types of phase inversion namely: catastrophic inversion and transitional inversion. Catastrophic inversion occurs when the volume fraction of the dispersed phase increases. It is irreversible. Transition inversion occurs due to the change in surfactant concentration and is

induced by changes in the HLB. These changes can be caused by an increase in temperature and/or addition of electrolytes (Tadros, 1994)

6. Flow of emulsions in pipes

6.1. **Reynolds Number**

The flow regime in pipes are described by Reynolds Number (Re). The general Reynold number for flow in circular pipe is given by:

$$Re = \frac{DV_{avg}\rho}{\mu} \tag{10}$$

Where D = hydraulic diameter of the pipe (the inside diameter if the pipe is circular) (m)

V_{avg} = mean velocity of the fluid (m/s)

ρ = density of the fluid (Kg/m^3)

μ = dynamic viscosity of the fluid (Pa.s)

Laminar flow occurs when Reynolds number is less than 2300 (Re < 2300). It is characterized by smooth streamlines and ordered motion. Transitional flow (2300 < Re < 4000) is the transition from laminar to turbulent flow. Turbulent flow occurs when Reynolds number is above 4000 (Re < 4000). It is characterized by velocity fluctuations and highly disordered motion.

For Non-Newtonian fluids, the Reynolds Number is given by the following equation:

$$Re' = \frac{v^{(2-n)}D^n\rho}{k'(8)^{n'-1}} \tag{11}$$

$$n' = n \tag{12}$$

$$k' = k\left[\frac{1+3n}{4n}\right]^n \tag{13}$$

Where Re' is the Metzner-Reed modified Reynolds number, n' and k' are Metzner-Reed modified power law constants for pipe flow and can be obtained from a viscometer (Darby, 1996; Wilkes, 1999).

When a water-in-oil emulsion transitions from laminar to turbulent flow regime, a significant delay is observed. Pouplin et al. (2010) declared that during this transition, a delay in Reynolds number Re can be observed up to 5000. This delay increases as the pipe diameter increases (Omer et Pal,2013).

6.2. **Pressure drop**

High pressure drop causes operational difficulties and it is one highly unwanted characteristics of water-in-oil emulsions as it can result in financial losses. Plasencia et al. (2013) reported that the pressure drop of a water-in-oil emulsion increase up to 8 times higher than the pressure drop of pure oil. On the other hand, Nädler and Mewes (1997) and Charles et al. (1961) predicted a decrease in pressure drop below that of pure water when the water volume fraction is increased beyond the phase inversion point. This behavior is called drag reduction (Nädler and Mewes, 1997) and it is due to the water layer flowing at a bottom section of the pipe wall that hinders the viscous dissipation of the emulsion. This implies that there will be less frictional losses along the flow thus leading to a reduced pressure drop.

Drag reduction is a behavior observed in unstable emulsions only (Omer et Pal, 2013: Pal, 1993) and is aggravated by the increase in the concentration of emulsions droplets (Cengel et al., 1962). Drag-reduction is not observed in surfactant-stabilized emulsions under turbulent flow (Omer et Pal, 2013). This is due to the fact such emulsions resist the turbulent currents and end up not being affected by them because they have low interfacial tension. This is more valid when the turbulence is higher than the dispersed droplets. Ashrafizadeh et al. (2012) confirmed this characteristic of

surfactant-stabilized emulsions by adding that it is due to the increase in viscosity. Pressure drop in pipe lines can be estimated using the Darcy-Weisbach equation which can be expressed as a function of the fanning friction factor as:

$$\Delta P = f \frac{L}{D} \rho 2 V_{avg}^2 \quad (14)$$

Where f = fanning friction factor (dimensionless)

L = Length of the measurement section (m)

D = Pipe diameter (m)

ρ = Density of fluid (Kg/m^3)

V_{avg} = Fluid velocity (m/s)

Equation (14) is valid for Newtonian and Non-Newtonian fluid whether in turbulent or laminar flow.

6.1.1 **Flow of Newtonian fluid**

For Newtonian fluid, the friction factor in smooth pipes can be calculated using:

$$f = {}^{16}/_{Re} \text{ , in laminar flow} \quad (15)$$

Alternatively, the Fanning friction factor can be calculated using:

$$f = {}^{2\tau_w}\Big/_{\rho V_{avg}^2} \quad (16)$$

Where τ_w is the shear stress at the pipe wall. τ_w can be expressed in Pa as:

$$\tau_w = \frac{D}{4} \left(\frac{\Delta P}{L}\right) \quad (17)$$

Shear rate at the wall of the pipe can be calculated as:

$$\gamma_w = \frac{8V}{D} \quad (18)$$

Where γ_w is shear rate at pipe wall in s^{-1}.

For Newtonian fluid experiencing turbulent flow, friction factor can be expressed as

$$f = {}^{0.079}/_{Re^{0.25}} \text{ , in turbulent flow} \quad (19)$$

Alternatively, Prandtl-Karman proposed an equation for estimating friction factor:

$$\frac{1}{\sqrt{f}} = 4.0 \log_{10}(Re\sqrt{f}) - 4.0 \quad (20)$$

Colebrook proposed an equation which applies to rough pipe when the flow is turbulent in order to account for the wall roughness effect (Darby,1996; Wilkes,1999):

$$\frac{1}{\sqrt{f}} = -4.0 \log_{10}\left[\frac{{}^{\varepsilon}/_{D}}{3.7} + \frac{1.255}{Re\sqrt{f}}\right] \quad (21)$$

Where ${}^{\varepsilon}/_{D}$ is relative roughness and ε is absolute pipe roughness in m.

6.1.2 **Flow of Non-Newtonian fluid**

Non-Newtonian fluid are described by equation (15) through (17) and equation (19). The shear rate of Non-Newtonian fluid is expressed as:

$$\gamma_w = \frac{8V}{D}\left[\frac{3n+1}{4n}\right] \quad (22)$$

Dodge and Metzner (1959) proposed an alternate equation for evaluating the friction factor in turbulent region for Power Law Non-Newtonian fluid by extending the Prandtl-Karman's equation:

$$\frac{1}{\sqrt{f}} = \frac{4}{n'^{0.75}}\log_{10}\left[Re' f^{1-\frac{n'}{2}}\right] - \frac{0.4}{n'^{1.2}} \quad (23)$$

6.3. **Viscosity of emulsions**

Flow assurance issues imposed by emulsions arise because of the change in their viscosity. It is known from the literature that the viscosity of emulsions increases with the increase in the water phase fraction. Therefore, the volume fraction of the dispersed phase is the most important factor that impacts the viscosity of emulsions. Emulsion viscosity is generally expressed as relative viscosity η_r:

$$\eta_r = {}^{\eta_e}/_{\eta_c} \tag{24}$$

Where η_r = Relative viscosity

η_e = Emulsion viscosity

η_c = Continuous phase viscosity

Oliveira et al. (2018) investigated the viscosity 126 Brazilian crude oils having API gravity varying between 13° and 35°.They focused on three parameters: shear rate, temperature and water volume fractions. The following graphs were observed: From **Fig. 9**, it can be seen that overall, the higher the viscosity the higher the water-cut.

The literature on the rheological characterization of emulsions is very broad. Most of the correlations and models used for prediction of emulsion viscosity take into account the water volume fraction of the dispersed phase only (ϕ) (Dan et Jing,). Later literature accounts for the shear rate.

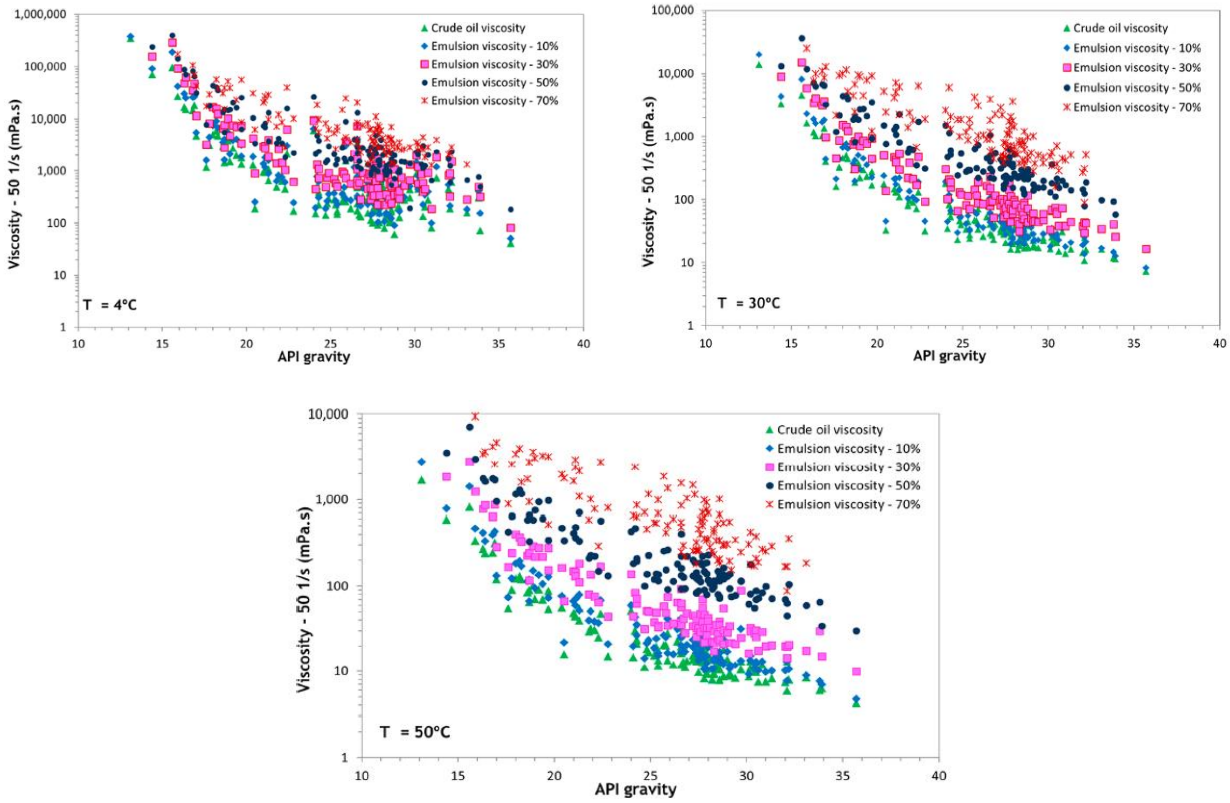

Fig. 9— Viscosity of different API gravity crude oils and their emulsions with different water cuts at 4°C, 30°C and 50°C (Oliveira et al., 2018)

The first correlation for emulsion viscosity was proposed by Einstein (1906) to represent dilute suspension:

$$\eta_e = \eta_c\,(1 + 2.5\phi) \tag{25}$$

Brinkman (1952) proposed a modification in Einstein equation taking into account the sphericity of the droplets surface:

$$\eta_e = \eta_c\,(\,1 - \phi\,)^{-2.5} \tag{26}$$

Taylor (1932) introduced a new model which incorporate modifiers to make models better fit emulsions having high concentration:

$$\eta_e = \eta_c\left[1 + 2.5\phi\,\left(\frac{\eta_d + 0.4\eta_c}{\eta_d + \eta_c}\right)\right] \tag{27}$$

Richardson (1933) proposed a simpler equation as it was observed that there was an exponential increase in relative viscosity as a function of volume fraction of dispersed phase:

$$\eta_r = e^{k\phi} \tag{28}$$

Where k is a constant.

Pal and Rhodes (1989) presented a new model that would be able to predict the viscosity of Newtonian and Non-Newtonian emulsions:

$$\eta_r = \left[\left(\frac{(\frac{\phi}{\phi^*})}{1.187-(\frac{\phi}{\phi^*})}\right)\right]^{2.49} \tag{29}$$

Where $\phi^*$is the dispersed phase concentration at which relative viscosity becomes 100.

Pal and Rhodes (1989) developed a more accurate model:

$$\eta_r = \left(1 - K_0 K_f(\gamma)\, \phi\right)^{-2.5} \tag{30}$$

New parameters were incorporated in this equation: K_0 is the hydration factor (fluid-dependent) and $K_f(\gamma)$ is the flocculation factor and is used only for Non-Newtonian emulsions.

Rønningsen (1995) proposed a linear correlation for water-in-crude oil emulsions that includes temperature:

$$ln\eta_r = k_1 + k_2 T + k_3 \phi + k_4 T\phi \tag{31}$$

Where $k_1 - k_4$ are the shear rate-dependent coefficients. But Eq. (31) is not representative of fluids expect the experimental ones because it does not contain any system dependent coefficient (Dan et Jing, 2006).

Pal (2000) proposed a new model to predict the relative viscosity of concentrated emulsions:

$$\eta_r \left[\frac{2\eta_r+5K}{2+5K}\right]^{3/2} = (1 - K_0\, \phi)^{-5/2} \tag{32}$$

Where K_0 is a factor representing the adsorbed surfactant on the surface of the droplets that is constant for a particular system.

The most recent correlation was proposed by Dan and Jing (2006). The authors claimed that their model fit the experimental data better when compared to Pal and Rhodes (1989). The following correlation was proposed:

$$K_e(\phi_{min}) = \frac{K_e(\gamma,\phi)|_{\phi=\phi_{min}}}{K_e(\gamma)|_{\phi=\phi_{max}}} = \frac{\frac{1-\eta_r^{-0.4}(\gamma,\phi_{min})}{\phi_{min}}}{\frac{1-\eta_r^{-0.4}(\gamma,\phi_{max})}{\phi_{max}}} \quad (33)$$

Fig.10 shows that the improved model fits the data better but it cannot be used for water cut near the inversion point due to the high dispersed phase fraction which can cause collision and distortion possibly making the rheological characterization more challenging.

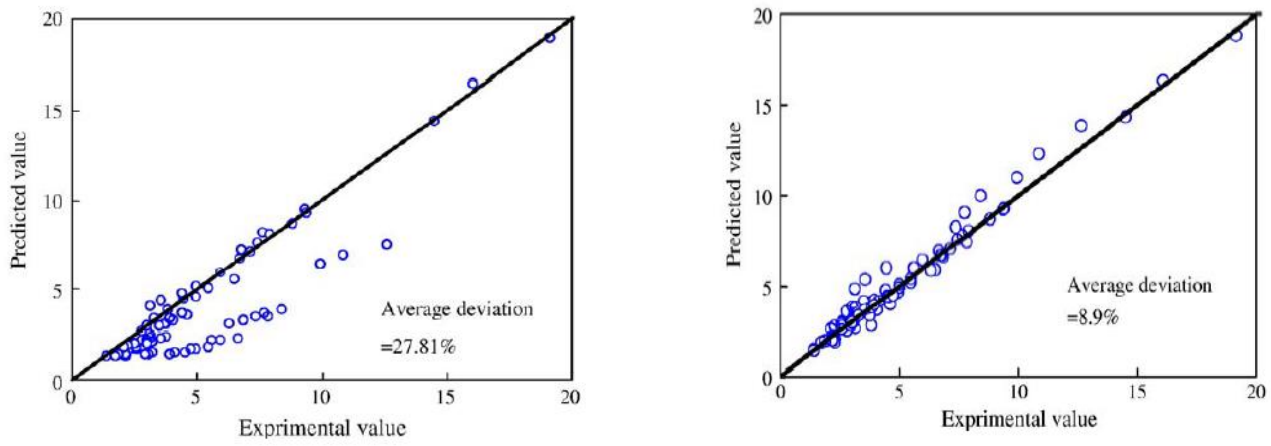

Fig. 10— Comparison between the experimental data with the Pal and Rhodes model and the Improved Pal and Rhodes model (Dan et Jing, 2006)

7. Total Acid and Base Number (TAN & TBN)

Surface active agents are a very important factor affecting the stability of emulsions. Crude oil contains elements which naturally act as surfactants. These natural elements are heavy polar

fractions which include asphaltenes, carboxylic organic acids, bases, and fine inorganic particles (Kilpatrick, 2012). Several authors have identified asphaltene as a compound severely impacting the stability of emulsions. Strassner (1968) studied the effect of asphaltene content on the stability of emulsion by removing asphaltene from a crude oil sample. It resulted that after the asphaltene removal the interfacial film weaken and became more mobile creating an unstable emulsion. In contrast, when asphaltenes were added a rigid film was formed and a more stable emulsion was formed. McLean (1997) and Kilpatrick (2012) demonstrated through laboratory tests that there is a relationship between the asphaltene precipitation point and the stability of water-in-oil crude oil emulsions. They made the similar observation that the most stable emulsions were observed near the asphaltene precipitation point. Thus, the acids and bases contained in crude oil affect the stability of emulsions.

Their effects can be observed through Total Acid Number (TAN) and Total Base Number (TBN). TAN represents the acid concentration and TBN represents the alkaline concentration. TAN is expressed in milligrams of potassium hydroxide required to neutralize the acid in 1 gram of oil. TBN is expressed mg KOH/g. Acids groups in crude oil mostly include carboxylic acids, hydroxyl, pyrrole and thiol acids while the basic group includes pyridines and quinolones. Overall, these groups are complex organic compounds that have diverse chemical and physical properties. Subramanian et al. (2017) revealed that the stability of the emulsion is improved when in an acidic environment. Brandal et al. (2006) found that removal of the acidic groups leads to a more stable emulsions and a decrease of interfacial tension. This was demonstrated by reducing the total acid number through removal of the acid component which caused the asphaltene to become more surface active and the interfacial tension to increase forming a more stable emulsion. Barth et al.

(2005) investigated twenty different crude oils and reported that there is a strong correlation between the asphaltene content and TBN.

With this comprehensive review of emulsion work in the literature and factors affecting the stability and viscosity of emulsions, we now transition to the relevant experiments performed in this study.

From the literature review, it reflects that the studies on emulsions are extensive. But the studies focus on specific parameters possibly due to the complexity of the emulsions. The pressure drop and velocity are the most studies parameters. When the flow rate is being measured, there is no correlation to the viscosity. When the pressure is studied , the estimated viscosity is derived from calculation and express as the emulsion relative viscosity that is the viscosity of emulsion divided by the viscosity of the base oil. The present literature agree that water-in-oil emulsions commonly show a shear thinning behavior that is described by the power law model. Dol et al. (2016) investigated the effect of sudden change and gradual change of constrictions on the emulsions. This study was realized by flowing the emulsion in a flow loop while the pressure drop across the pipeline was recorded. The results indicated an increase in pressure drop as the water fraction increased and the change in constriction increase the reduction in water droplets. The effect was tested at different water-cut but the viscosity of the emulsion was not evaluated during the study.

Dan and Jing (2006) realized a study on the apparent viscosity of the emulsion. The viscosity of the emulsion is once again expressed as relative viscosity hence a separated independent value of the emulsion itself it not present. In addition, the equation will be applicable to low water cut and the experiment was performed on waxy oils having a relatively high viscosity (59.6- 534 mPA.s).Hence the need for the current to investigate the rheology of the emulsion independently.

Chapter III: Experimental Procedure

1. Experimental Work flow summary

The current chapter will discuss the experimental work flow, the techniques used and the laboratory materials as well as equipment used through the research. The first step in this research was to conduct single phase flow tests with deionized water, and two crude oils of different viscosity (Texas oil). Once the data from the flow test were analyzed, the emulsions were prepared with deionized water and their stability were tested. A researcher from the same lab has previously carried out extensive tests on a similar oil from the same provider (Oluwatosin, 2016). His finding set the first concentration (1%) and type of surfactants to try (Span 85). The crude oils used originated from wells in a Texas field same as the oil used by Oluwatosin (2016). Note that oil from this field does not readily emulsify with water, hence the need to add a surfactant to stabilize the emulsion and allow us to study its characteristics. The oil used in this research and the oil used by Oluwatosin (2016) happened to be dissimilar in their reactions to the 1% Span 85 concentration, thus a series of trial-and-error tests was carried out to determine the concentration and type of surfactant that would create a stable emulsion that is consistent in properties. The surfactants used were not selected on a particular basis: they were readily available in the lab in sufficient amount and were then used to carry the research. Surfactants were mixed using an IKA Ultra Turrax T18 at 2 preset speeds for a define period of time estimated in second. The stability of the emulsions was tested through two tests: the bottle test and the centrifuge test. The emulsions proven to be stable has their viscosity and density recorded over time to observe possible changes in stability and/or viscosity. All the viscosity measurement carried before flow tests were carried out with the appropriate size of a Cannon Fenske Capillary viscometer. The most stable emulsion was tested with the flow loop. Overall, flow tests were carried out for 100% Deionized water, 100% oil (oil

A), 100% oil (oil C), and the most stable emulsion. Oil C is a very viscous oil that was tested in order to verify the ability of the emulsions to flow through the flow loop and provide accurate results with our equipment as the anticipated viscosity of the emulsion was expected to be similar to that of this viscous oil C. Density throughout the research was measured with a pycnometer. Once an emulsion demonstrated stability over time, 3.1 L of the emulsion was made to carry the flow test experiments. All the flow test experiments were carried out using a laboratory scale flow loop. The measured data was obtained from the metal pipe section consisting of two different stainless-steel pipes of 1/4" and 3/8" outside diameters mounted horizontally. The parameters recorded during the investigation were flow rate, viscosity (before and after the flow), pressure (inlet and outlet). The Anton Paar rheometer MCR 72 and the Cannon Fenske capillary viscometer were used to determine the rheological parameters of the emulsions. All the experiments were carried at room temperature of 25°C.

2. Fluids and Chemicals

The fluids used throughout the research were deionized water, crude oils (Texas crude oil) and the emulsion made from them. All the crude oils used were obtained from the same field (Texas crude oil). The crude oils and water were emulsified using Span 85, Span 80, Triton™ X-100, Merpol® A, Tergitol®, Tween®80, Merpol®SE. All the surfactants used are non-ionic. All fluids and surfactants were used at room temperature. The characteristics of the fluids and surfactants used are listed in **Table 3** and **Table 4.**

Table 3— Surfactants Properties

Name	Chemical name/group	Density g/cc (25°C)	Viscosity Cp (25°C)	HLB	Supplier
Merpol® A	Alcohol Phosphate	1.07	90	6	Sigma-Aldrich
Merpol® SE	Alcohol Ethoxylate	0.97	60	10	Sigma-Aldrich
Span 80	Sorbitan Monooleate	0.99	1000-2000	4.3	TCI
Span 85	Sorbitan Trioleate	0.95	200-300	1.8	Sigma-Aldrich
Tergitol®	Alcohol Ethoxylate	1.006	60	13.3	Sigma-Aldrich
Triton™ X-100	Octylphenol Ethoxylate	1.061	240	13.5	Sigma-Aldrich
Tween ® 80	Polyoxyethylene Sorbitan Monooleate	1.076	375-480	15	Fisher BioReagents

Table 4— Fluid properties at 25ºC

Fluid Properties	
Deionized Water	API = 10 ρ = 0.9971 g/cc μ = 1 cP
Oil A1	API = 35 ρ = 0.8498 g/cc μ = 8.43 cP
Oil A2	API = 34.97 ρ = 0.850 g/cc μ = 7.01Cp
Oil B	API = 34.38 ρ = 0.853 g/cc μ = 16.75 cP
Oil C	API =24 ρ = 0.9099 g/cc μ = 369.38 cP
Oil D	API = 34.97 ρ = 0.850 g/cc μ = 6.54 cP

3. Emulsion Formation

All the emulsions made were 100 cc to 150 cc. The first step in making the Water-in-crude oil is to dissolve the surfactants into the crude oil. The required the amount of each liquid to be known from prior calculations and then measured with a scale. The required volume of surfactant was estimated as a percentage of the total volume of oil used, but measurements were carried out based on their corresponding weight for accuracy purposes. Different concentrations and combination of surfactants were used. The agitation required to make emulsion was provided by the IKA Ultra Turrax T18 (**Fig. 11**). The IKA Ultra Turrax T18 has speed ranging from 3000 to 25000 RPM and produces high turbulence and high accelerations through the application of an extremely strong shear as well as thrust forces supplied by the rotor and stator **(Fig. 11**). The disperser provides fine dispersed droplets and the set up prevents air entrapments.

Fig. 11— IKA Ultra Turrax T18 disperser (left) and Anton Paar MCR 75 rheometer (right)

The surfactant and oil mixture is first mixed for 30 seconds at 10,000 RPM.The weighted deionized water is slowly added while stirring is carried out upto 1minute. Finally, the speed is increased to 20,000 RPM and mixing continues for an additional 2 minutes. Overall, the emulsion is mixed for 3 minutes. The following water fractions were investigated: 10%, 15%, 20% and 30%, but the focus was shifted to the 30% emulsion for the graeter part of this study. The emulsion was allowed to cool down and reach room temperature (25°C). It was then put in two separate tubes of 15 mL. The viscosity was measured using a routine Cannon Fenske viscometer. **Fig. 12** shows the viscometer and **Table 5** the viscosity ranges for routine Cannon Fenske viscometers. The density was measured using a pycnometer according to ASTM D854 (**Fig.12**).

Table 5— Recommended Viscosity Ranges for Cannon-Fenske Routine Viscometers

size	approx. C (cSt/s)	viscosity range (cSt)	
		from	to
25	0.002	0.5	2
50	0.004	0.8	4
75	0.008	1.6	8
100	0.015	3	15
150	0.035	7	35
200	0.1	20	100
300	0.25	50	250
350	0.5	100	500
400	1.2	240	1200
450	2.5	500	2500
500	8	1600	8000
600	20	4000	20000
650	45	9000	45000

The first stability tests were investigated through the bottle test. In a bottle test, the emulsion is allowed to separate into a distinct oil layer and a water layer on its own (gravity) without the

application of any external force. Stability is a measure of separation: if an emulsion does not separate into an oil layer and a water layer , it is said to be stable.

Fig. 12— 400 size Cannon-Fenske Viscometer (left) 25mL pycnometer (right)

If an emulsion separates into an oil layer and a water layer, the volume of oil separated (Vo) and the volume of water (Vw) separated is recorded (**Fig. 13)**. The separation is expressed in % as follows:

$$\%\, Separation = \frac{Vo+Vw}{Ve} \tag{34}$$

Where , Vo = Separated oil volume (mL)

Vw = Separated water volume (mL)

Ve = Total emulsion volume (15 mL)

Stability varies from seconds to years. The bottle test was carried out from 0 to upto 72 hours depending on the stability. The crude oil was not responding to the first surfactants concentration and type trials. Bottle tests being time consumming, the stability test was replaced by the centrifuge test. The centrifuge used was is a Clay Adams Dynac 420063, the speed ranges from 1000 RPM to 10000 RPM. The tubes are placed in the centrifuge for a cumulative period of 30 minutes in 5 minutes increments at 2000 RPM. The volume of separated oil and water is recorded at every interval and the separation % is calculated. If there is separation, the centrifuge test is stopped and the emulsion is kept aside. If there is no separation after the 30 minutes, the emulsion is centrifuged further at 10,000 RPM (maximum speed on the centrifuge) for 7 minutes. Emulsions which could pass this additional test, have not shown any separation till date. After all these tests, the remaining volume of the emulsion is kept in a 125mL for futher observation and viscosity measurements.

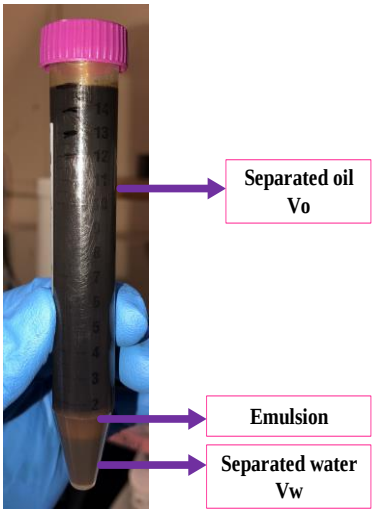

Fig. 13— Emulsion separation

In the later part of the study, the emulsion rheology was identified by the use of the Anton Paar MCR75 rheometer which use a concentric cylinder system (**Fig.11**). The automated rheometer is equipped with a ball-bearing motor that provides measurements in rotational mode. An oscillatory mode is also available for special applications.

4. Flow Experiment

The flow test experiment was performed using a laboratory scale flow loop. This flow loop consists of two stainless steel pipes of 1/4" and 3/8" outside diameter respectively. The fluids are first introduced into the system in tank A. The tank has a capacity of 3.1 L but for a continuous circulation a volume of 3.1 L is required. The experimental flow loop is represented in **Fig. 14** and the dimensions are listed below:

Table 6— Pipe characteristics

OD (in)	ID (m)	ΔP measuring Length	Thickness (m)
3/8	0.00775	2.055	0.00089
1/4	0.004572	2.06	0.00089

The flow test equipments are presented in **Fig. 18.** The Cole Parmer variable speed pump is used to pump the fluid and operate from speed of 90 to 9000 RPM. The speed is adjusted by rotating the knob to the required speed. The speeds are not explicitly written on the pump hence from the marking on the wheel around the knob, the speeds were assigned values that ranges from 1 to 11. **Fig. 18** shows that the variable speed pump is a constant pressure pump. This characteristic was observed throughout the flow test runs.

The mass flow rate was recorded manually. Once the desired speed has been selected, the fluid is allowed to stabilize and circulate for few seconds. A beaker is selected, and its weight is measured.

Fluid is then collected and the time the beaker takes to be filled is recorded. The filled beaker weight is measured. The difference between both weights is the weight of fluid collected for the current fluid. The mass flow rate is in turn converted into velocity. Then the beaker is emptied, and the new empty weight is recorded.

The pipes, valves, and fittings are provided by Swagelok. Flow tests were carried in one pipe diameter while the other one remained closed. Each line has two pressure recording points: P1 and P2 on the 3/8”, P4 and P5 on the 1/4" pipe. Pressure drop was recorded in Psi using pressure gauge and digital pressure transducers (**Fig. 18).** For the flow test, the data was recorded in three runs and each run consists of data measurement from a minimum speed to the maximum speed (11). 3 runs were conducted in order to provide accurate results. The pressure recorded and the velocity calculated were repeatable overall. **Fig.15 and Fig.16** shows the repeatability of the velocity for water in the 1/4” pipe and the repeatability of pressure for crude oil A1 in the 1/4” pipe. This demonstrate that the equipment is reliable and that the pump delivers a constant pressure. It should be noted that there were instances in which the Run 2 and Run 3 exhibited a behavior out of trend when compared to the Run 1. This can be due to the fact that the additional Run might deform the shear of the fluids causing the data to behave erratically, or it could be due to changes in pipe wetting characteristics. An example is shown in **Fig**. **17**.

It was then observed that Run 1 provides the most accurate data. Hence all the flow tests data were analyze using data provided by the first run, Run 1.

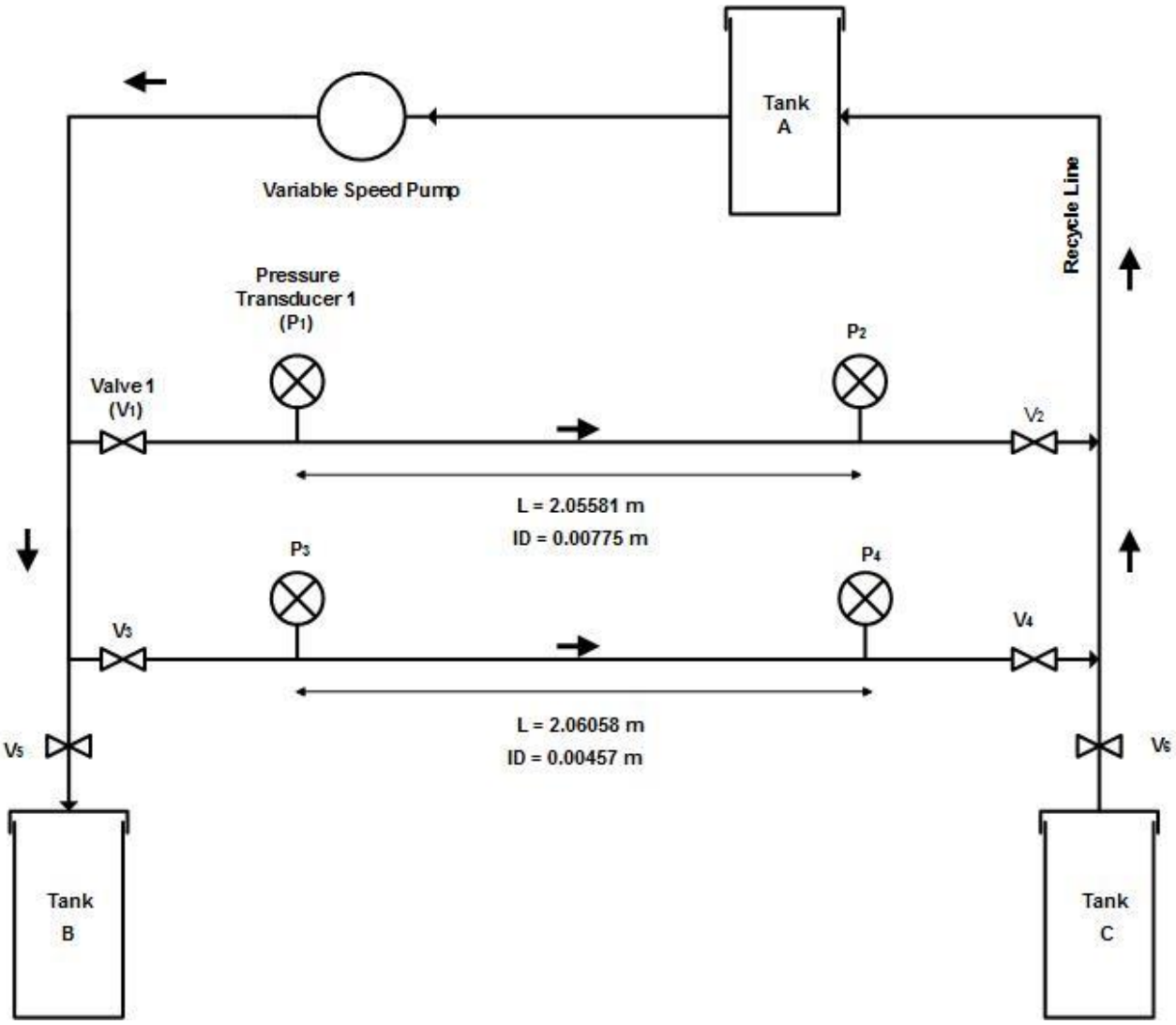

Fig. 14— Experimental flow loop

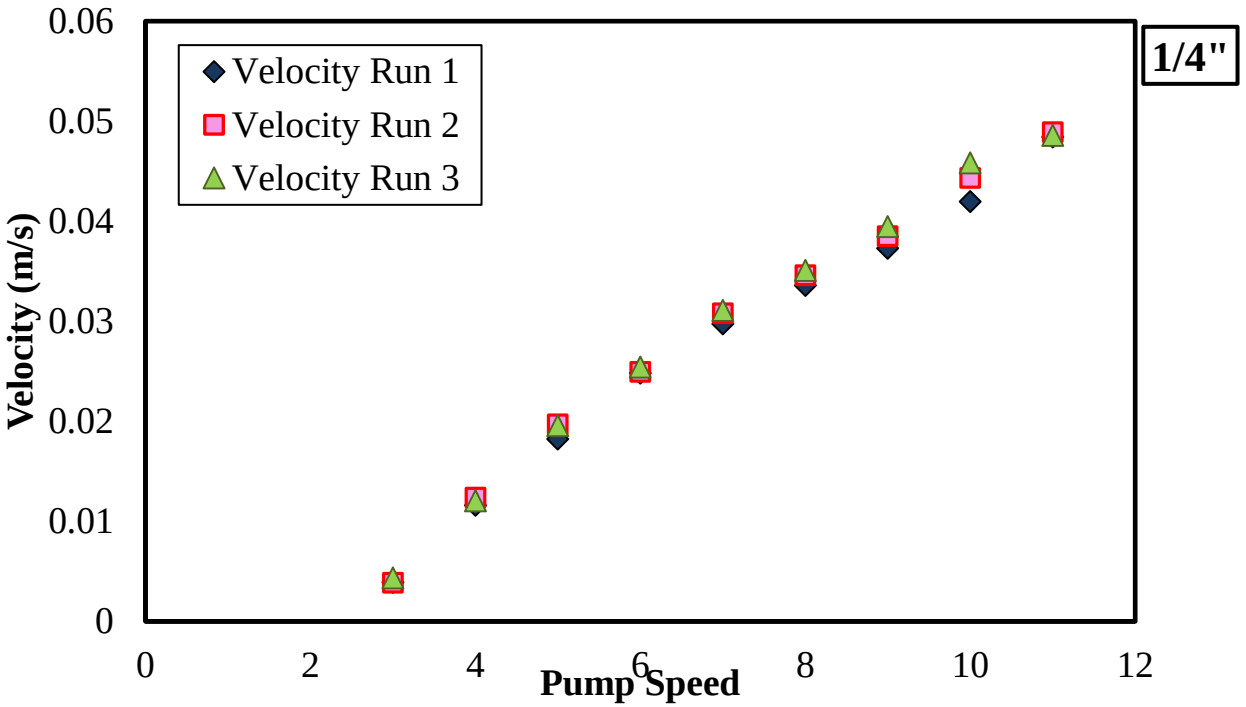

Fig. 15— Reproducibility of the measured velocity for water in 1/4" pipe

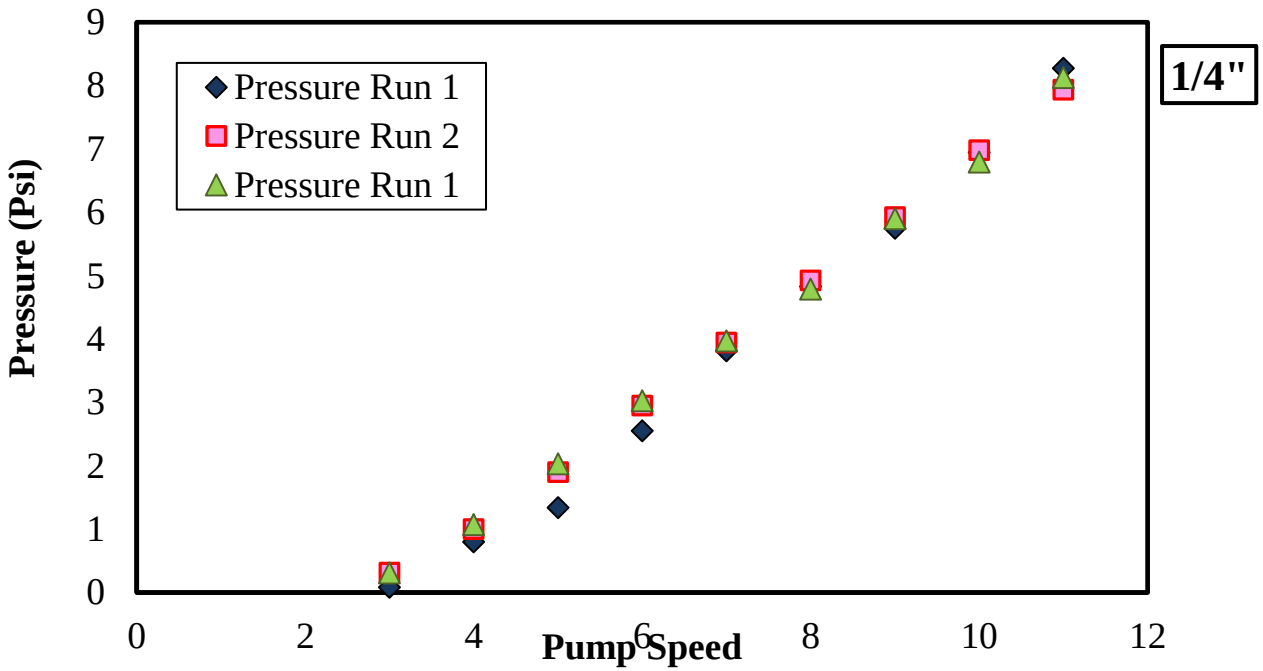

Fig. 16— Reproducibility of the measured pressure for crude oil A1 in 1/4" pipe

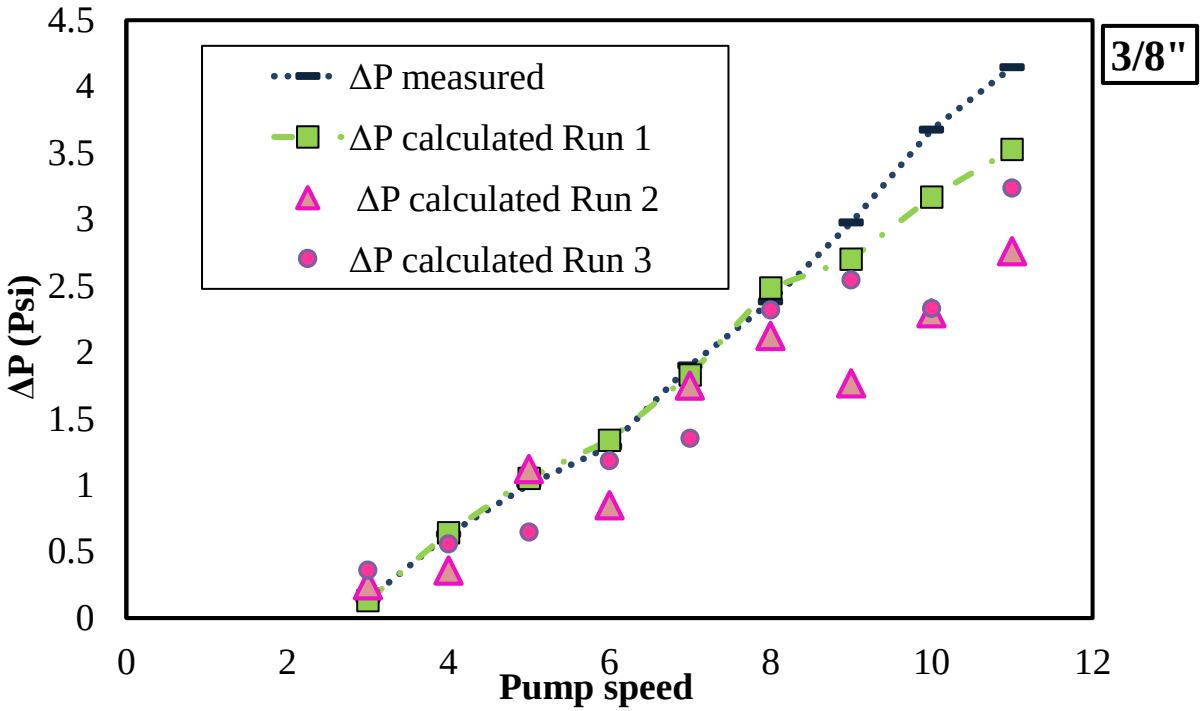

Fig. 17— Comparison between the measured data and the calculated data for different runs (1,2,3) for Crude oil A1 in 3/8”

The flow tests investigation debuted with single phase fluid namely water, crude oil A1 and crude oil C. Each time, tests were run in the bigger diameter, 3/8 size first. The experiment started for each run by filling the tank with a fluid and then starting the pump at the lowest speed which provide a continuous recirculation. The collected fluid weight is measured and the pressure at P1 and P2 are recorded (P3 and P4 for 1/4") upon reaching a steady state flow. Following this step, the speed pump is shortly adjusted to the next higher speed. After the flow test was conducted, the fluid under study was collect in Tank B by opening valve V_5. Air was added through V_6 and the pipe were slightly lifted to make sure the fluid is extracted. As the majority of the oil was consumed through the search for the adequate concentration of surfactant, only one water fraction of 30% was tested in this study.

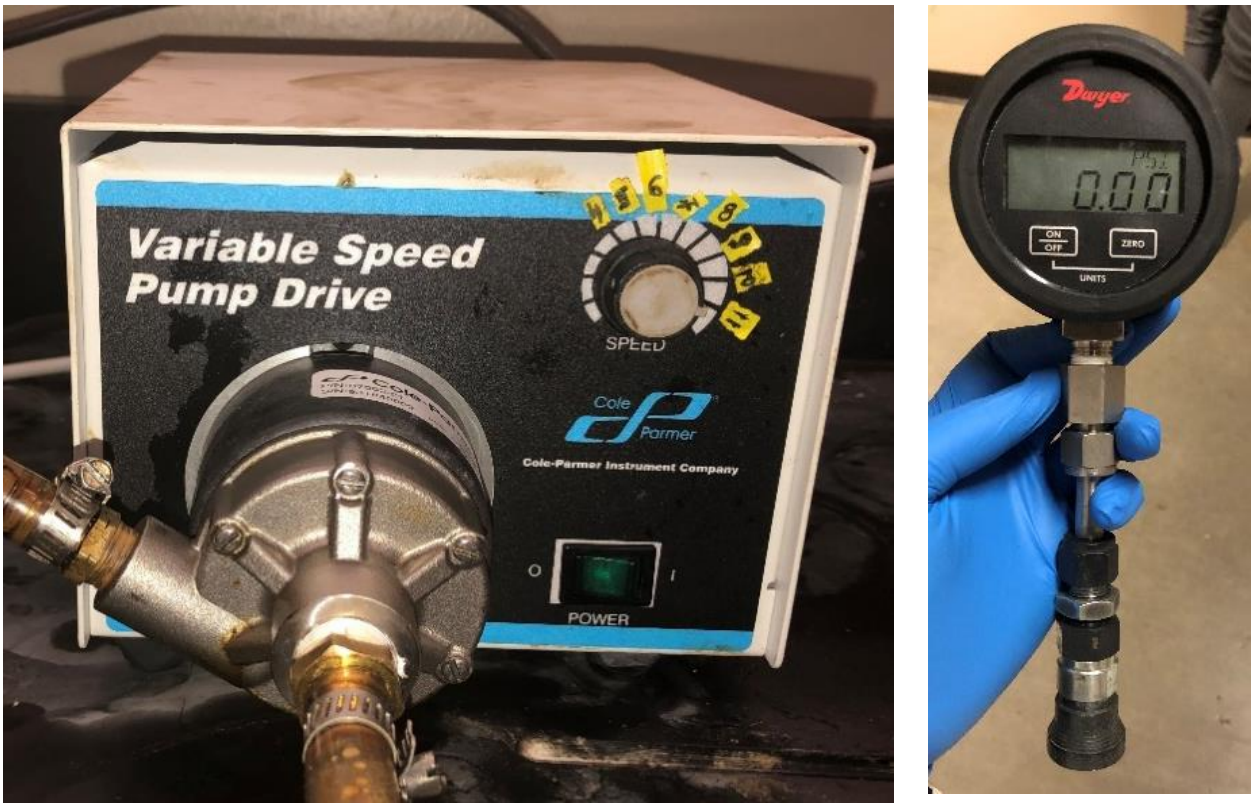

Fig. 18— Cole Parmer variable speed drive (left) and pressure gauge (right)

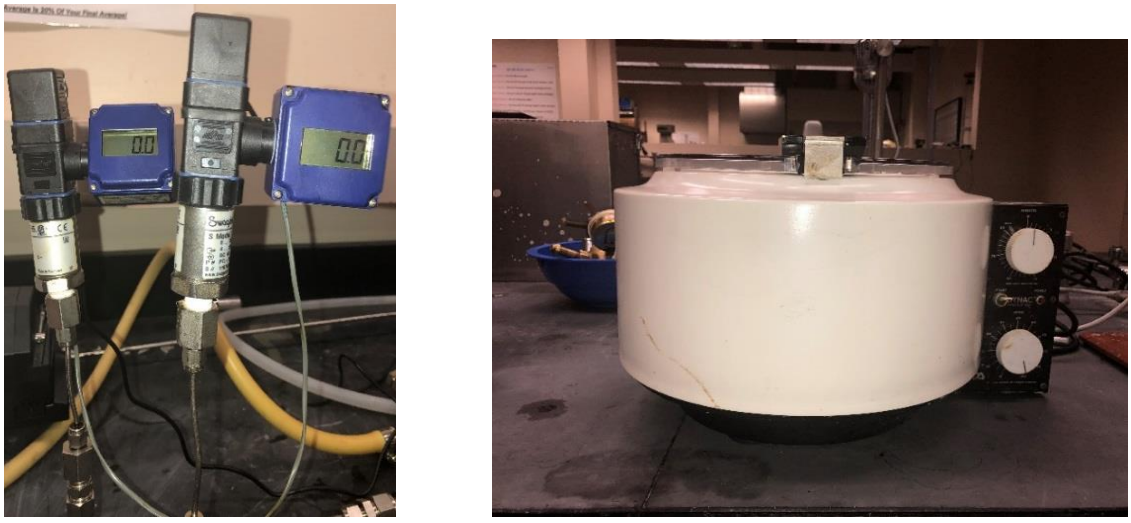

Fig. 19— Digital transducers (left) and Centrifuge (right)

Chapter IV: Results and Discussions

1. Surfactant selection and emulsification

A stable emulsion is required for these flow tests, otherwise it is difficult to interpret the data. The crude oil and water emulsions will be stabilized with surfactants. The first step is to find the optimum concentration of surfactant that will yield a stable emulsion. Oluwatosin (2016) conducted prior tests on a similar type of Texas oil used in this current research. He investigated the effect of six different surfactants on emulsion stability and found that the most stable emulsion was obtained using only 1% of Span 85 and that the surfactant stabilized emulsion are reproducible. The effect of surfactant concentration was investigated at different water fractions **(Fig. 20)**. Overall it is clear that 1% of Span 85 yields the highest stability at all water fractions (10% to 70%). Therefore 1% Span 85 was the first concentration used to test the emulsion in the current research.

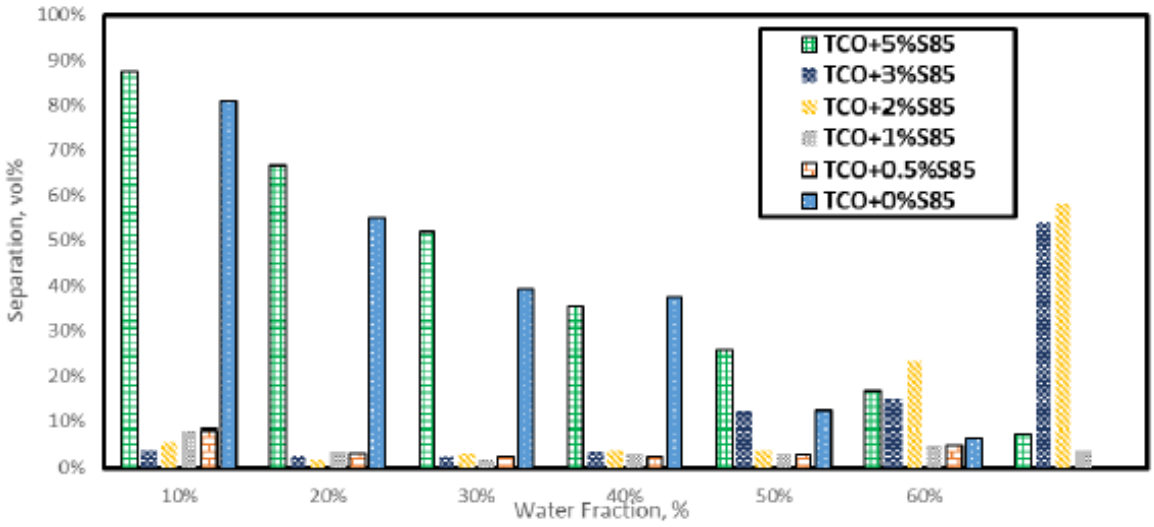

Fig. 20— Effect of different surfactant concentration on stability of emulsion (Oluwatosin, 2016)

The emulsion was tested at 30% water cut with 1% Span 85. The bottle test for this emulsion showed that separation occurred within the first 30 minutes (**Fig. 21**). Hence further tests needed to be conducted to obtain the most stable emulsion. 85 different combinations of different types of surfactants at different concentrations were made. The list of the combination can be found in **Appendix A**.

Fig. 21—30% water-cut (left) showing separation after 30 minutes (right)

Selecting the concentration and the type of surfactant is still a trial-a-error method. Single surfactants were tried first. After unsatisfactory stability, blends of surfactants were created. Overall, the most stable emulsions for all crude oils was obtained from a blend of TX100 and Span 80.

Fig. 22 illustrate the physical appearance of few of the emulsions made. When using a low HLB surfactant, oil separated first on top followed by little or no bottom water separation. When a high HLB was used, water separation was observed first followed by oil separation. The color of the separated water varies from surfactant to another.

Fig. 22— Different emulsion appearance

Fig. 22 from left to right shows:

- 3% Merpol SE + 1.5 % Span 85 + 3.20 % Span 80, Oil B
- 10% water cut, 2% TX 100 + 1% Span 80 + 1% Merpol A, Oil B
- 30% water cut, 2.4% Span 85, Oil A1
- 30 % water cut,2.5% Span 85 + 1.5% Tergitol Oil B
- 30% water cut, 3.4% TX100 + 3 % Span 80 + 2.5 % Merpol A, Oil B
- 20% water cut 1%TX100+ 0.66% Span80, Oil B
- 30% water cut, 3.9% TX100+ 3.9% Span 80, Oil D

The most stable emulsion was obtained at 30% water cut are listed below in **Table 7:**

Table 7— Most stable emulsion obtained

Base Oil	Surfactant and concentration of blend	Water Cut	HLB of the Blend
Oil A1	**1.5% TX100 + 1% Span 80**	**30%**	**9.97**
Oil A2	**3.5% of TX100 + 3.4% of Span 80**	**30%**	**9.13**
Oil D	**3.6% TX100 + 3.4% Span 80**	**30%**	**9.131**

None of the emulsions made with oil B remained stable over 24 hours. The emulsions made from oil B were very light from visual observation when compared to the other made with oil A2 and D. Even though oil B showed separation, the following combination of surfactants exhibited the least separation after 5 minutes, but it did not last for more than 24 hours (see Appendix):

- 3.9% TX100 + 3.8% Span 80 (1% separation)
- 3.9% TX100 + 3.9% Span 80 (1% separation)
- 4% TX100 + 3.9% Span 80 (2% separation)
- 3% TX100 + 2.5% Span 80 + 2% Merpol A (3% separation)
- 3% TX100 + 3% Span 80 + 2% Merpol A (2% separation)
- 3.6% TX100 + 3.5% Span 80 + 1.5% Merpol A (0% separation)

The addition of Merpol A to the TX100 and Span 80 mixture for oil B showed encouraging results. But the trial-and-error method uses a considerable amount of oil and started causing delay in the realization of the study thus it could not be investigated further.

Oil A1 demonstrated to contain traces of water separation after centrifugation, hence it was not carried forward in the study but the presence of water might explain the reason why emulsion made with this oil showed stability at low surfactant concentration (1.5% TX100 + 1% Span 80). It is

important to note that this emulsion from this oil have showed stability for 2 months. The separated water volume after centrifuging oil A1 is shown in **Appendix A**.

An emulsion using oil A2 as the base oil using 3.5% Tx100 + 3.4% Span 80 at 30% water cut maintained its stability for several days (Stable till date). Hence this blend is carried forward for the investigation (**Fig. 24**). It is very important that the emulsion demonstrate a constant viscosity behavior over time. Therefore, the viscosity was recorded over 24 hours before starting the flow test experiments and the results were satisfactory (see **Appendix A**).

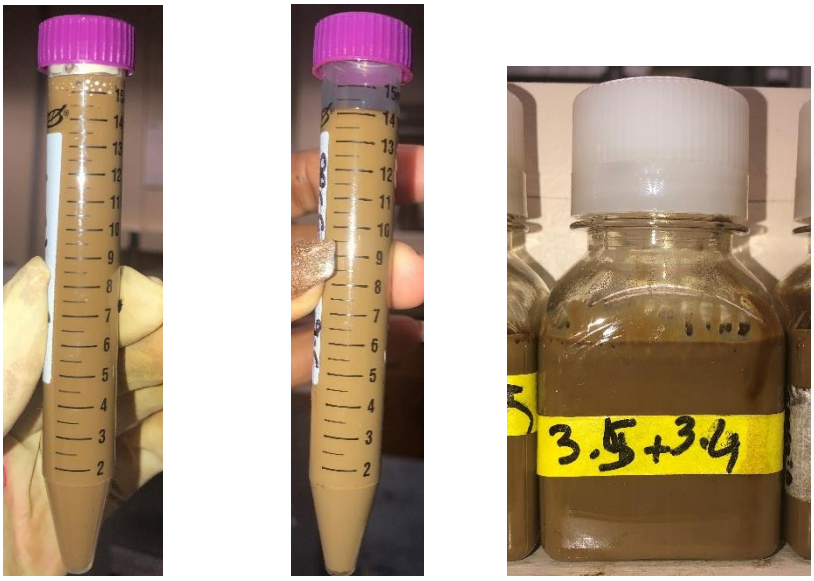

Fig. 23— 3.5%TX100 + 3.4% Span 80 at 30% water cut before centrifuge test(left), after centrifuge test (middle) and after 1 week (left)

As mentioned in chapter 3, 3.1 L of emulsion is need for adequate circulation. The volume of emulsion prepared per batch is 150 cc. In order to speed up the emulsion formation process, I considered increasing the volume of emulsion prepared from 150 cc to 300 cc. A 30% water cut emulsion containing 1.5% TX100 and 1% Span 80 was created at two different volumes: 150 cc and 300 cc. The protocol followed was the same for both emulsions. Even though both emulsions showed the same color and stability (0% separation), they have different densities and viscosity which are presented in **Table 8**. It is observed that the viscosity of the emulsion increased

significantly when creating an emulsion volume of 300 cc. This is likely due to the shape of the mixing tool and the location of the water-oil interface. The water was likely exposed to more turbulence, dispersing it into smaller droplets within the oil and resulting in a higher viscosity.

Table 8— Effect of the increase of emulsion formation volume

Surfactant concentration	Volume made	Viscosity (cP)	Density (g/cc)
1.5% TX 100 + 1% span 80	150 cc	231.224349	0.884726
1.5% TX 100 + 1% span 80	300 cc	1588.437181	0.845638

2. Single phase flow test

The flow test was carried out with single phase fluids in the following order: deionized water, oil A1, oil C, and then with a 30% water cut emulsion. The volumetric flow rate and the pressure were recorded. For the 3/8" pipe, pressures were recorded at the inlet at P1 and outlet at P2. For the 1/4" pipe, pressures were recorded at inlet at P3 and outlet P4. The Reynolds number was calculated using Eq. (10) and the pressure difference (ΔP) was calculated. Then the calculated ΔP and the measured ΔP were compared to verify the equations for each pipe diameter. There is a match between the calculated ΔP and the measured ΔP for water and oil A1 **(Fig. 24 and 25)**. This match confirms that the water under flow is exhibiting a Newtonian behavior. Therefore, in this case n=1 and it reflects that the viscosity is independent of the shear rate. Once the water and Oil A1 flow test were carried out, crude oil C was test with the same flow loop. Oil C has higher viscosity compared to oil A1. In order to test the ability of the equipment to handle viscous emulsions, viscous oil C was used with the equipment. This flow test was performed to verify the recirculation of a potential emulsion having the approximate viscosity.

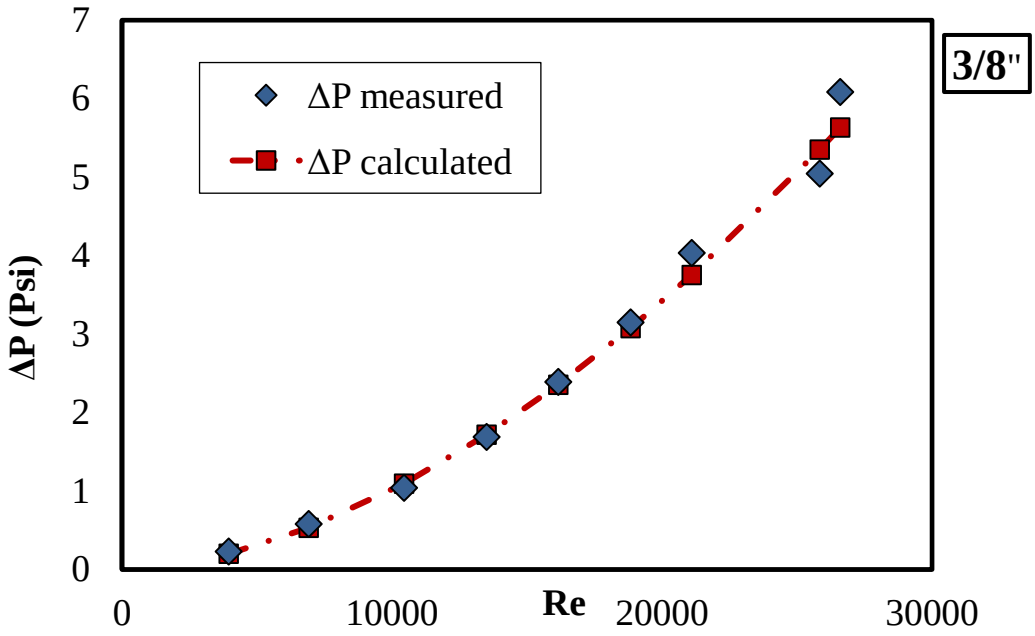

Fig. 24— A plot of measured and calculated pressure drop for water flow in a 3/8" pipe.

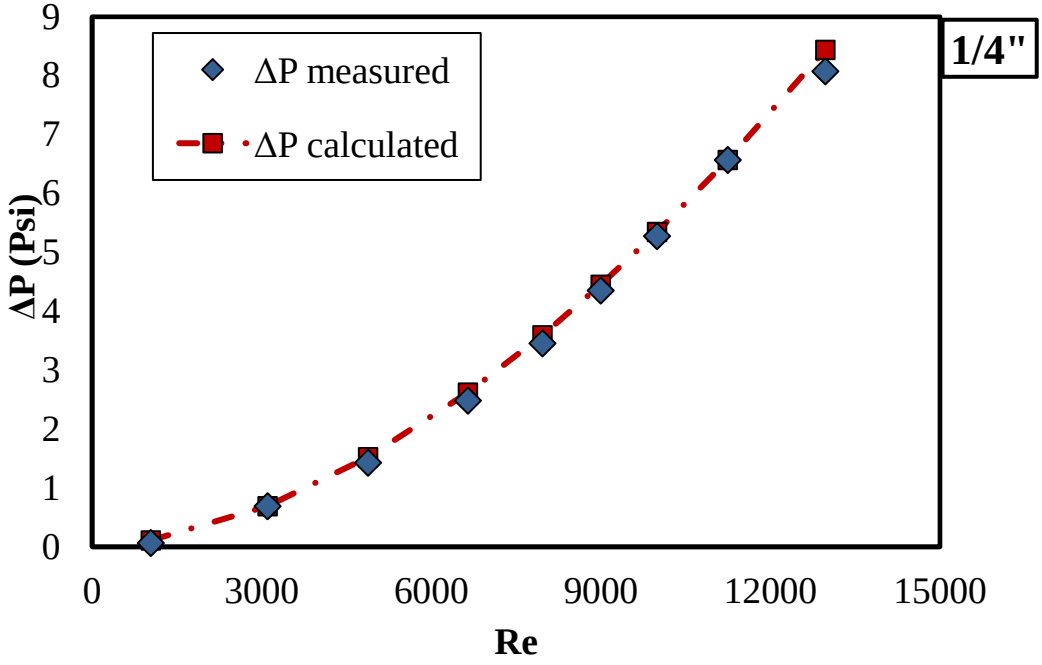

Fig. 25—A plot of measured and calculated pressure drop for water flow in a 1/4" pipe.

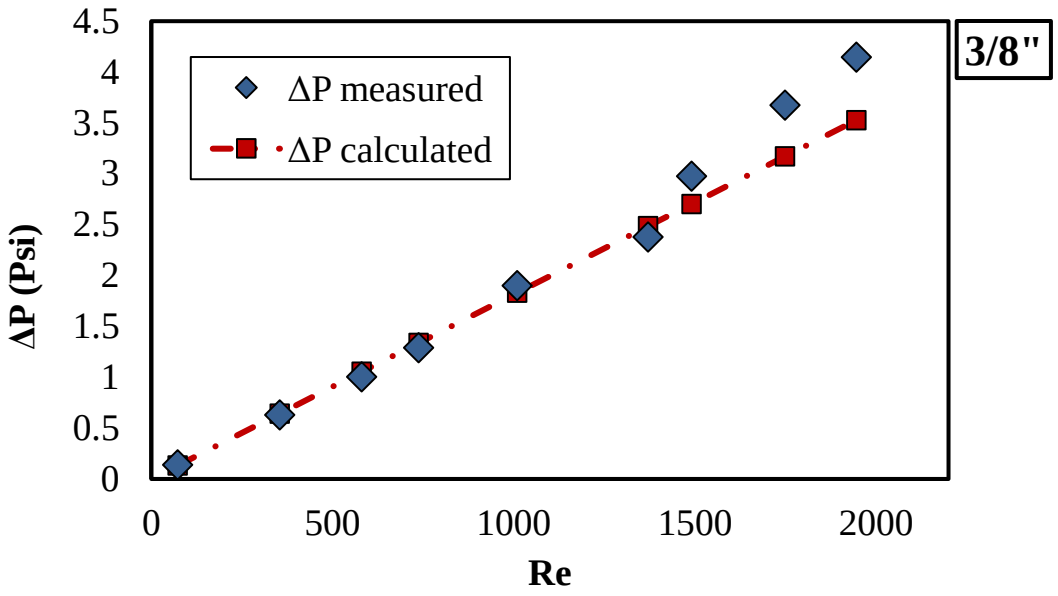

Fig. 26—— A plot of measured and calculated pressure drop for crude oil A1 in 3/8" pipe.

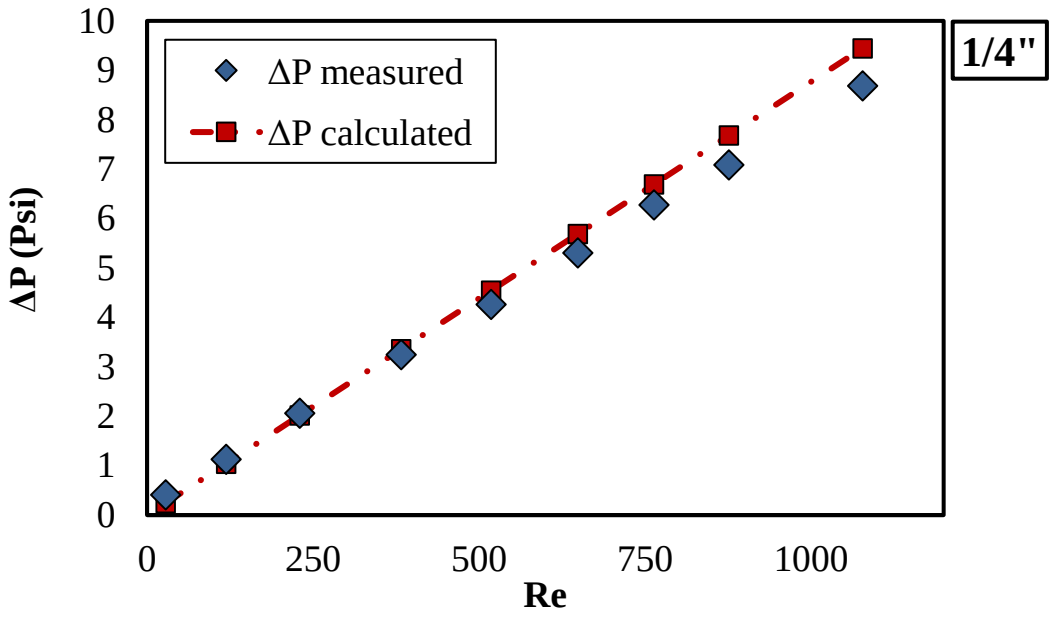

Fig. 27— A plot of measured and calculated pressure drop for crude oil A1 in 1/4" pipe.

Oil C is heavy and make the pipe difficult to clean. In order to prevent the wetting of the inside wall of the 1/4", oil C was flow tested only with pipe 3/8". The results are presented in **Fig. 28** and it shows that the equipment can handle the flow of the emulsions. The calculated ΔP and the measured ΔP do not match for oil C. The results are discussed later in this chapter.

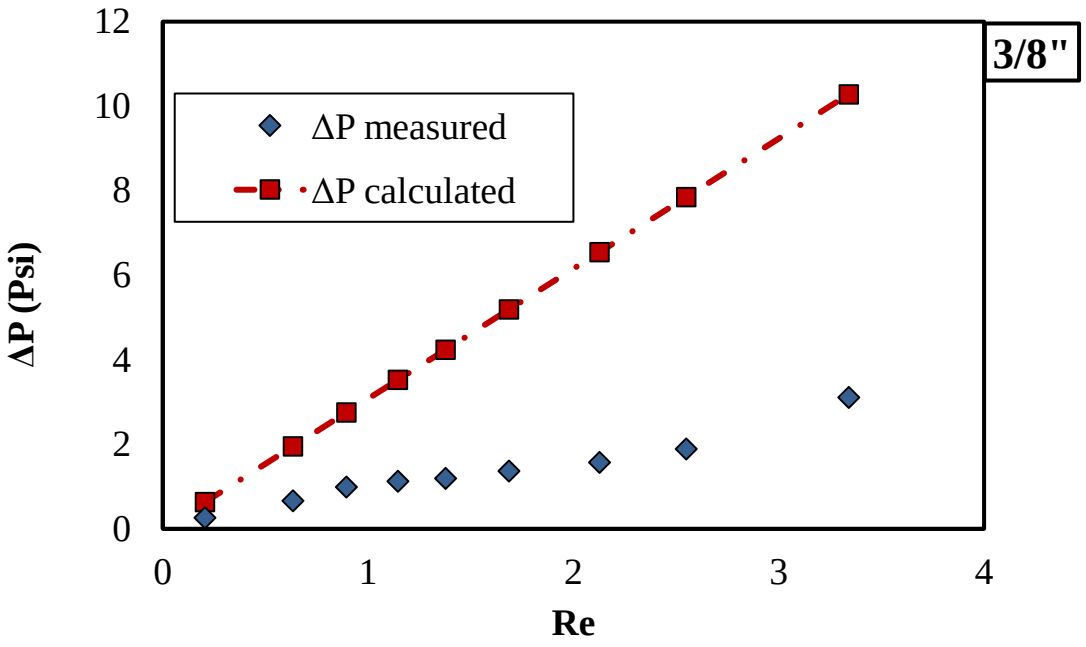

Fig. 28— A plot of measured and calculated pressure drop for crude oil C in 3/8" pipe.

3. Emulsion flow test

The flow test was carried out with the pre mixed 30% water cut emulsion containing 3.5% Tx 100 +3.4% Span 80. The protocol followed for the flow test of the emulsion is the same that was followed for the single phase flow tests using deionized water, oil A1 and oil C. The results obtained from the first three runs are presented below:

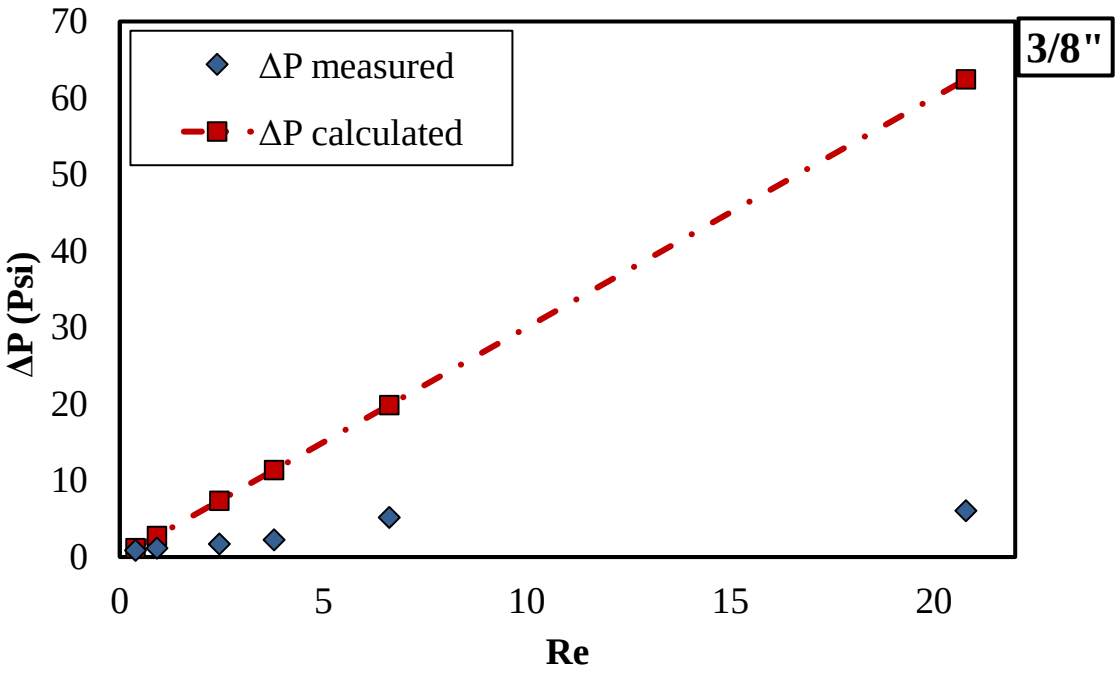

Fig. 29— A plot of measured and calculated pressure drop for the emulsion in 3/8" pipe run 1.

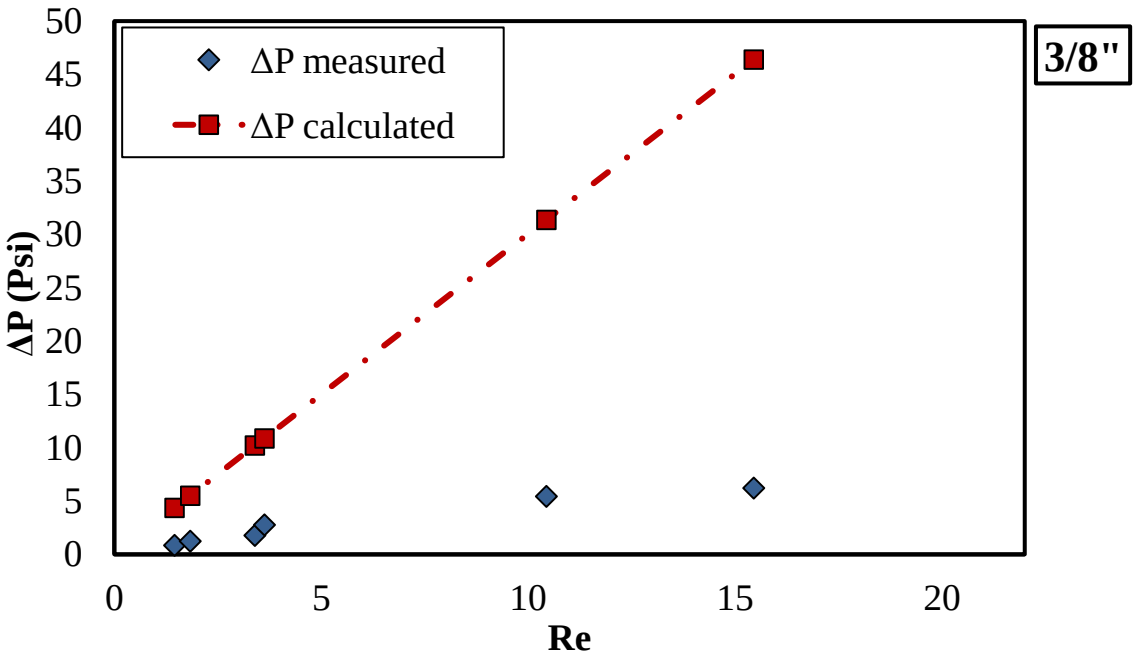

Fig. 30—A plot of measured and calculated pressure drop for the emulsion in 3/8" pipe run 2.

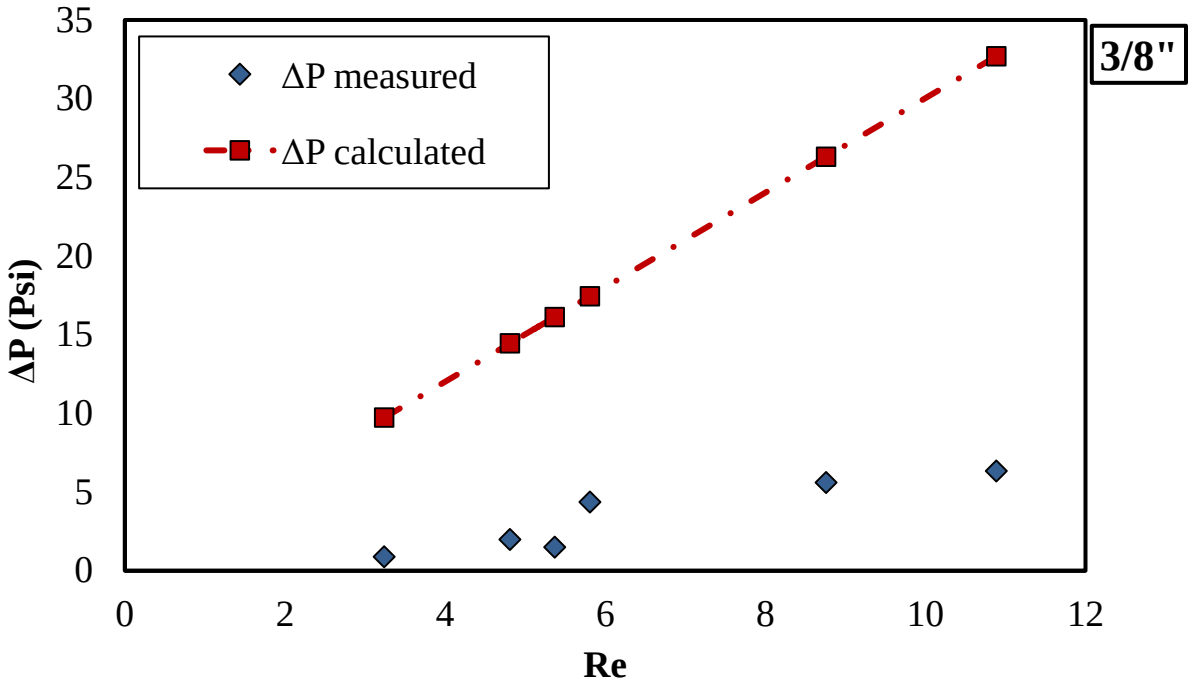

Fig. 31— A plot of measured and calculated pressure drop for the emulsion in 3/8" pipe run 3.

It should be noted that only the data obtained from the first run was used in futher analysis as the data become more erratic after Run 1. **Fig.32** confirms again that the pump is a constant pressure pump. The calculated ΔP and the measured ΔP do not match for the emulsion. The pressure drop was estimated considering the Newtonian flow equation Thus , the discrepancy between the calculated pressure drop and the measured pressure drop implies that the emulsion do not follow a Newtonian behavior for both diameter pipes. Therefore, the next step is to analyze the type of behavior that the emulsion follows. This resume in estimating the shear rate and shear stress experienced by the fluid during the flow test. Once the values are obtained, they can be plotted on a cartesian plot with the shear rate on the x-axis and shear stress on the y-axis. The trend followed by the data will help us predict the rheological model followed by the emulsion (**Fig.5**).

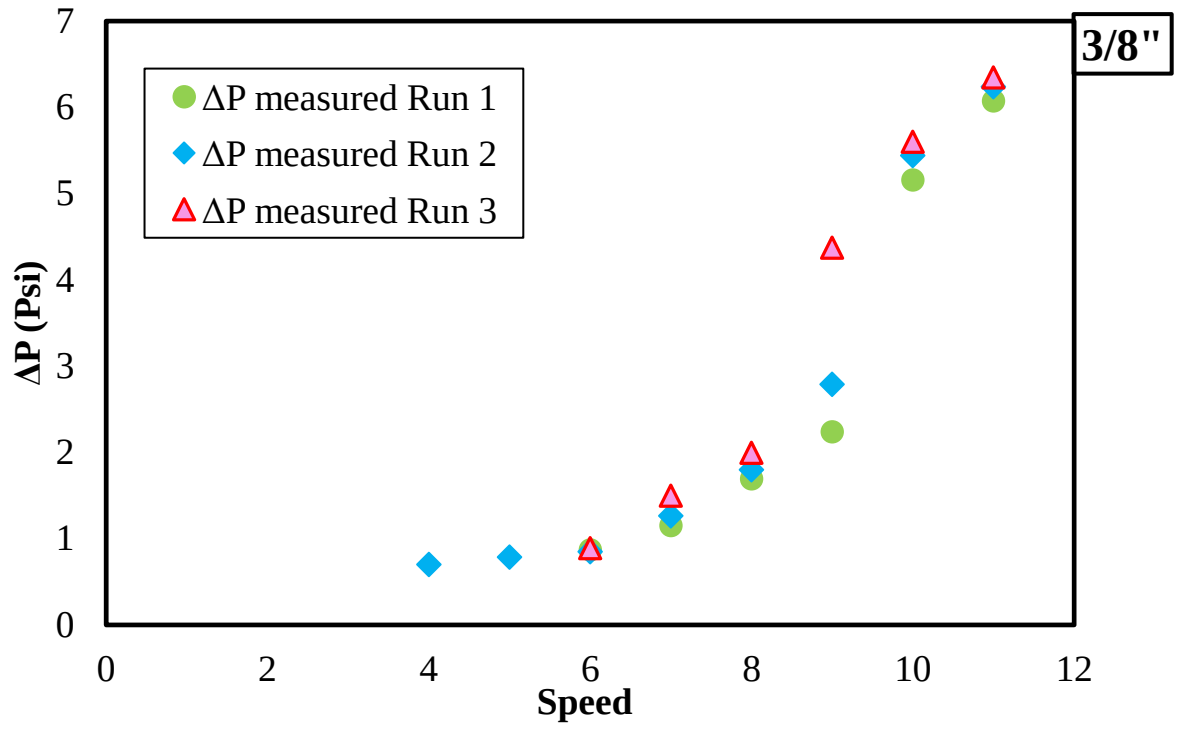

Fig. 32— A plot of measured pressure drop for the emulsion in 3/8" pipe for run 1,2 and 3.

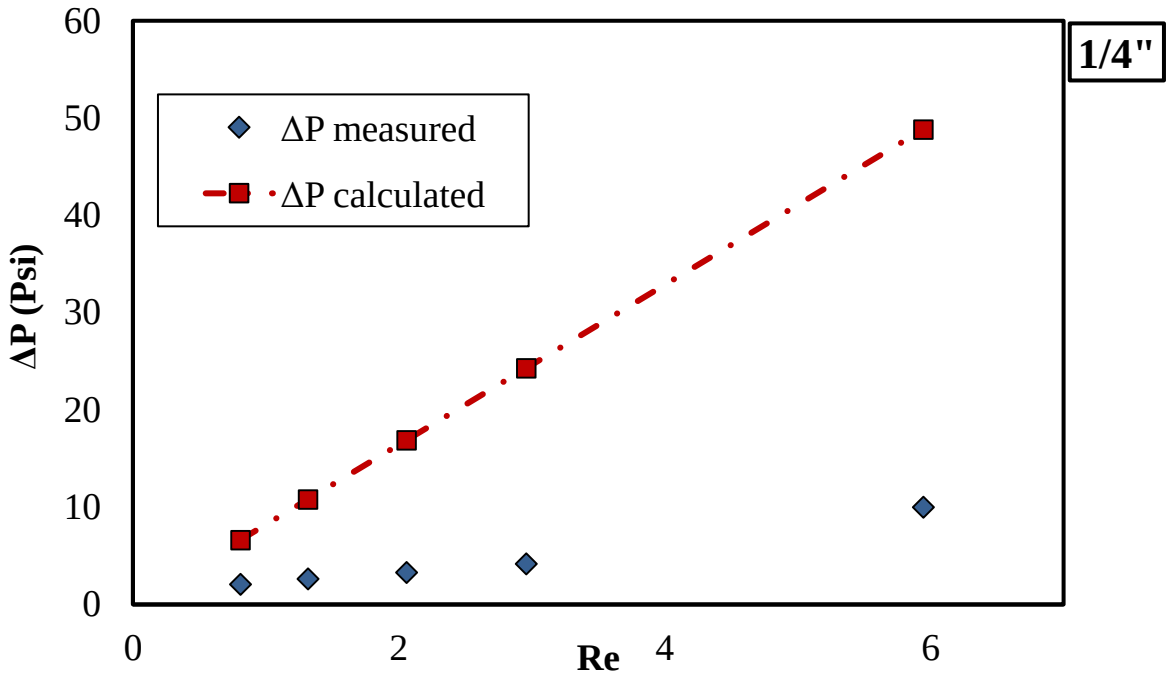

Fig. 33— A plot of measured and calculated pressure drop for emulsion in 1/4" pipe.

4. Shear rate vs shear stress estimation

The recorded pressure and velocity from the flow test in 3/8” and 1/4" are converted into shear rate and shear stress using Eq (35) and (36) (Darby, 1996; Wilkes, 1999) :

$$\tau = \frac{D}{4}\left(\frac{\Delta P}{L}\right) \tag{35}$$

$$\gamma = \frac{8V}{D}\left(\frac{1+3n}{4n}\right) \tag{36}$$

When n=1, we have a Newtonian fluid and for pseudoplastic fluid, n is less than 1 (n<1).

Shear rate for Non-Newtonian fluids is commonly estimated by the power law model which requires parameters n and k. These can be obtained from the shear curves after rheology measurements if the data fits the power law. **Fig. 34** presents the shear curves of the emulsion obtained from the flow test assuming an n value of 1. The behavior starts to show indications of non-Newtonian flow since the shear-stress/shear rate relationship is not linear. Two distinct features; first, there are signs of some shear thickening, and second, the part of the data that appears to show constant slope behavior generates a line that doesn’t pass through zero. The early part of the data presented in **Fig. 34** suggests that the emulsion exhibits some shear-thinning behavior. For the 3/8” pipe diameter: shear rate varies from 0 to 1130 s^{-1} while shear stress varies from 0 to 40 Pa. For the 1/4" pipe diameter: shear rate varies from 0 to 680 s^{-1} while shear stress varies from 0 to 32 Pa. The 3/8” pipe experiences a wider range of shear rate.

In order to confirm the findings from the flow tests, the rheology of the emulsion is tested using the rheometer. The shear rate of the 3/8” was considered and the flow curve obtain is a plot of the shear rate against the shear stress.

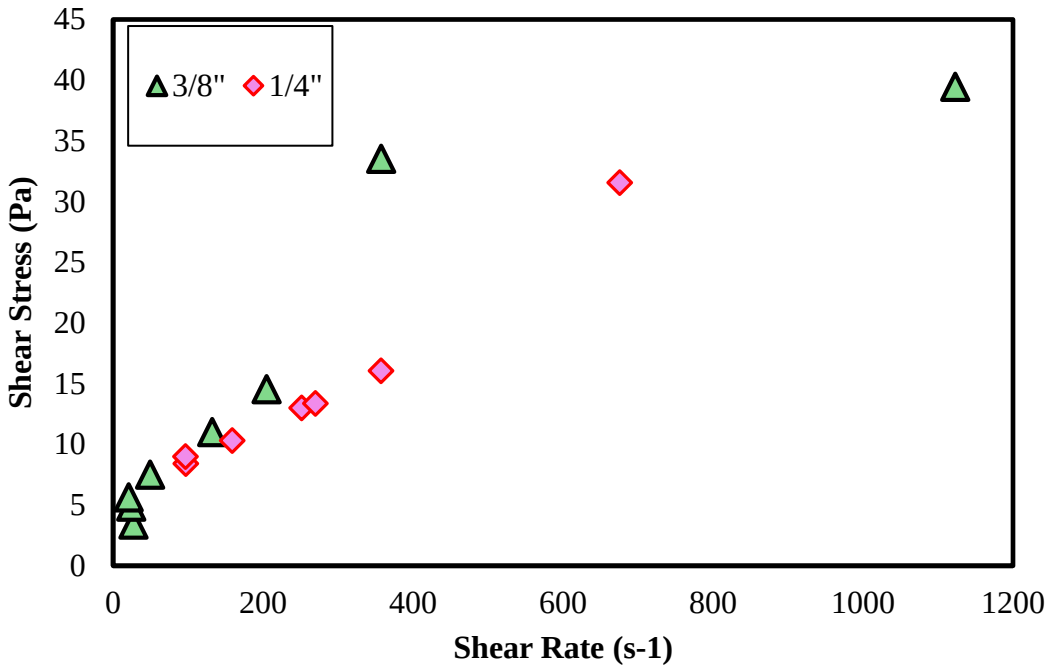

Fig. 34— Cartesian plot of shear rate and shear stress estimated from the flow test data for the emulsion in 3/8" and 1/4" pipe.

Table 9—Emulsion viscosity

Emulsion	μ (cP) Day 0	μ (cP) Day 1
3.5% TX 100 + 3.4 % Span 80	192.77	202.80
3.6% TX 100 + 3.5% Span 80	187.65	187.74

It should be noted that a new emulsion was prepared to run the rheological test. The base oil used in this case was oil D which is very similar to oil A2 used to create the first batch of the 30% water emulsion. These base oils have the same origin and are both Texas oil. The surfactant blend of the new emulsion varies slightly from the first one as shown in **Table 9**. The viscosity of both emulsions is very similar and both are identical as far as their behavior is concerned.

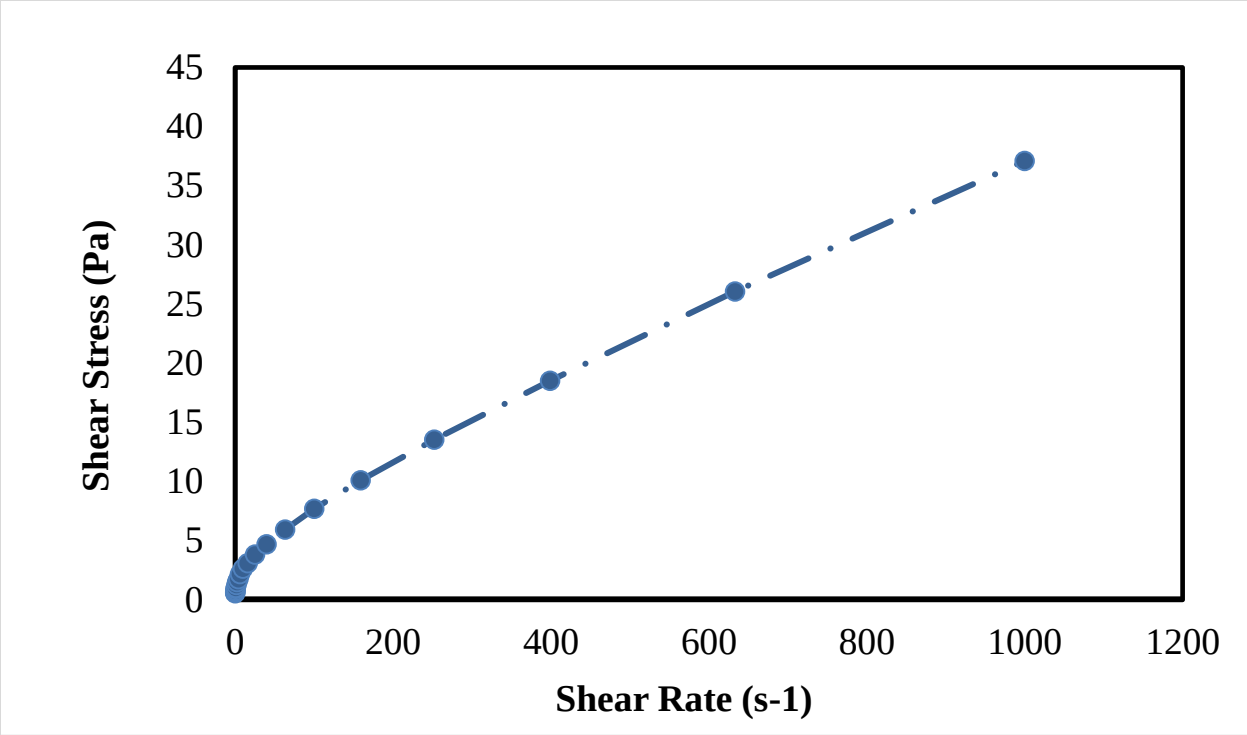

Fig. 35— Shear curve of the emulsion from Anton Paar rheometer

The emulsion rheological behavior was investigated using Anton Paar rheometer MC75. The results of the rheometer are presented as curves of shear stress (τ) vs shear rate (γ) shown in **Fig. 35**.

From the figure above, the emulsion follows a shear thinning behavior. The Non-Newtonian behavior is confirmed. Shear thinning fluids are commonly described by the power law model as mentioned earlier and the expected trend of shear rate and shear stress for these type of fluids is shown in **Fig. 36**. The flow behavior index n is less than 1 for shear thinning fluids.

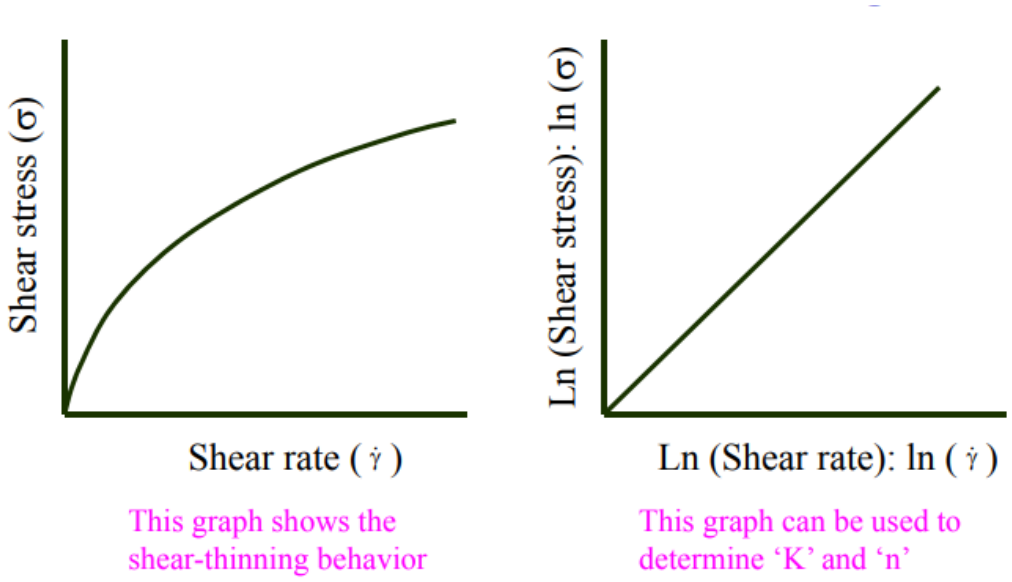

Fig. 36— Expected Flow behavior for a shear thinning fluid (pnl.org): on a cartesian plot (left) and on a Ln-Ln plot (right).

It is observed that the rheometer data, obtained in Fig.35 is similar to the behavior described in Fig. 36. Therefore, the emulsion is Non-Newtonian. Thus the next step is to obtained the parameters that are used to describe the fluid following the power law model. In order to obtain the n and k parameters for the emulsion from the shear curves using rheometer data, a ln-ln plot is generated (**Fig. 37**). The result of this plot is expected to be a straight line as shown in **Fig 36.** However, a quick look at these results from the rheometer clearly shows that the data doesn't fit the power law model as the Ln-Ln plot of the shear rate and shear stress do not follow a linear trendline. The results of **Fig.37** is indicating that the power law fit is not suitable for all fluids in particular for the emulsion under investigation. It is necessary to understand the cause of such behavior.

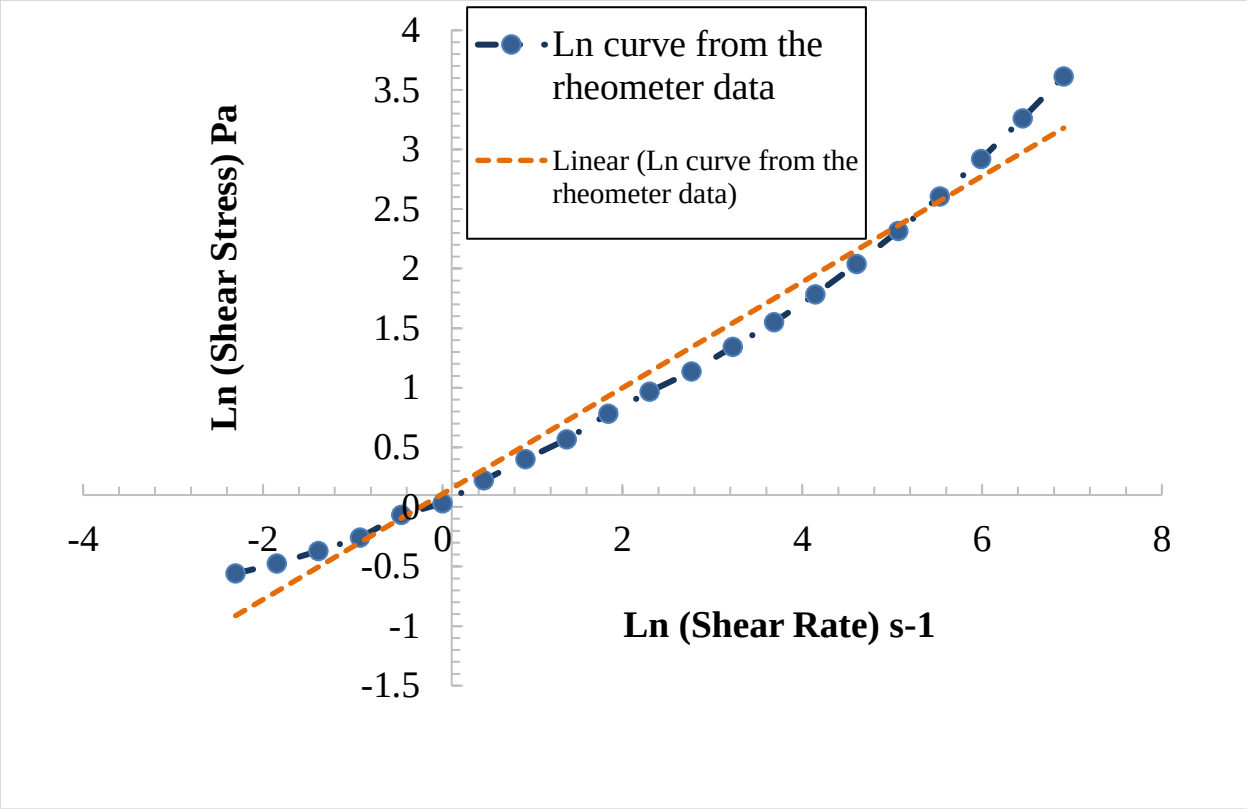

Fig. 37—— Power law model fit for the emulsion using from the rheometer

The shear rate and shear stress were then compared with the experimental data from the flow test (ΔP, V) for both pipe diameter 1/4" and 3/8" assuming n=1. The results were compared with the shear curve from the rheometer as shown in **Fig 38.**

It is observed that the shear rate and shear stress from both 1/4" and 3/8" diameter pipe follow the trend of the rheometer data when plotted on a logarithmic scale. The 1/4" diameter matches the data perfectly from shear rate of 100 to 800 s^{-1}. Therefore, we focus on the 1/4" data for further comparison in the initial analysis.

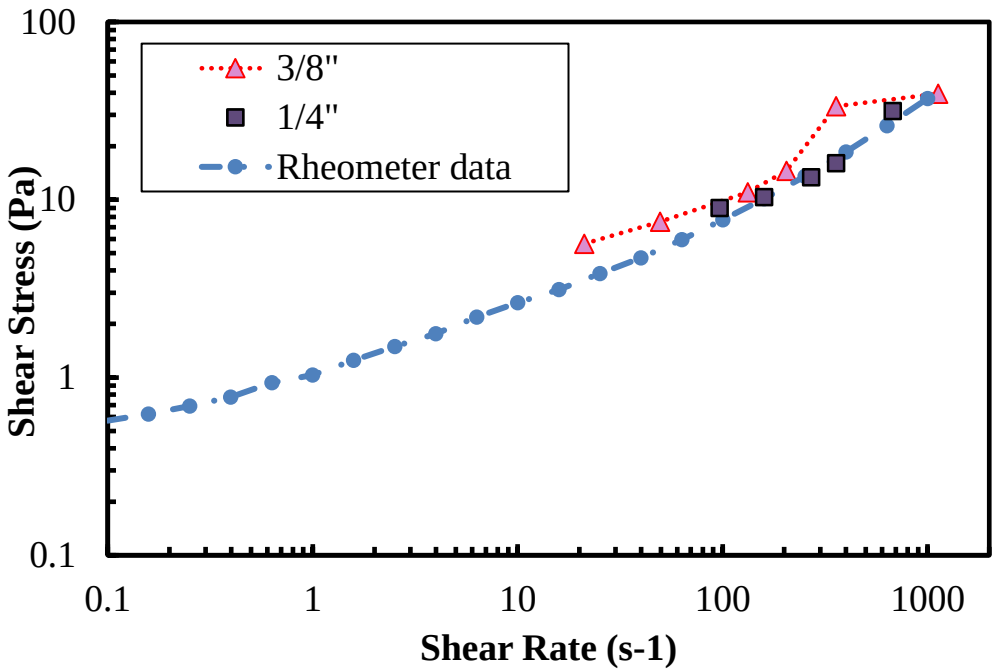

Fig. 38—— Comparison between the rheogram and the flow curves of the flow test of the emulsion.

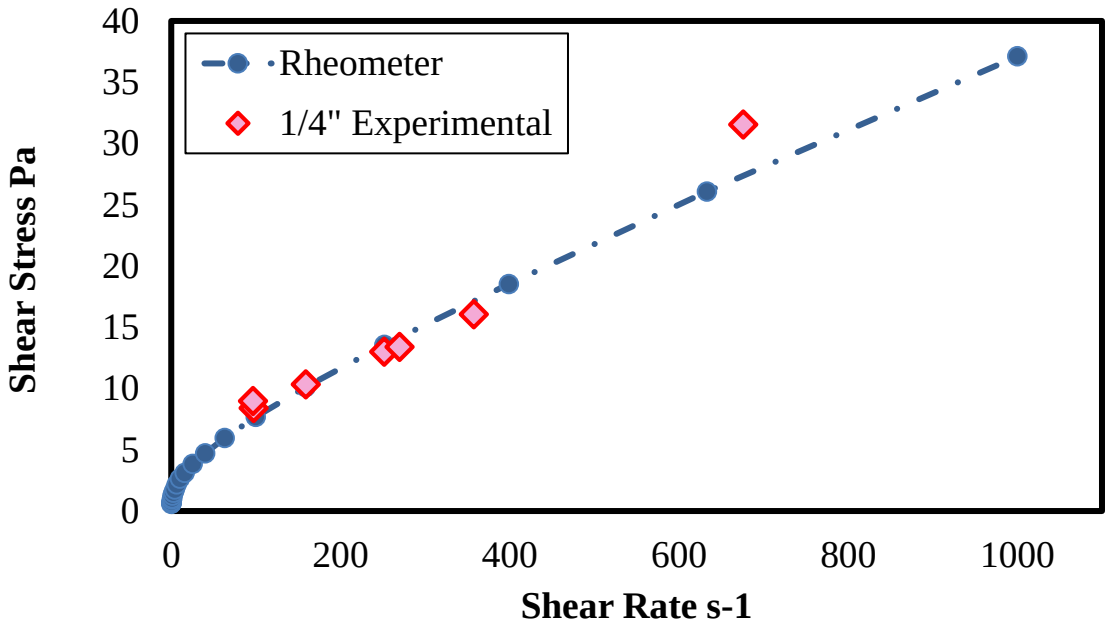

Fig. 39— Cartesian plot of shear rate and shear stress from flow test and rheometer.

The Cartesian plot of the 1/4" pipe and the rheometer shear curve maintains a very close match **Fig.39.**

5. Effect of the deviation from the Power Law model on the rheology of emulsion

The emulsion demonstrated a Non-Newtonian behavior and follow the trend of the rheometer data. Given that power law is the only model used to evaluate the rheology of emulsions, we decided to investigate the impact of the deviation from power law model on the rheological behavior. From the rheological data, as shown in **Fig.40**, we identified 3 ranges for the data: high shear, medium shear and low shear. For comparison purposes, here are the shear rate range used:

- High shear: 300- 1000 s^{-1}
- Medium shear: 10- 25 s^{-1}
- Low shear: 0.1- 0.251 s^{-1}
- Full range: 1.5 - 1000 s^{-1} (poor fit)
- Non-Power Law (polynomial equation)

In the medium shear range, the viscosity obtained from the capillary viscometer is close to the viscosity obtained from the rheometer. The medium shear range will be considered as capillary viscometer range for simplification. The parameters obtained from **Figs.41**-**43** are listed in **Table 10**. In addition to using these parameters to see its impact on pressure/rate relationships, we captured the full range of data using a polynomial equation for shear stress as a function of shear rate. We call that, non-power law/full range; the polynomial equation is shown in **Fig. 40**.

Table 10— Rheological parameters

Emulsion Shear	n	K
High shear	0.756	0.313
Medium shear	0.4061	1.0271
Low shear	0.2038	0.9113
Full range shear	0.5133	0.8261

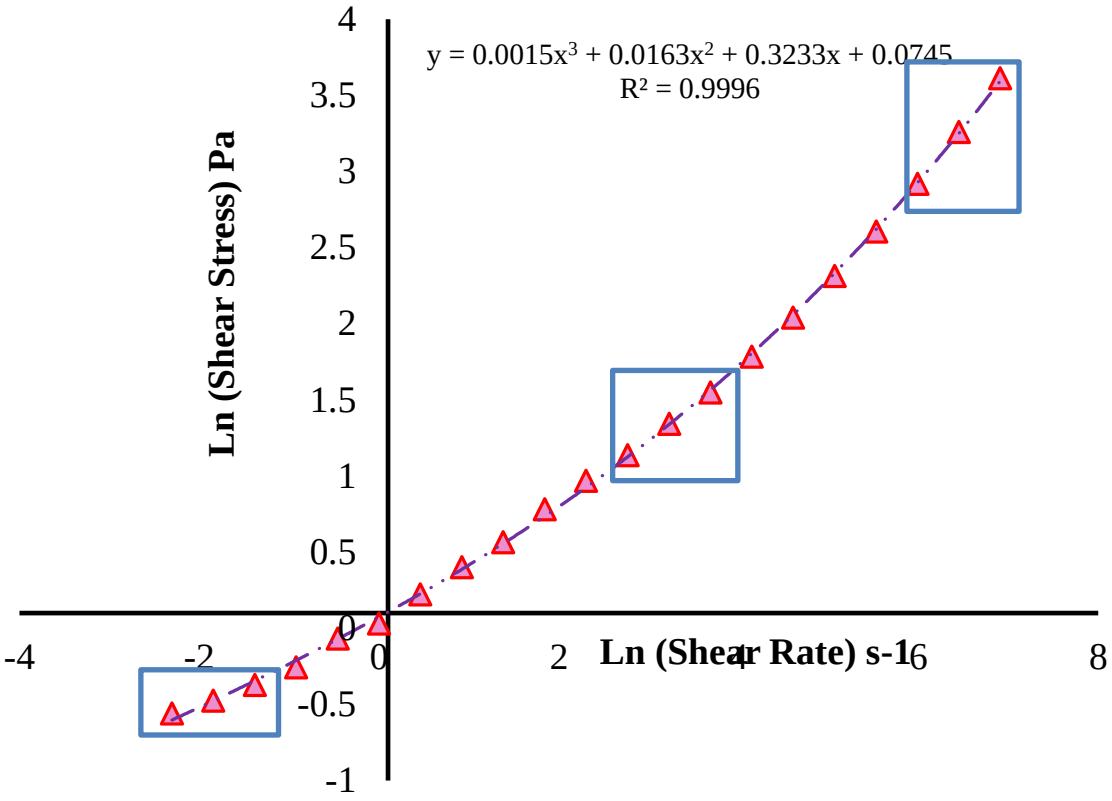

Fig. 40—Ln-Ln plot of the shear stress and shear rate from the rheometer data

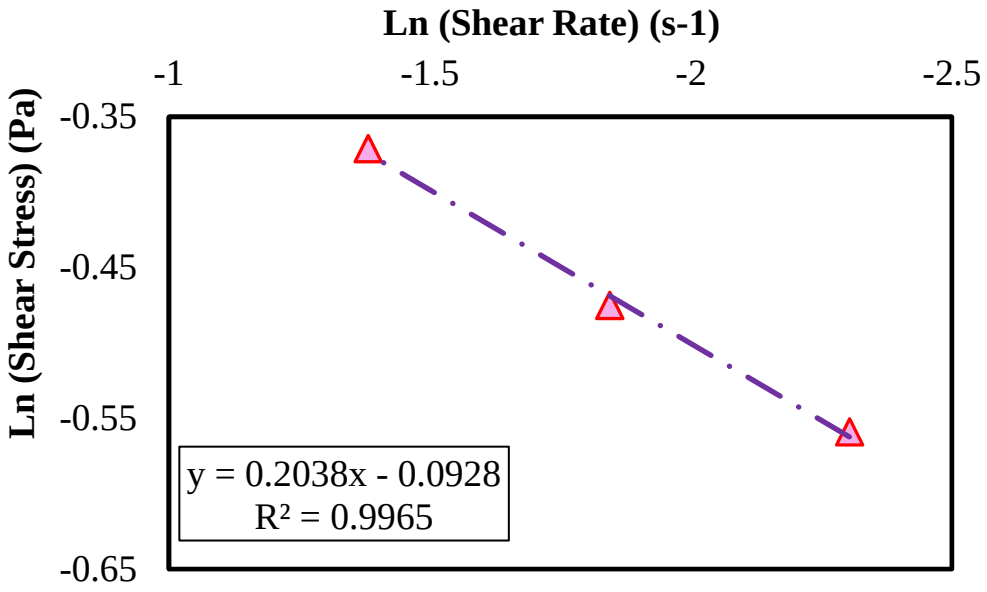

Fig. 41— Ln-Ln plot of the shear stress and shear rate from the rheometer data at low shear

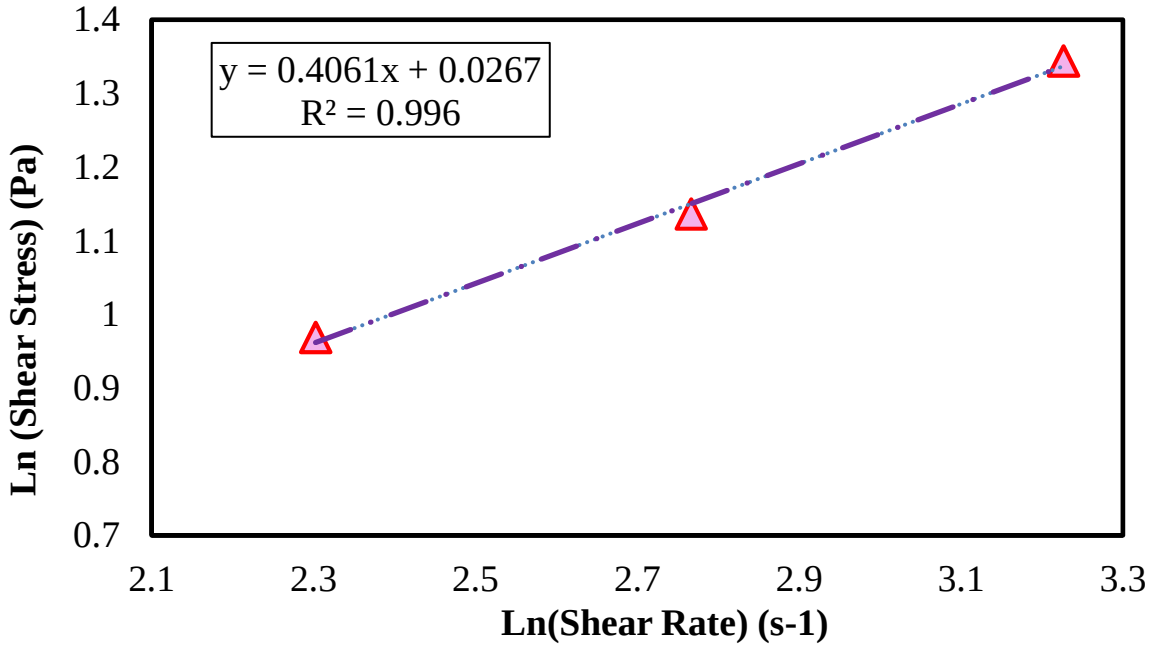

Fig. 42— Ln-Ln plot of the shear stress and shear rate from the rheometer data at medium shear(Capillary Viscometer)

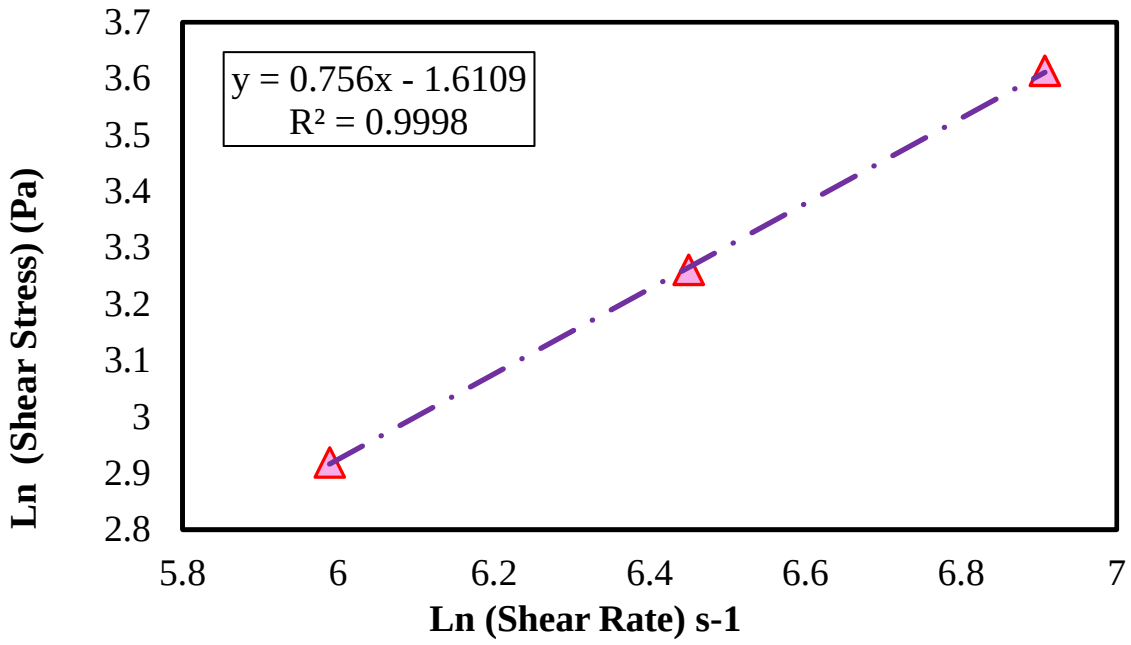

Fig. 43— Ln-Ln plot of the shear stress and shear rate from the rheometer data at high shear

6. Verification of the impact of the deviation from the Power Law model

In order to test the real-life application of the rheometer and compare its efficiency to that of the rotational viscometer, the parameters obtained from the rheometer were used to estimate the pressure drop in a hypothetical pipe. The characteristics of the hypothetical pipe of 500 ft was selected to replicate field conditions and are listed in **Table 9** below.

Table 11— Hypothetical 4" pipe characteristics

OD = 0.1016 m ID = 0.09 m	L = 152.4 m Q= 10 - 2000 bbl/d	ε = 0.00862 m

For each of the 4 cases of power law parameters described earlier, and for the polynomial function case, the flow rate was transformed into an equivalent shear rate, then the appropriate equation was used to calculate the shear stress depending on the model being used. Eventually, the pressure drop was calculated from shear stress. It is important to note that polynomial fit was used has a

hear rate varying from within 0.5 -100 s^{-1} and the experimental shear rate obtained is between 0.1-1000 s^{-1}; The polynomial fit I within the range of the experimental data. The use of the polynomial fit is not describing the relation between shear rate and shear stress through a correlation. It is one way to express the exact relationship within the range in order to capture the behavior in that same range. The result for the pressure drop as a function of flow rate for the various models is shown in **Fig. 44**. It shows that when low shear-range data is used, pressure can be highly underestimated. Another observation is that when high shear-rate rheometer data is used, pressure is underestimated for low flow rates and overestimated for high flow rates. The use of the full range of data while keeping a forced fit to the power law model results in further over-estimation of pressure. It is interesting to note however, that the use of the data in the range of the capillary viscometer results in the closest match to the pressure estimated from the capturing the exact correlation between shear rate and shear stress. The pressure difference might not be too large in this specific example, but considering longer pipes transporting emulsions at higher rates, the pressure difference can be significant.

These results show that the use of the power law model with the full range of rheometer data can be misleading; note that this is a common practice in evaluating emulsions. We now have direct evidence of why some companies elect to quantify emulsion viscosity using capillary viscometers. Note that in addition to the limitation we indicate, rotational rheometers can change the rheology of an emulsion. In our case however, the emulsion was stable-enough not to be affected by the rotation (**Fig. 45**). Although capillary viscometers do not provide access to non-Newtonian behavior characterization, our data indicates that it could be possible to use two different ranges of capillary viscometers to capture the behavior.

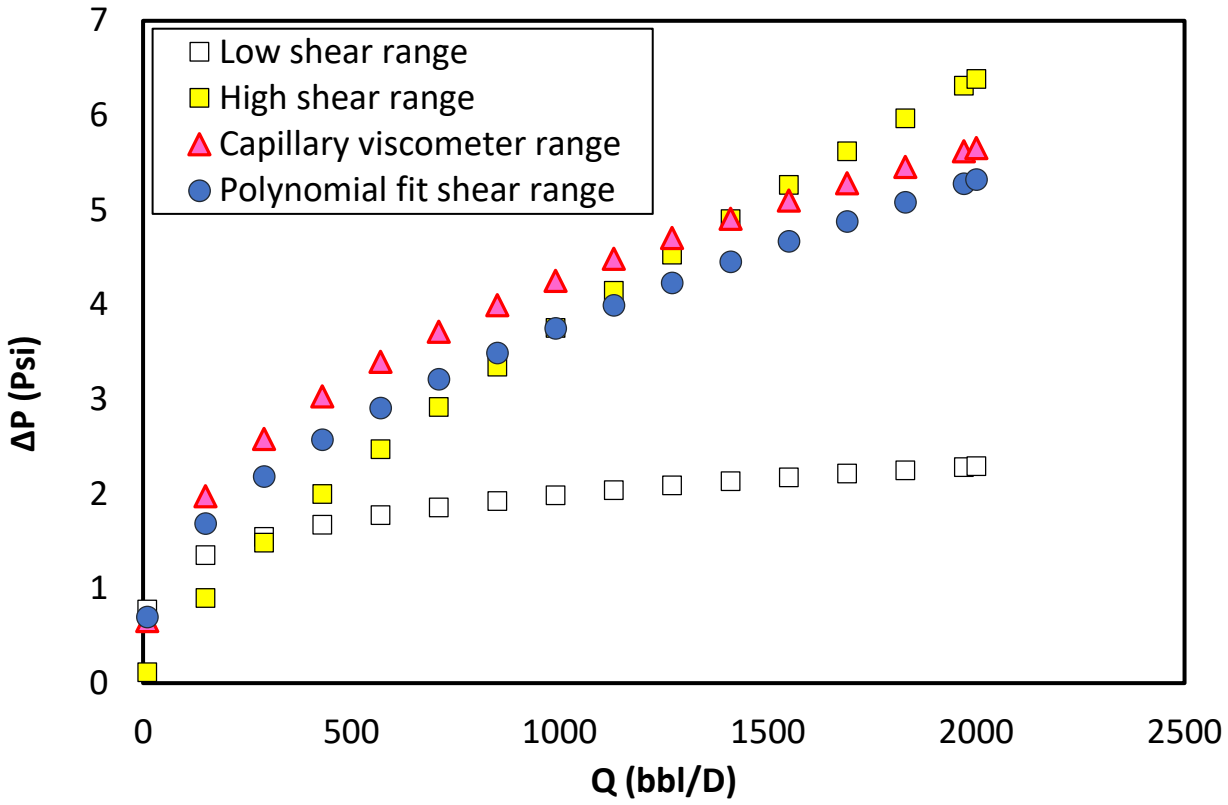

Fig. 44— Estimation of ΔP from the n and k parameters of rheometer for different shear range

In to analyze the 3/8" flow data in light of these findings, we decided to explore the relationship between shear rate and velocity. This relationship for Non-Newtonian fluids is dependent on the value of "n". Taking the actual measured velocity data and pressure data, we calculated the shear stress from pressure, we then calculated shear rate from the exact polynomial fit of the rheometer data (representing the true relationship between shear stress and shear rate for this fluid). We then plotted the shear rate and velocity, which gave a straight line as shown in **Fig. 46**. The slope of that line is 1446 (1/m). The slope in the case of a Newtonian fluid (8/D) would have been 1032 (1/m). The factor to correct for non-Newtonian behavior is thus 1.4, which is equivalent to an "n" value of 0.38446 if the following equation is to be use:

$$\gamma = \frac{8V}{D}\left(\frac{1+3n}{4n}\right) \tag{37}$$

Performing the same analysis for the ¼" pipe, we identify an "n" value of 1.37; a value larger than 1. These results go to show the limitation of the power law in describing the behavior of emulsions. Based on these results, in the next chapter, we outline our conclusions and recommendations for further work and best practices in this regard.

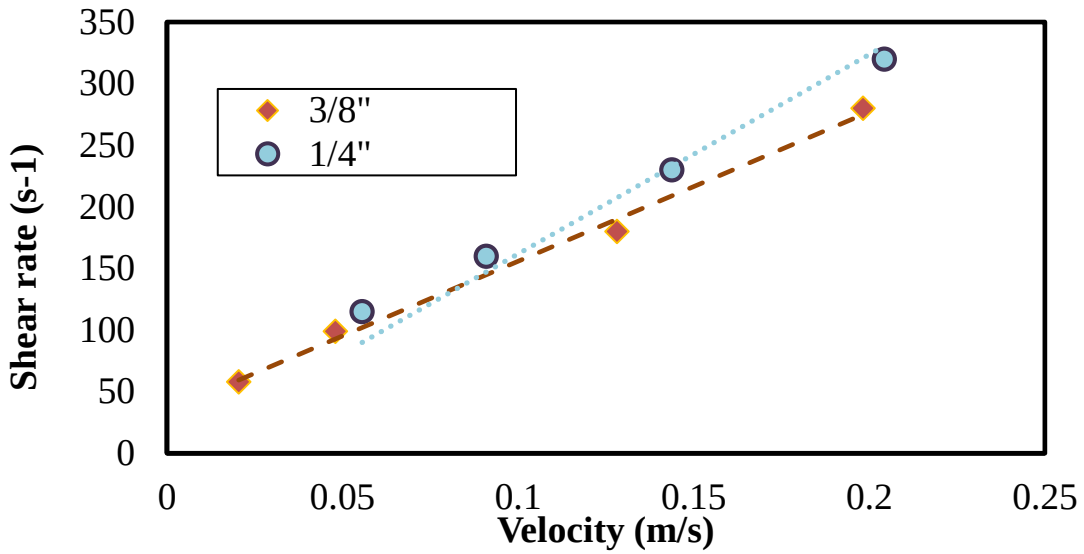

Fig. 45—— Verification of the relationship between shear rate and velocity for 3/8"

Chapter V: Conclusion and Recommendations

In this study, the flow and rheology of water-in-crude oil emulsions were investigated.

First, using a laboratory scale flow loop, a single phase flow test was performed with deionized water, crude oil A1 and crude oil C. Through the single phase flow the capacity of the equipment to handle subsequent experimental work was confirmed. Second, a stable emulsion was prepared at 30% water cut and was tested through a Cannon Fenske capillary viscometer and an Anton Paar MCR 75 rheometer. In addition, the shear rate and shear stress were both generated from the flow test performance and from the rheometer.

The focus was to compare and analyze the possible divergence between the two tests. The following are the conclusion derived from this research:

- In searching for the blend of surfactants that yield a stable emulsion, a technique needs to be identified to mitigate the loss of oil during trials. Although a 1% span 85 was perfect for the Texas Crude Oil batch received in 2016 with a 20 to 60-cp viscosity, the new oil received in 2018 needed a blend of TX100 and Span 80 to establish stability. An attempt to correlate this with HLB was made which guided us to reduce the number of trials needed, however, more work is required to establish better correlations that can be generalized to more oil types.
- The rheology of the water-in-oil emulsion presented in this study cannot be estimated using the power law model. This forced-fit of this model can result in over-estimating the pressure required during transport in most cases.
- The analysis of the equation describing the shear rate as a function of velocity for non-Newtonian fluids failed the test of our experimental data for flow in ¼ and 3/8” pipes. One

"n" value can't describe the flow of the same emulsion in both pipes. This lends itself to yet another project one can undertake.

- The use of capillary viscometers in characterizing the rheology of emulsions is possible. The use of one viscometer range would not capture the non-Newtonian behavior, but the development of a methodology of using two ranges of viscometers to capture the behavior seems highly possible.

References

Abdurahman, H. S., R. M. Yunus and Anwaruddin H. 2008. Stabilization Mechanism of Water-in-Crude Oil Emulsion.Journal of Applied Sciences, Vol. 7, 571-1575.https://doi.org/10.3923/jas.2007.3512.3517.

Al-Yaari, M., Al-Sarkhi, A., Hussein, et al. 2013. Pressure Drop Reduction of Stable Water-in-Oil Emulsion Flow: Role of Water Fraction and Pipe Diameter, International Petroleum Technology Conference, Beijing, China, 26-28 March.https://doi.org/10.2523/IPTC-16883-MS.

Angeli, P., "Droplet Size in Two-Phase Liquid Dispersed Pipeline Flows" Chem. Eng. Tech., 24(4), 431-434 (2001).

Ashrafizadeh S.N., Motaee E. and Hoshyargar V. 2012. Emulsification of Heavy Crude Oil in Water by Natural Surfactants. Journal of Petroleum Science and Engineering, 86–87, 137–143.

Ashrafizadeh, S.N. and Kamran, M. 2010. Emulsification of Heavy Crude Oil in Water for Pipeline Transportation. Journal of Petroleum Science and Engineering, Vol. 71, Isssues 3-4, 205 – 211. https://doi.org/10.1016/j.petrol.2010.02.005.

Barth T.,Høiland S.,Fotland P. et al. 2005.Relationship Between The Content Of Asphaltenes And Bases In Some Crude Oils, Energy Fuels, 19 (4), 1624–1630, Bergen Norway,https://doi.org/10.1021/ef049750a.

Becher, P. 1957.Emulsions: Theory and Practice. Reprint,New York: Robert E. Krieger Publishing.

Bhardwaj A. and Hartland S. 1998. Studies on Build up of interfacial film at the crude oil / water interface. Journal of Dispersion Science and Technology. 19. 465-473.https://doi.org/10.1080/01932699808913189.

Boukadi F., Singh V., Trabelsis R. et al. 2012. Appropriate Separator Sizing: A Modified Stewart and Arnold Method. Modelling and Simulation in Engineering.Volume 2012, Article ID 721814.http://dx.doi.org/10.1155/2012/721814.

Brandal, Ø., Hanneseth A.-M. D., Hemmingsen P.V.et al. 2006. Isolation and Characterization of Naphthenic Acids from a Metal Naphthenate Deposit: Molecular Properties at Oil-Water and Air-Water Interfaces. Journal of Dispersion Science and Technology. 27 (3). 295-305.https://doi.org/10.1080/01932690500357909

Brauner, N. and A. Ullmann, "Modeling of Phase Inversion Phenomenon in Two-Phase Pipe Flow", Int. J. Multiphase Flow, 28, 1177–1204 (2002).

Brinkman H.1952. The Viscosity of Concentrated Suspensions and Solutions. J. Chem. Phys. 20 (4), 571–584.

Calabrese P.V.,Chang T.P.K. and Dang P.T. 1986. Drop Breakup in Turbulent Stirred-Tank Contactors. Part I: Effect of Dispersed-Phase Viscosity. AIChE,3(2) () 657.https://doi.org/10.1002/aic.690320416.

Cengel J. A., Faruqui A. A., and Finnigan J. W. et al.1962. Laminar and Turbulent Flow of Unstable Liquid-Liquid Emulsions. AIChE J., 8(3), 335.

Charles M., Govier G.W. and Hodgson G. W. 1961. The Horizontal Flow of Equal Density Oil-Water Mixtures. Can. J. Chem. Engng., 39, 27-36.

Dan D., and Jing G. 2006. Apparent Viscosity Prediction Of Non-Newtonian Water-In-Crude Oil Emulsions, Journal of Petroleum Science and Engineering,Volume 53, Issues 1–2,113-122,ISSN 0920-4105,https://doi.org/10.1016/j.petrol.2006.04.003.

Darby R., "Chemical Engineering Fluid Mechanics" Marcel Dekker, Inc. (1996).

Dodge D.W. and Metzner A.B.1959.Turbulent Flow of Non-Newtonian Systems, AIChE J., 5(2), 189-204 (1959).

Dol S. S.,Chan M. S,Wong S. F. et al. 2016. Experimental Study on the Effects of Water-in-Oil Emulsions to the Pressure Drop in Pipeline Flow (Version 10007627), World Academy of Science, Engineering and Technology, International Journal of Chemical and Molecular Engineering.Vol:10,No:12. http://doi.org/10.5281/zenodo.1131613.

EinsteinA.1906. Eine neue bestuimmung der molekulardimensionen. Ann. Phys. 9, 289–306.

Fan T. 2001.Viscosity Measurement Using CANNON-FENSKE Viscometers,October 26,http://www.prrc.nmt.edu/groups/petrophysics/media/pdf/viscometer.pdf.

Gomez S. 2018.MS Thesis. *Experimental Characterization of Brine in Crude Oil Emulsions and Its Performance in Artificial Lift Systems*. University of Oklahoma, Norman, Oklahoma, (2018).

Griffin, W.1949. Classification of Surface-Active Agents By HLB. Journal of Cosmetic Science, 1, 311-326.http://journal.scconline.org/contents/cc1949/cc001n05.html.

Hawkins watts. https://www.hawkinswatts.com/wp-content/uploads/2016/01/Hawkins-Watts-HLB-Balance.pdf.

Henríquez, C. J. 2009. W/O Emulsions: Formulation, Characterization and Destabilization. Ms Thesis, Technischen Universität Cottbus zur Erlangung, Caracas (February 2002).

Hesketh, P., F. Russell and A. Etchells, "Bubble Size in Horizontal Pipelines", A.I.Ch.E. J., 33(4), 663-667, (1987).

Hinze, J., 1995. Fundamentals of the Hydrodynamic Mechanism of Splitting in Dispersion Processes. AIChE, 1 (3), 289–295.https://doi.org/10.1002/aic.690010303.

ICI Americas Inc. 1976. The HLB System A Time-Saving Guide to Emulsifier Selection.Revisited 1980. Wilmington, Delaware: ICI Americans Inc.

Isaacs E. E., Chow R.S. 1991. Practical Aspects of Emulsion Stability in Emulsions Fundamentals and Applications in the Petroleum Industry, Chap. 2, 51-77. Alberta, Canada: Advances In Chemistry Series.

Johnsen E. E, and Rønningsen H. P., 2003.Viscosity Of 'Live' Water-In-Crude-Oil Emulsions: Experimental Work And Validation Of Correlations, Journal of Petroleum Science and Engineering,Volume 38, Issues 1–2, 23-36, ISSN 0920-4105,https://doi.org/10.1016/S0920-4105(03)00020-2.

Joses T. J., Neustadter E.L, Whittingham K.P et al. 1978. Water-In-Crude Oil Emulsions Stability and Emulsion Destabilization by Chemical Demulsifiers. Journal of Canadian Petroleum Technology . 7(2) April-June, 100-108.http://dx.doi.org/10.2118/78-02-08.

Kilpatrick, P. K. 2012. Water-in-Crude Oil Emulsion Stabilization: Review and Unanswered. Energy & Feuls, 26(7), pp 4017–4026. ,30 May.https://doi.org/doi:10.1021/ef3003262.

Kokal, S. 2005. Crude Oil Emulsions: A State-Of-The-Art Review. SPE Production and Facilities, 20 (01),SPE 77497-PA.http://dx.doi.org/10.2118/77497-PA.

Kubie and Gardner G.C. 1977. Drop Sizes and Drop Dispersion in Straight Horizontal Tubes and in Helical Coils, Chem. Eng. Sci., 32 (2), 195–202.https://doi.org/10.1016/0009-2509(77)80105-X.

Leone G.,Delfini M., Di Cocco M.E. et al. 2008. The Applicability Of An Amidated Polysaccharide Hydrogel As A Cartilage Substitute: Structural And Rheological Characterization, J. Mater. Sci. Mater. Med. 19 (8) (2008) 2873–2880.

Lim J.S., Wong S.F., Law M.C., et al. 2015. A Review on the Effects of Emulsions on Flow Behaviours and Common Factors Affecting the Stability of Emulsions. Journal of Applied Sciences, 15: 167-172.ISSN 1812-5654.http://dx.doi.org/10.3923/jas.2015.167.172.

Lunde M. B. 2017. Rheology and Flow Properties of Water-in-Oil Emulsions - Comparing Measured Flow Rates to Predicted Flow Rates Based on the Rheological Results From the Laboratory. MS Thesis, Norwegian University of Science and Technology, Trondheim (June 2017) .

McLean J. 1997. Effects of Asphaltene Aggregation in Model HeptaneToluene. Journal of Colloid and Interface, 196, pp 23-34.

Metzner, A.B. and M.G. Park, 1964.Turbulent Flow Characteristics of Viscoelastic Fluids. Journal of Fluid Mechanics, 20(2), 291-303.http://dx.doi.org/10.1017/S0022112064001215.

Mohammed, S.2009. Characterization and Rheology of Water-in-Oil Emulsion from Deepwater Fields. MSc. Thesis, Rice University, Houston, Texas (2009).

Nadler, M. and Mewes D.1997. Flow Induced Emulsification In The Flow Of Two Immiscible Liquids In Horizontal Pipes. International Journal of Multiphase Flow,Volume 23, Issue 1, February,55-68,https://doi.org/10.1016/S0301-9322(96)00055-9.

Oliveira M. C K.,Miranda L. R. O., Carvalho A. B. M., et al. 2018. Viscosity of Water-in-Oil Emulsions from Different American Petroelum Institute Gravity Brazilian Crude Oils, Energy & Fuels, **32**, 2749-2759.

Oluwa I. 2016. MS Thesis. *Experimental Study of The Rheology And Stability Behaviour of Surfactant Stabilized Water-In-Oil Emulsion* .University of Oklahoma, Norman, Oklahoma,(2016).

Omer A. 2009. *Pipeline Flow Behavior of Water-In-Oil Emulsions*, PhD thesis, University of Waterloo, Ontario.

Omer A. and Pal R. 2013. Effects Of Surfactant And Water Concentrations On Pipeline Flow Of Emulsions. Ind. Eng. Chem. Res., 52, 9099 – 9105.

Opawale A., O. S. 2013. Tools for Troubleshooting Emulsion Problems in Producing Oilfields. Presented at the SPE Production and Operations Symposium, Oklahoma City, Oklahoma, 23-26 March,USA, SPE -164512-MS .http://dx.doi.org/10.2118/164512-MS.

Otsubo, Y. and Prud'homme, R.K. 1994. Effect of Drop Dize Distribution on the Flow Behaviour of Oil-In-Water Emulsions. Rheologica Acta, Vol 33, 303–306.

Pal R.2000. Viscosity–Concentration Equation for Emulsions of Nearly Spherical Drops. J. Colloid Interface Sci. 231, 168–175.

Pal, R. 1993 .Pipeline Flow of Unstable and Surfactant Stabilized Emulsions, AIChE J., November , 39 (11), 1754-1764.https://doi.org/10.1002/aic.690391103.

Pal, R., 1987. Emulsions: Pipeline Flow Behavior, Viscosity Equations and Flow Measurement,PhD thesis, University of Waterloo, Ontario.

Plasencia J., Pettersen B., and Nydal O. J. 2013. Pipe flow of Water-in-Crude Oil Emulsions: Effective Viscosity, Inversion Point and Droplet size distribution.Journal of Petroleum Science and Engineering, 101,35-43.https://doi.org/10.1016/j.petrol.2012.11.009.

Pouplin A., Masbernat O., Decarre S., et al. 2010. Transition To Turbulence In A Dispersed Liquid-Liquid Horizontal Flow. In Proceedings of the 7th International Conference on Multiphase Flow ICMF 2010. Tampa, FL, USA.

Richardson E.G.1933. Uber Die Viskositat Von Emulsionen. KolloidZ. 65 (1), 32–37.

Rønningsen, H. 1995. Correlations For Predicting Viscosity Of W/O-Emulsions Based On North Sea Crude Oils. Presented at the SPE International Symposium on Oilfield Chemistry,San Antonio, Texas,14-17 February. SPE-28968-MS.https://doi.org/10.2118/28968-MS.

Russell, T.W.F., G.W. Hodgson and W. Govier, 1959.Horizontal Pipelines Flow of Mixtures of Oil and Water. The Canadian Journal of Chemical Engineering. , 1959, Vol.37(1),9-17. ISSN: 0008-4034.https://doi.org/10.1002/cjce.5450370104

Schramm, L.L. 1992. Emulsion: Fundamentals and Applications in the Petroleum Industry.Advances in Chemistry.Series-231.Washington DC.

Schubert, H., and Armbroster, H. 1992. Principles of Formation and Stability of Emulsions. International Chemical Engineering Series, No. 1, 14-28.

Silset, A.2008. Emulsions (w/o and o/w) of Heavy Crude Oils Characterization, Stabilization,Destabilization and Produced Water Quality. PhD Thesis, Norwegian University of Science and Technology, Trondheim (November 2008).

Sjoblom A.J..2016. .Emulsions and Emulsion Stability, Second edition. Norway: Taylor & Francis Group.https://doi.org/10.1201/9781420028089.

Som, S.K. and Biswas, G. 2003. Introduction To Fluid Mechanics And Fluid Machine, Second Edition.New Delhi: Tata McGraw-Hill.

Souto E.B. and Müller R.H.. 2006. The Use Of SLN And NLC As Topical Particulate Carriers For Imidazole Antifungal Agents, Pharmazie 61 (5),431–437.

Strassner J. E., 1968. Effect of pH on Interfacial Films and Stability of Crude Oil-Water Emulsions. Journal of Petroleum and Technology. March.https://doi.org/doi:10.2118/1939-PA.

Subramania D., May N. and Firoozabadi A. 2017. Functional Molecules and the Stability of Water-in-Crude Oil Emulsions. Energy & Fuels. 31. 10.1021/acs.energyfuels.7b01039.

Tadros F. T., 2016. Emulsions: Formation, Stability , Industrial applications , Berlin,Boston : De Gruyte .ISBN 978-3-11-045217-4.

Tatar C., Sumnu B.,., and Sahin , G. S. 2017. Rheology of Emulsions. In J. Ahmed, P. Ptaszek, & S. Basu , Advances in Food Rheology and Its Applications. Oxford: Woodhead Publishing Ltd.

Taylor G. 1932. The Viscosity of a Fluid Containing Small Drops of Another Fluid. Proc. R. Soc. Lond. 138, 42–48.

Tjoeng, A. Y. and Loro, R. 2016. Viscosity Modelling of Pyrenees Crude Oil Emulsions. Presented at the SPE Asia Pacific Oil & Gas Conference and Exhibition, Perth, Australia, 25–27 October, SPE-182326-MS, https://doi.org/10.2118/182326-MS.

Urdahl O., Fredheim A.O. and Loken K.-P. 1997. Viscosity Measurements of Water-In-Crude-Oil Emulsions under Flowing Conditions: A Theoretical and Practical Approch, Colloids and Surfaces A: Physicochemical and Engineering Aspects Volumes 123–124, 15 May ,623-634.Norway.https://doi.org/10.1016/S0927-7757(96)03801-0.

Whorlow R.W. 1980.Rheological Techniques, England, Chichester: Ellis Horwood Ltd, M. Laso, L. Steiner and S. Hartland, Chem. Eng. Sci., 42(10) (1987) 2429.

Wilkes J., “Fluid Mechanics for Chemical Engineers” Prentice Hall, inc. (1999).

Zaki N.N. 1997. Surfactant Stabilized Crude Oil-in-Water Emulsions for Pipelines Transportation of Viscous Crude Oils. Colloids and Surfaces A: Physicochemical and Engineering Aspects, **125** (1), 19-25.https://doi.org/10.1016/S0927-7757(96)03768-5.

Appendix A: Experimental Data & Plots

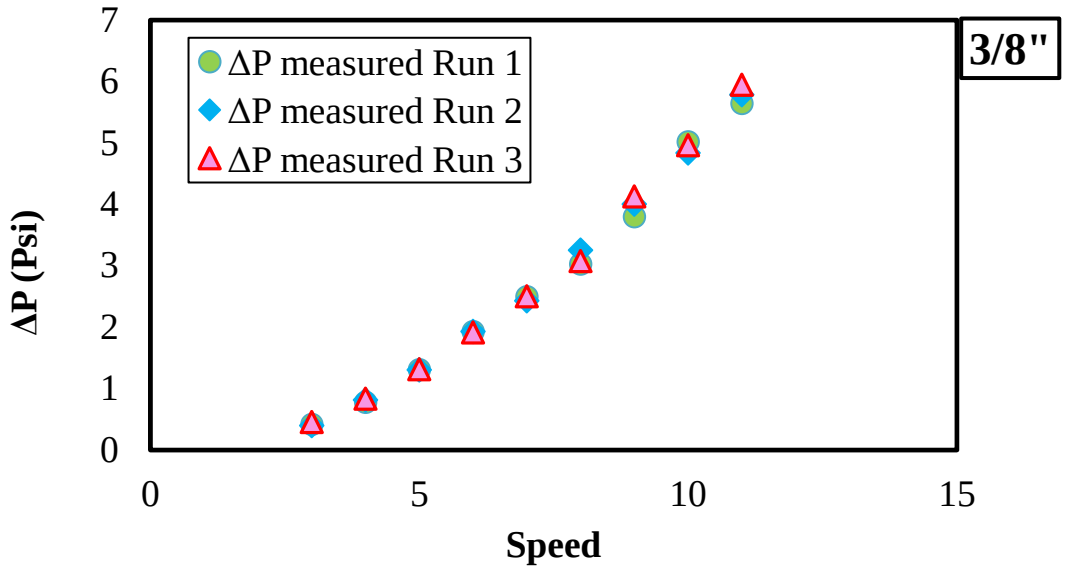

Fig. A.1— Reproducibility of measured pressure for water 3/8" considering the pump speed

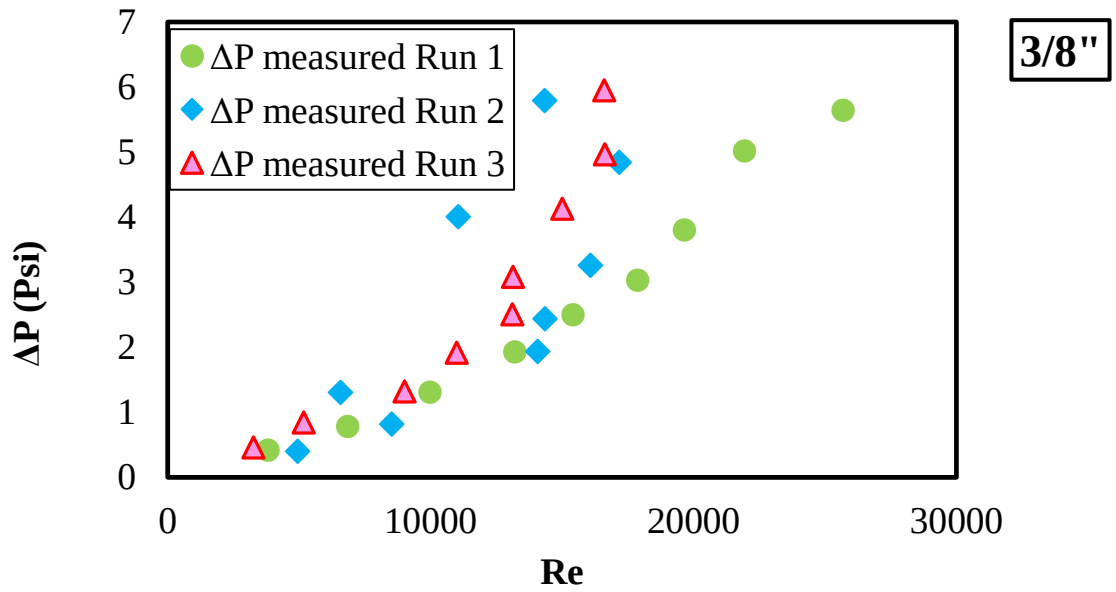

Fig. A.2— Reproducibility of measured pressure for water 3/8" with Reynolds Number

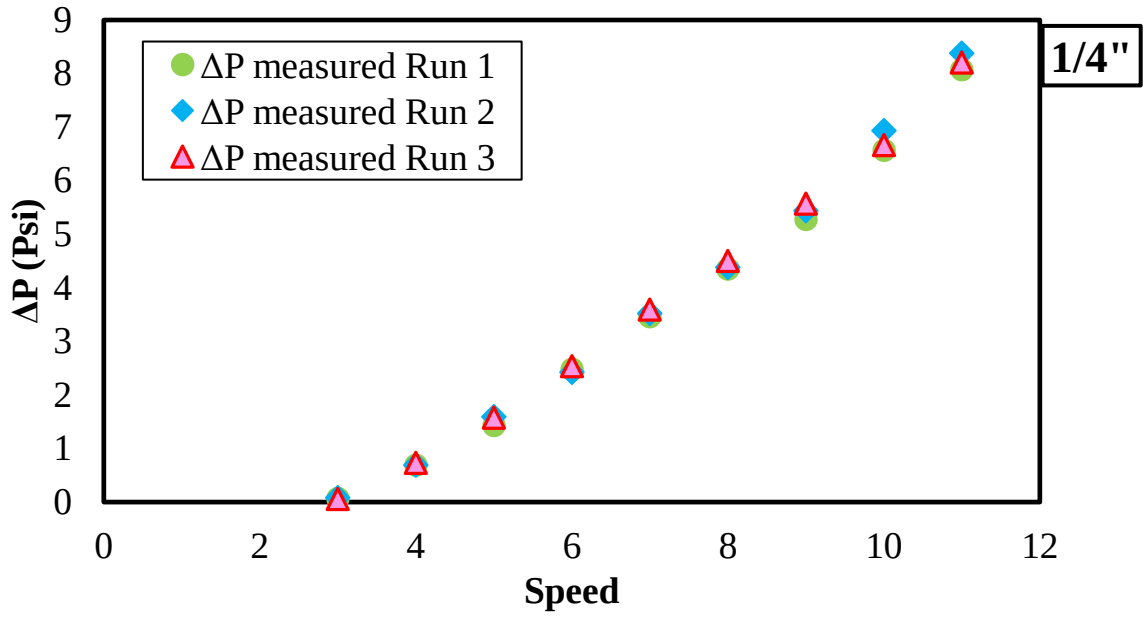

Fig. A.3— Reproducibility of measured pressure for water 1/4" considering the pump speed

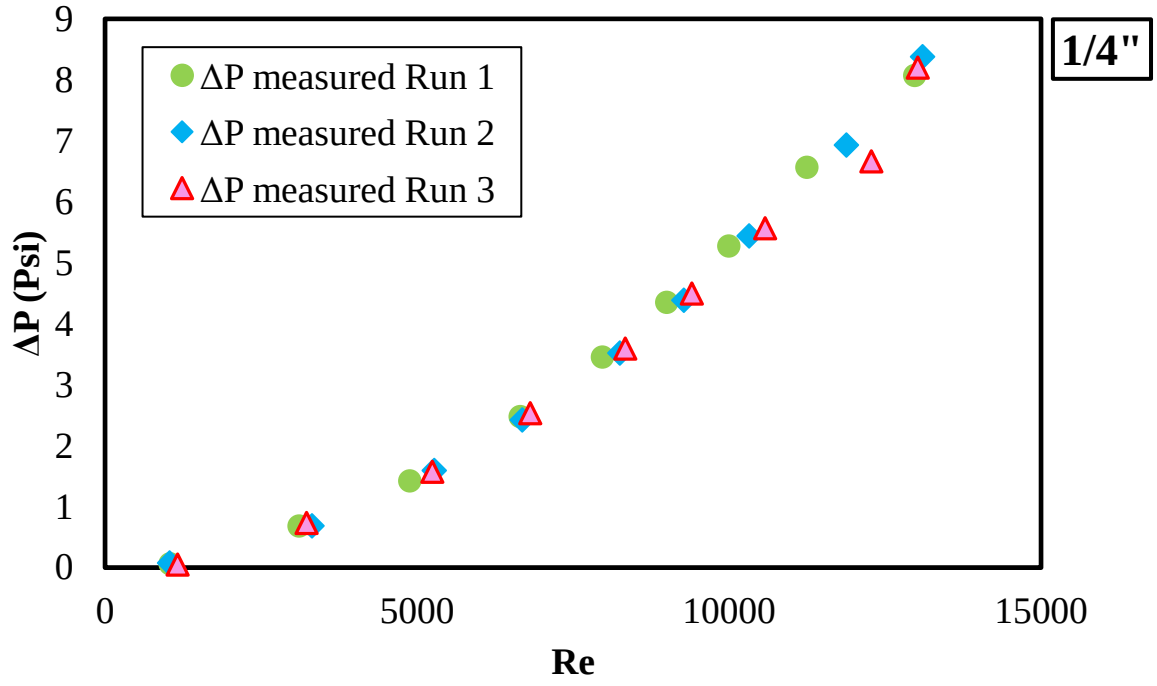

Fig. A.4— Reproducibility of measured pressure for water 1/4" with Reynolds Number

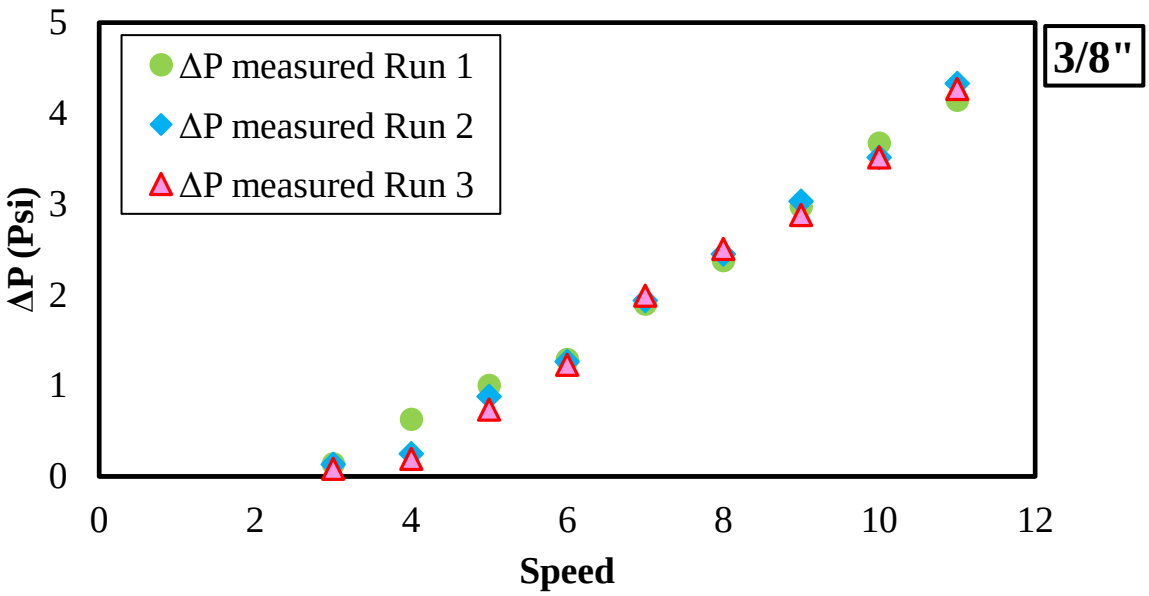

Fig. A.5— Reproducibility of measured pressure for crude oil A1 3/8" considering the pump speed

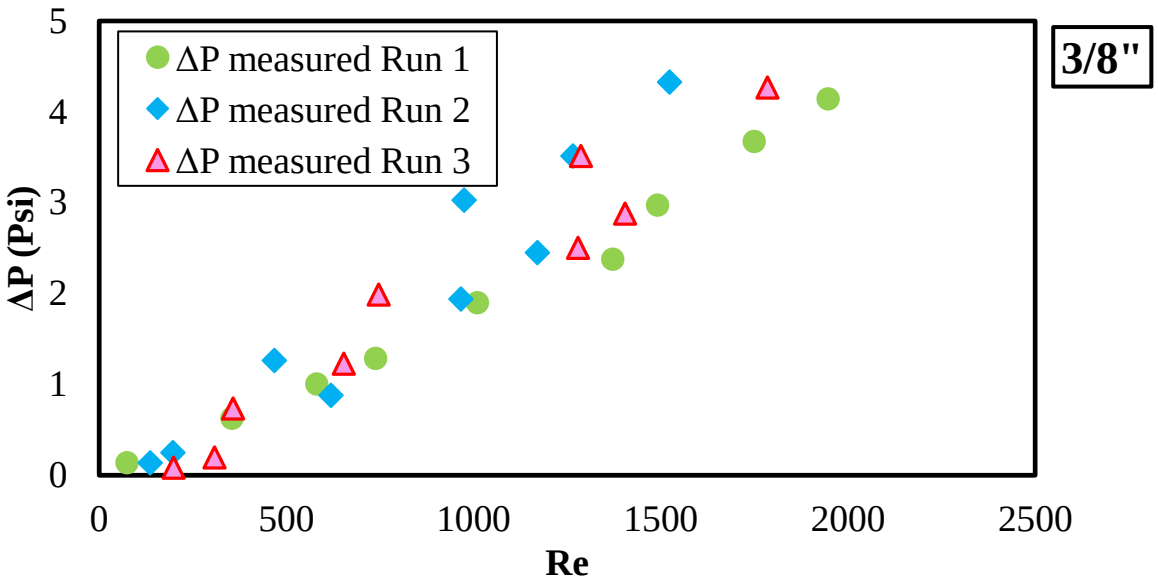

Fig. A.6— Reproducibility of measured pressure for crude oil A1 3/8" with Reynolds Number

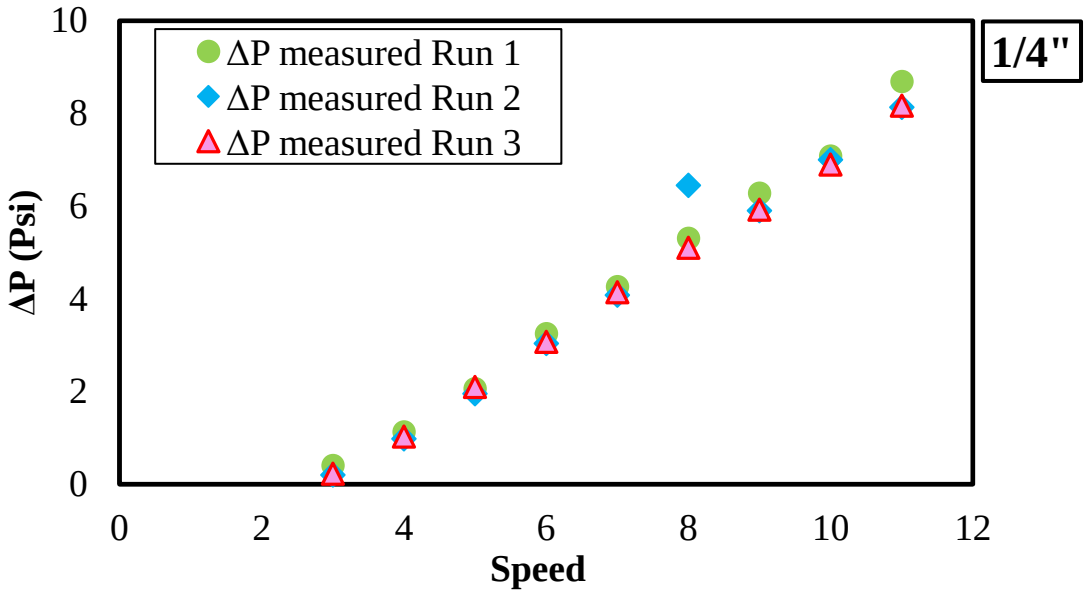

Fig. A.7— Reproducibility of the measured pressure for crude oil A1 for 1/4"

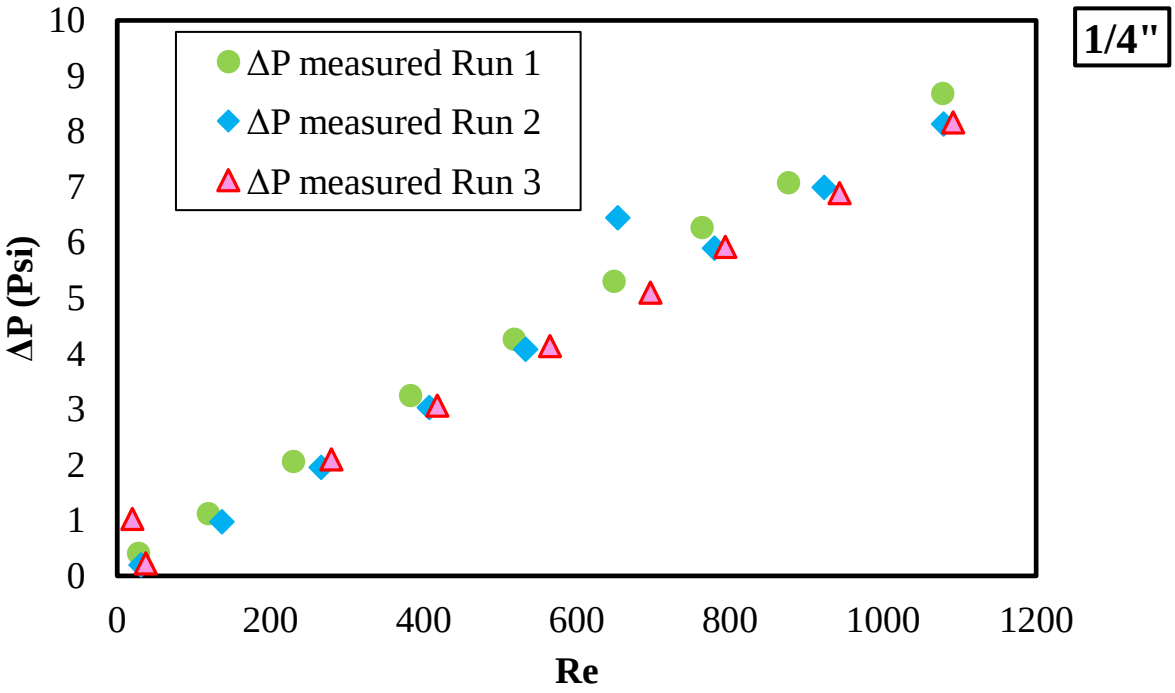

Fig. A.8— Reproducibility of the measured pressure for crude oil A1 for 1/4" with Reynolds Number

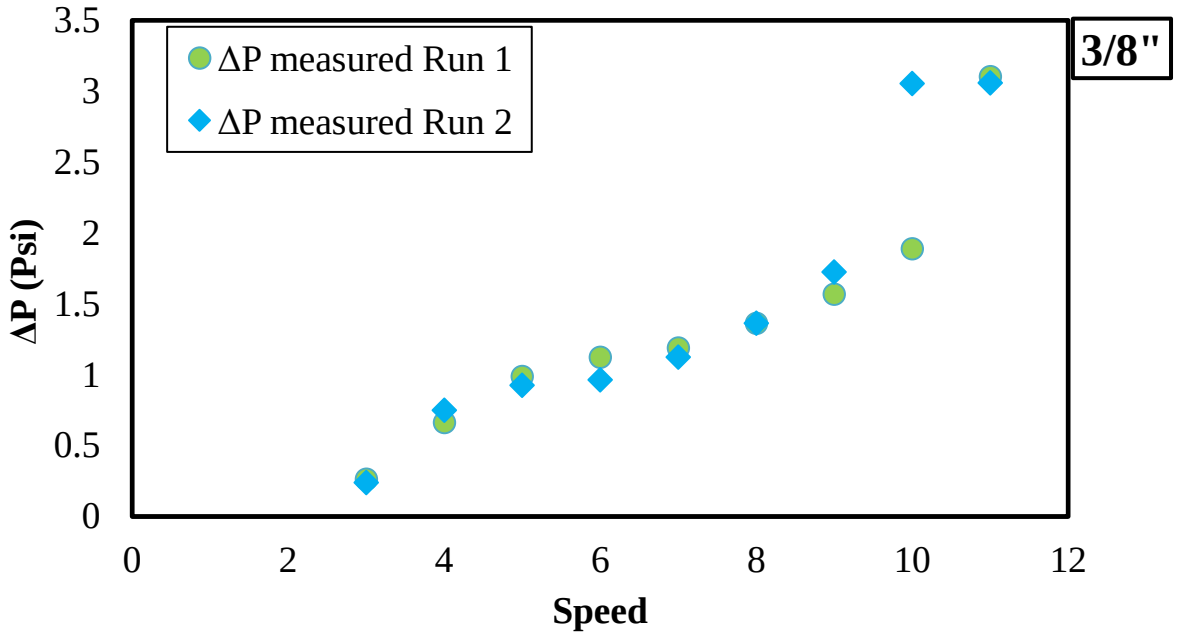

Fig. A.9— Reproducibility of the measured pressure for crude oil D for 3/8" considering the pump speed

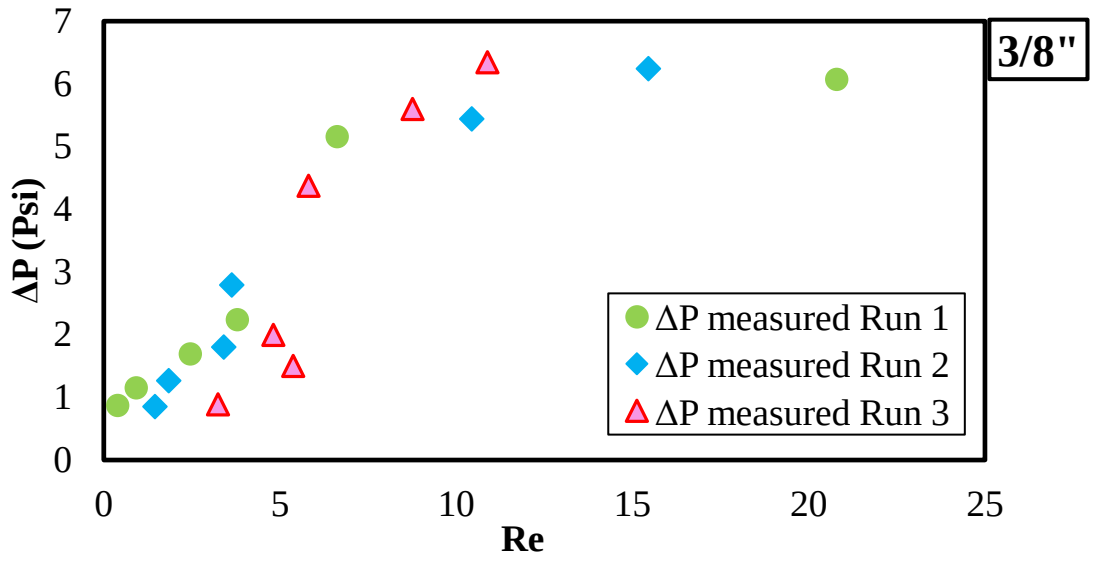

Fig. A.10— Reproducibility of the measured pressure for emulsion for 3/8" with Reynolds Number

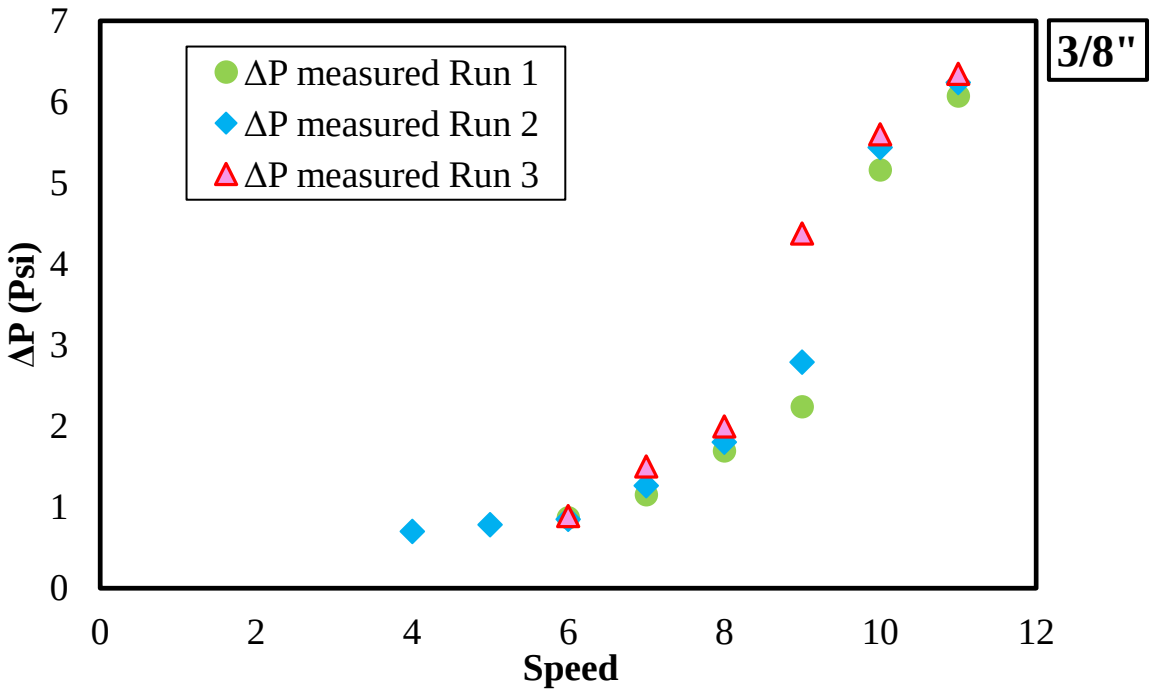

Fig. A.11— Reproducibility of the measured pressure for emulsion for 3/8" considering the pump speed

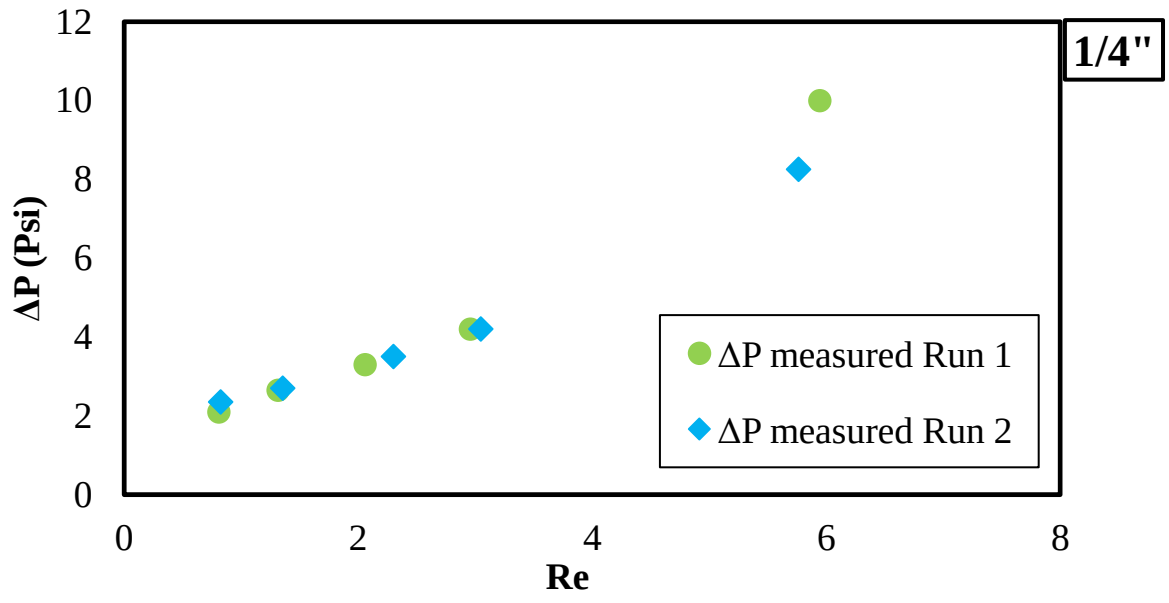

Fig. A.12— Reproducibility of the measured pressure for the emulsion for 1/4" with Reynolds Number

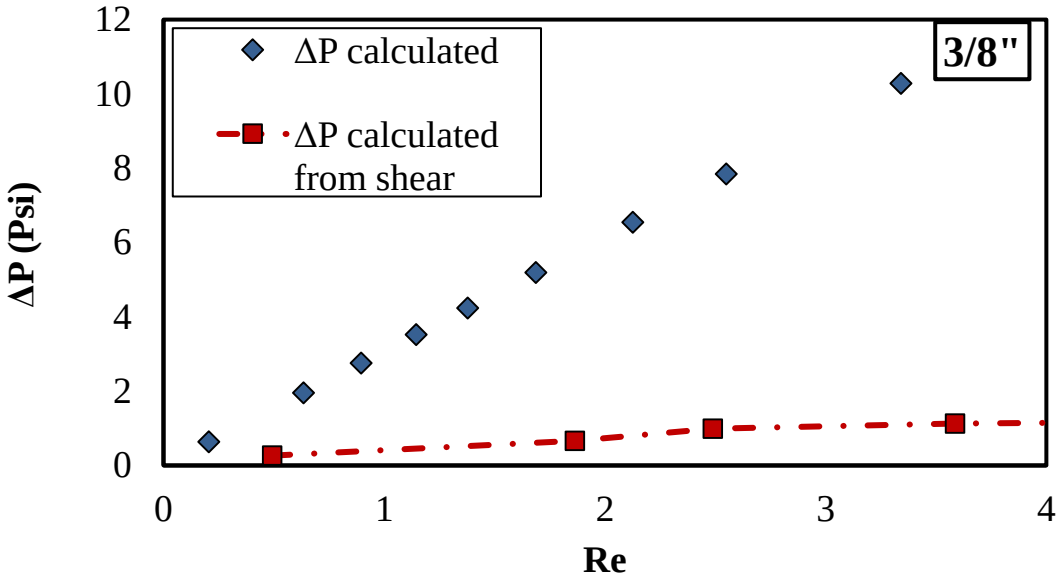

Fig. A.13—— Comparaion of ΔP for 100% crude oil C in 3/8”

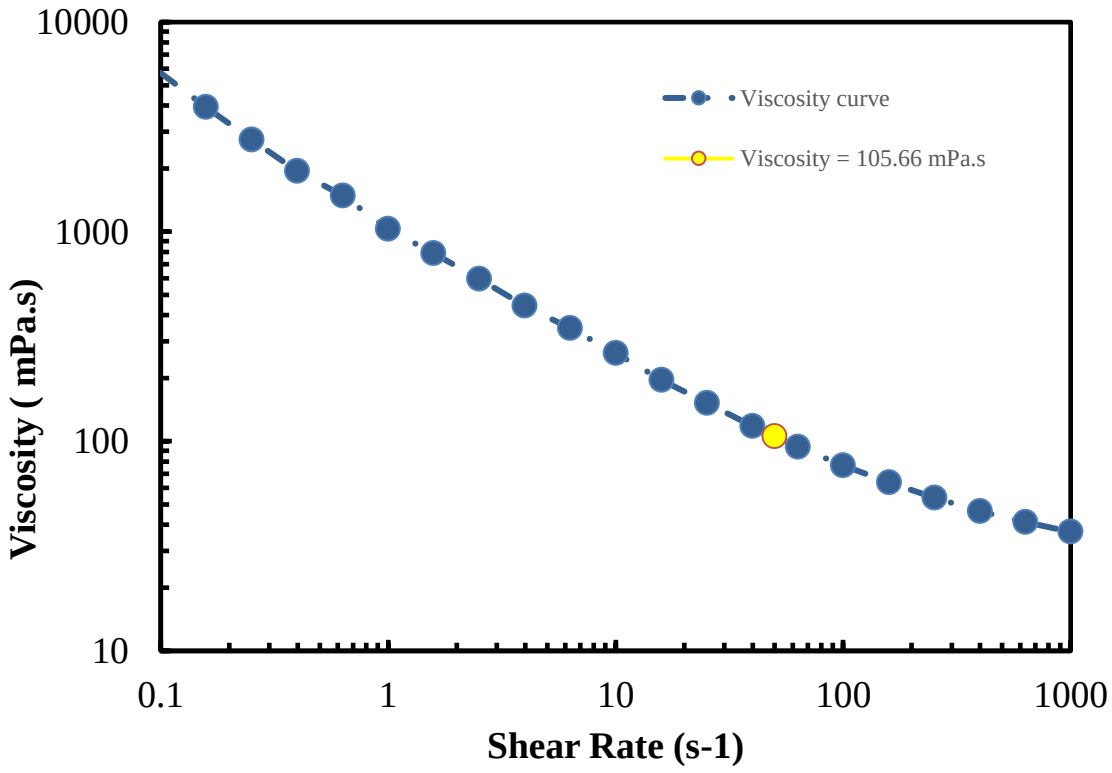

Fig A.14— Viscosity curve from rheometer

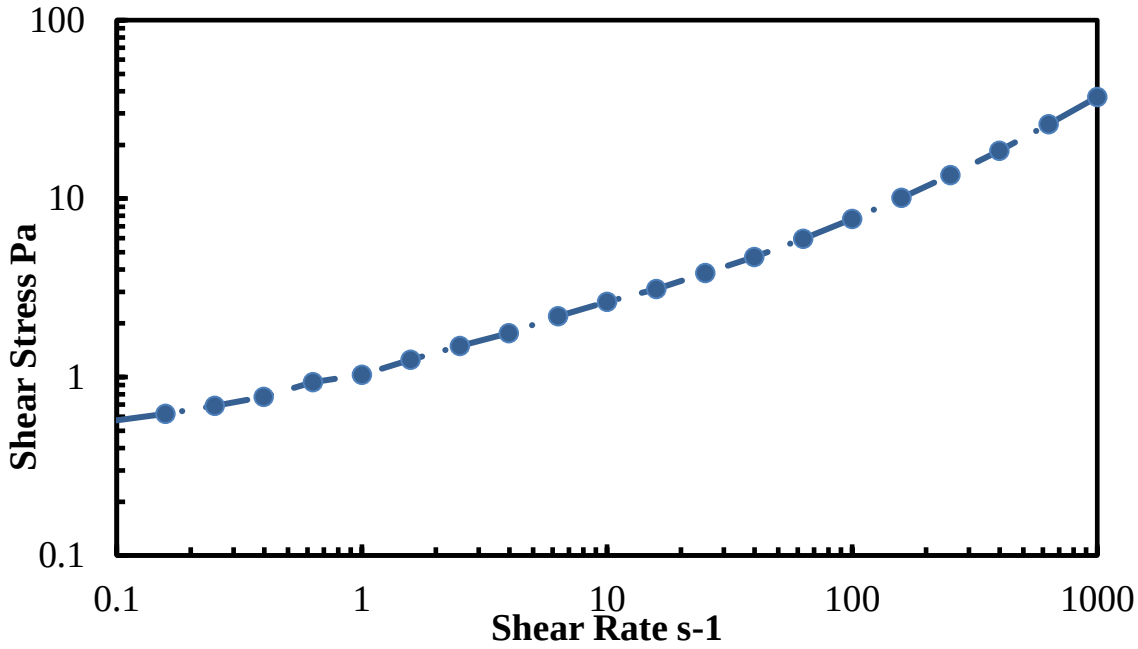

Fig. A.15—Shear rate Vs shear stress from rheometer

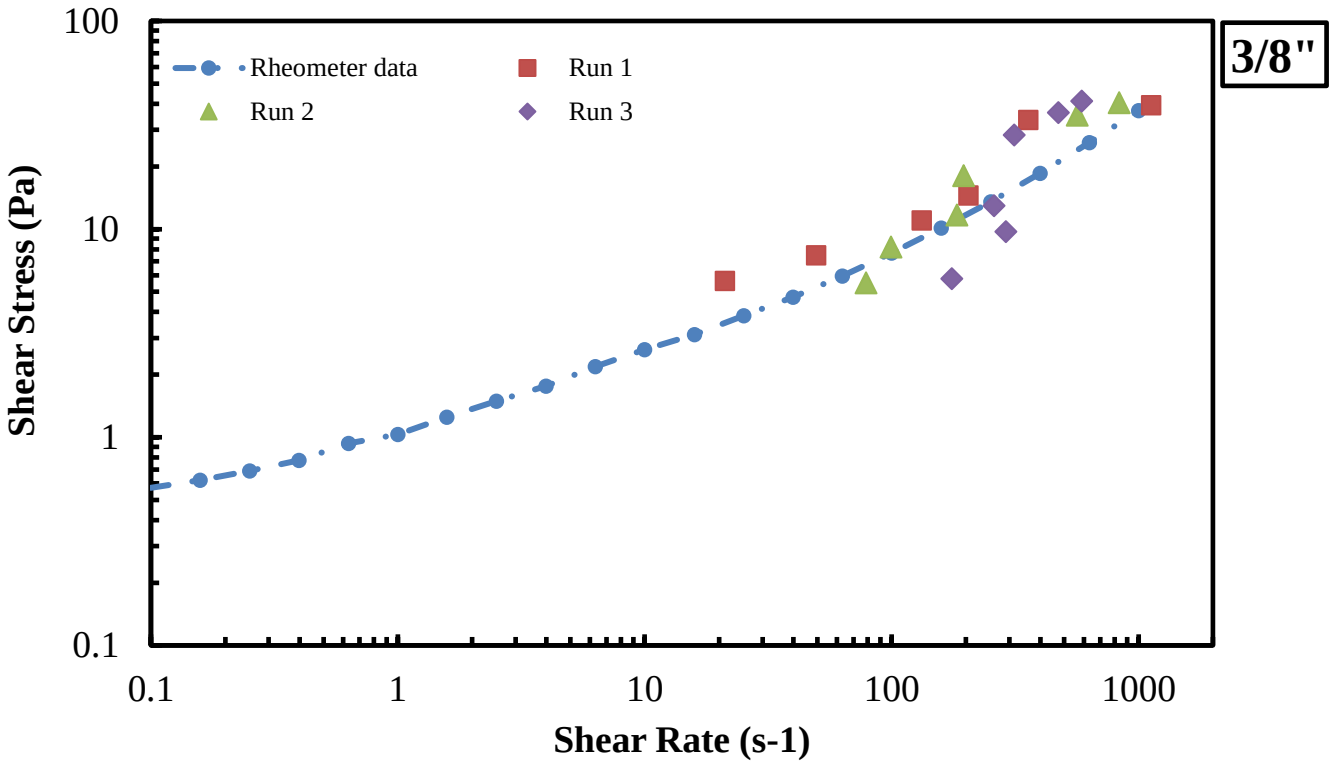

Fig. A.16— Shear rate data comparison 3/8”

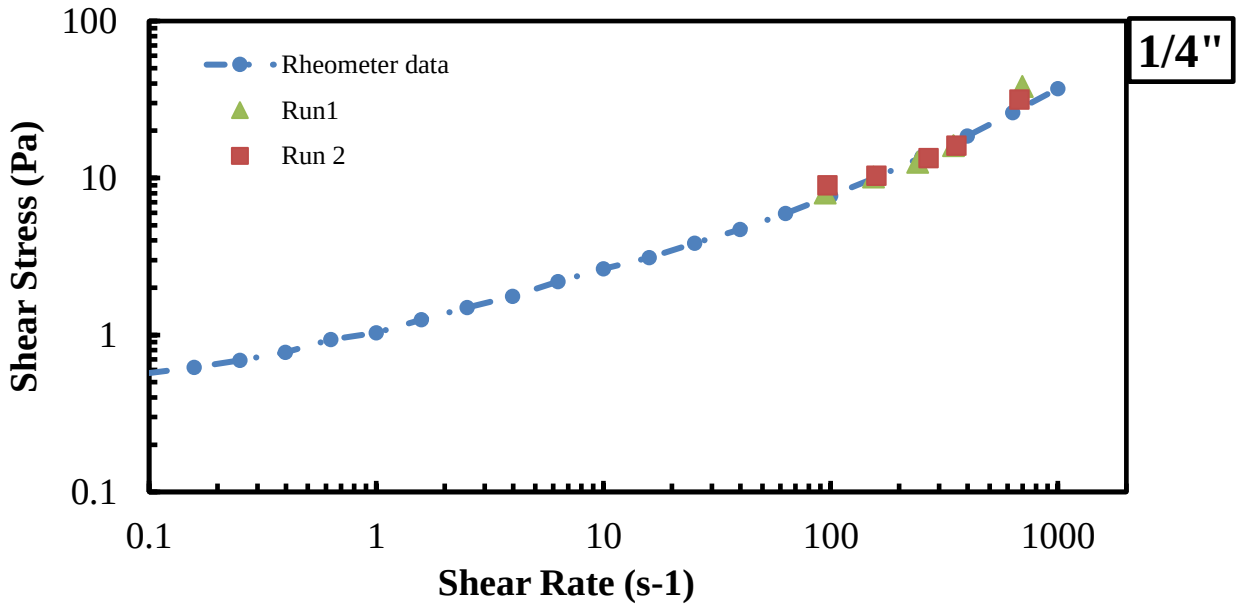

Fig. A.17— Shear rate data comparison 1/4”

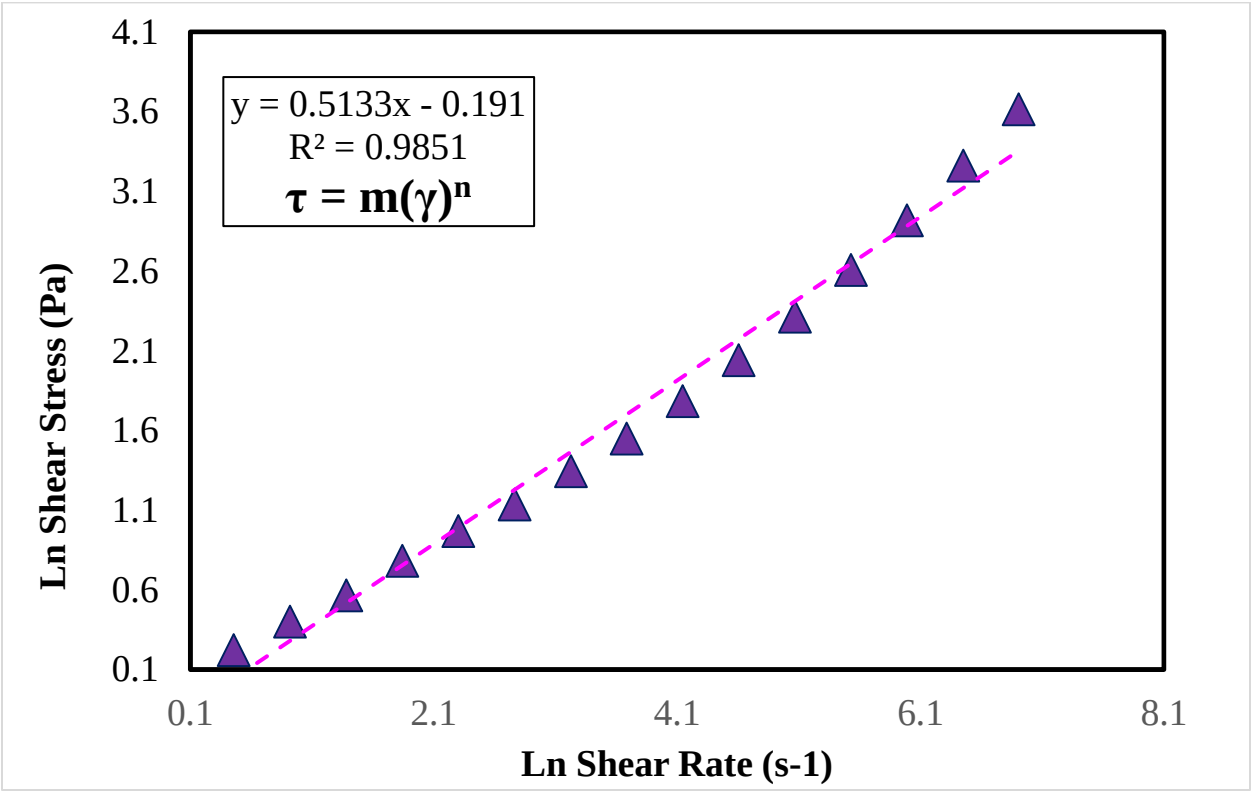

Fig. A.18—Ln – Ln plot of the emulsion

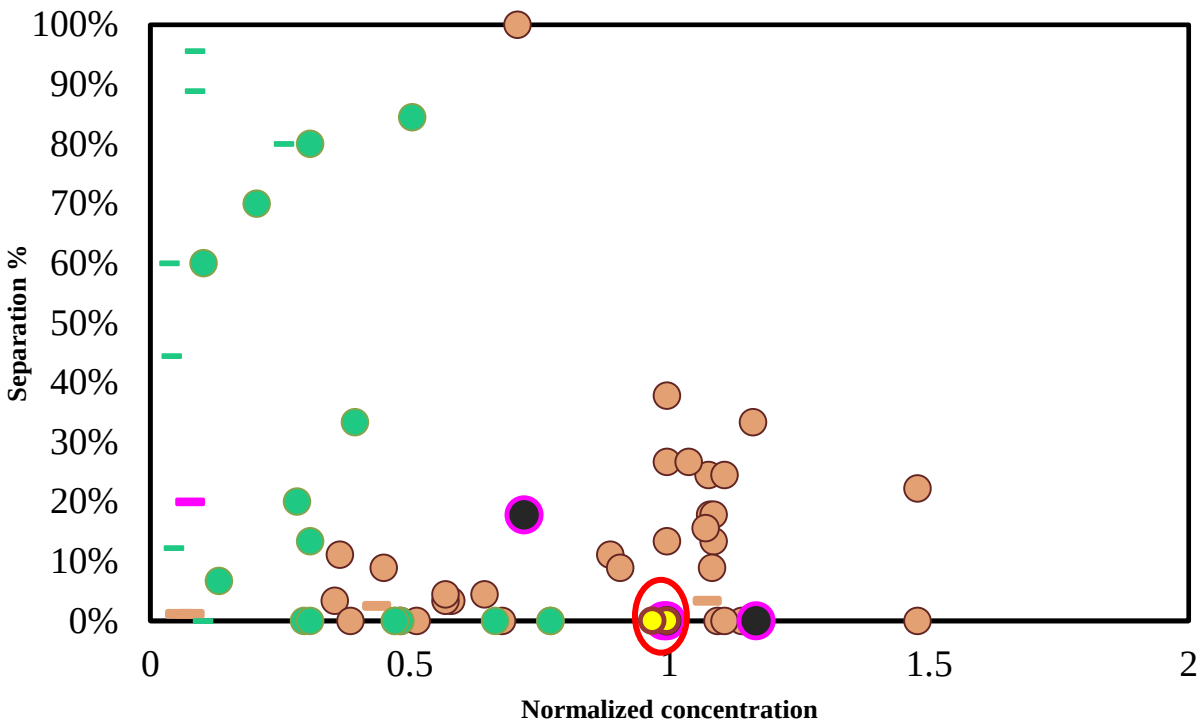

Fig. A.19— Separation exhibited by the emulsion tested

An attempt to correlate HLB to the emulsion separation after 5 minutes in the centrifuge at 10,000 RPM was made. The HLB of the surfactant blend was calculated using **Eq.2**. (The total amount of surfactant was estimated as a function of the HLB value; total weight of emulsion out of oil multiplied by the hlb of the blend and the total is divided by 100). Then the total concentration of surfactants in each blend was multiplied by the calculated HLB of the blend. The value obtained from multiplying the total weight of emulsion by the hlb of the blend and the dividing the total by 100 is plotted against separation obtained after 5 minutes . Due to the fact that separated oil in the emulsion tend to be as dark as the emulsion in some cases, and that the separation between layers is not always properly defined, the separation % after 5 minutes was expressed in terms of water separated in order to provide accurate results. The results are shown in **Fig. A.19**. A clear correlation is not observed but for oil A2 and oil D.

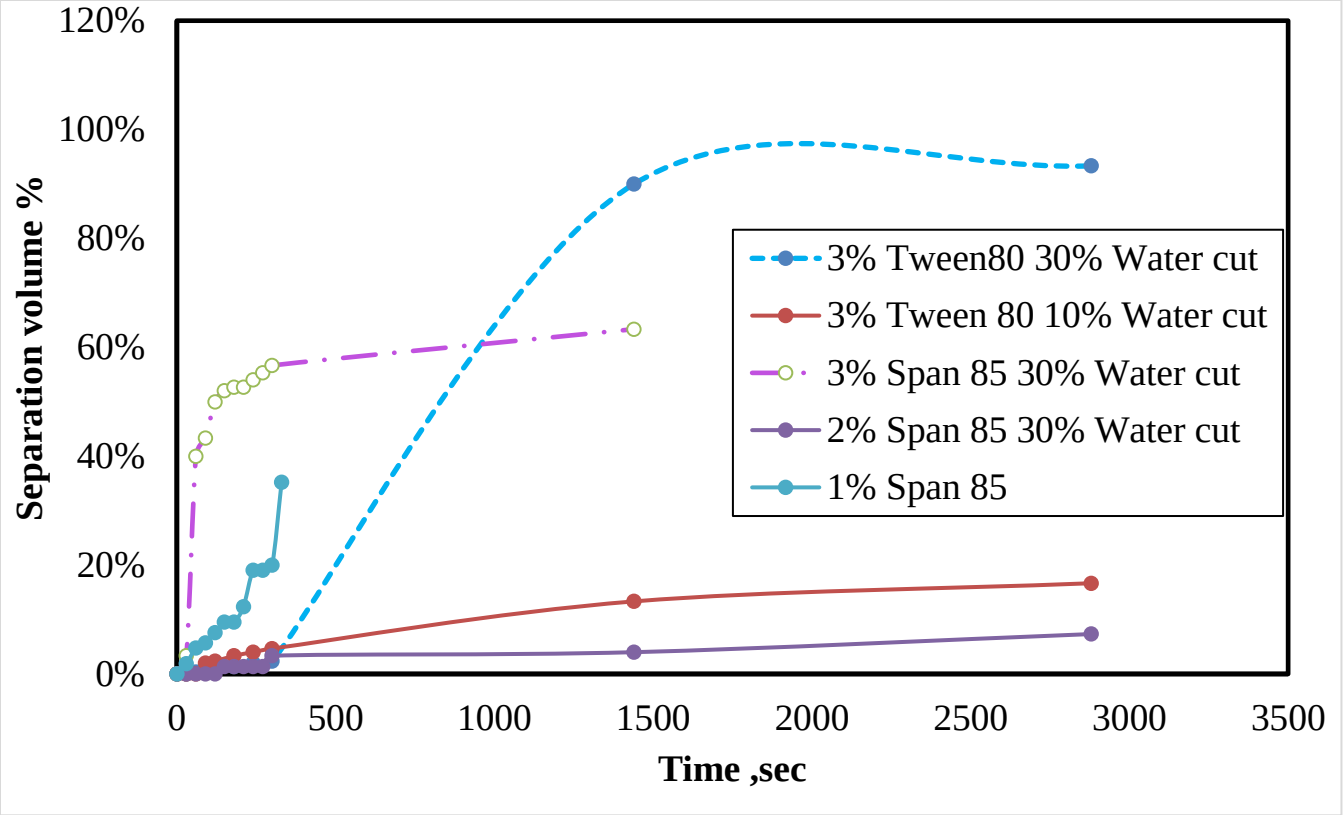

Fig. A.20— Initial bottle test

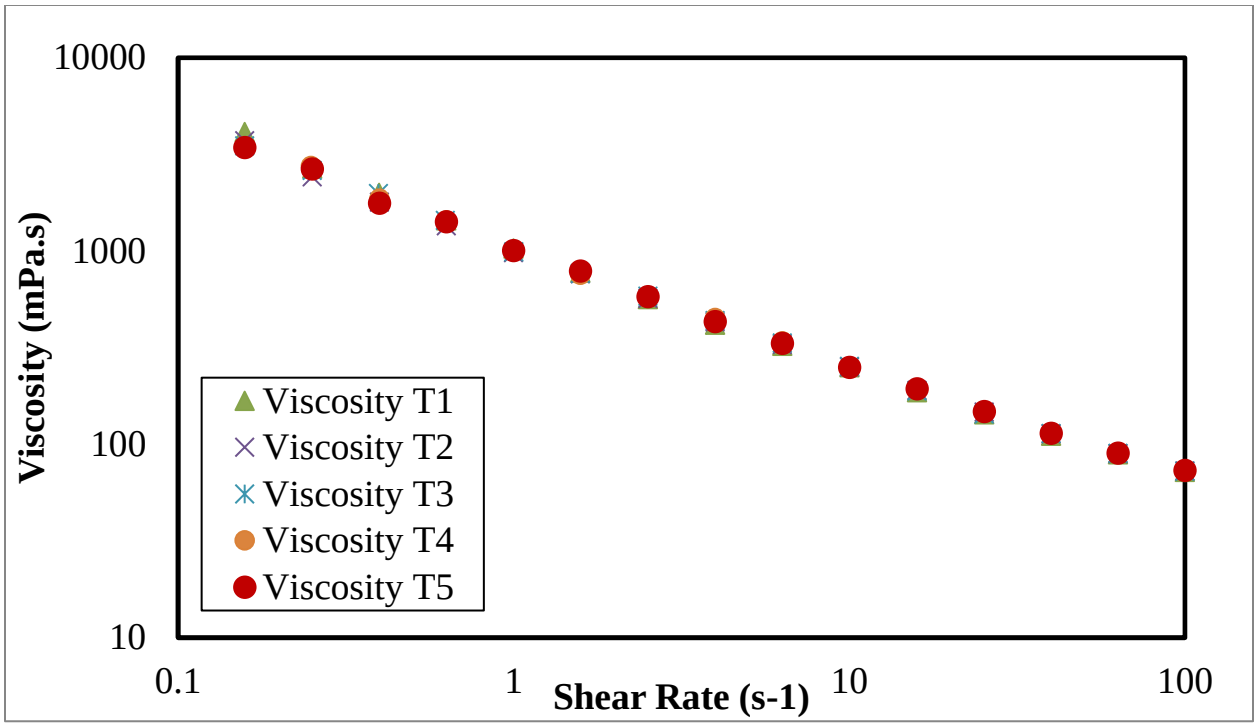

Figure A.21— Reproducibility of the viscosity curve measurement for the rheometer

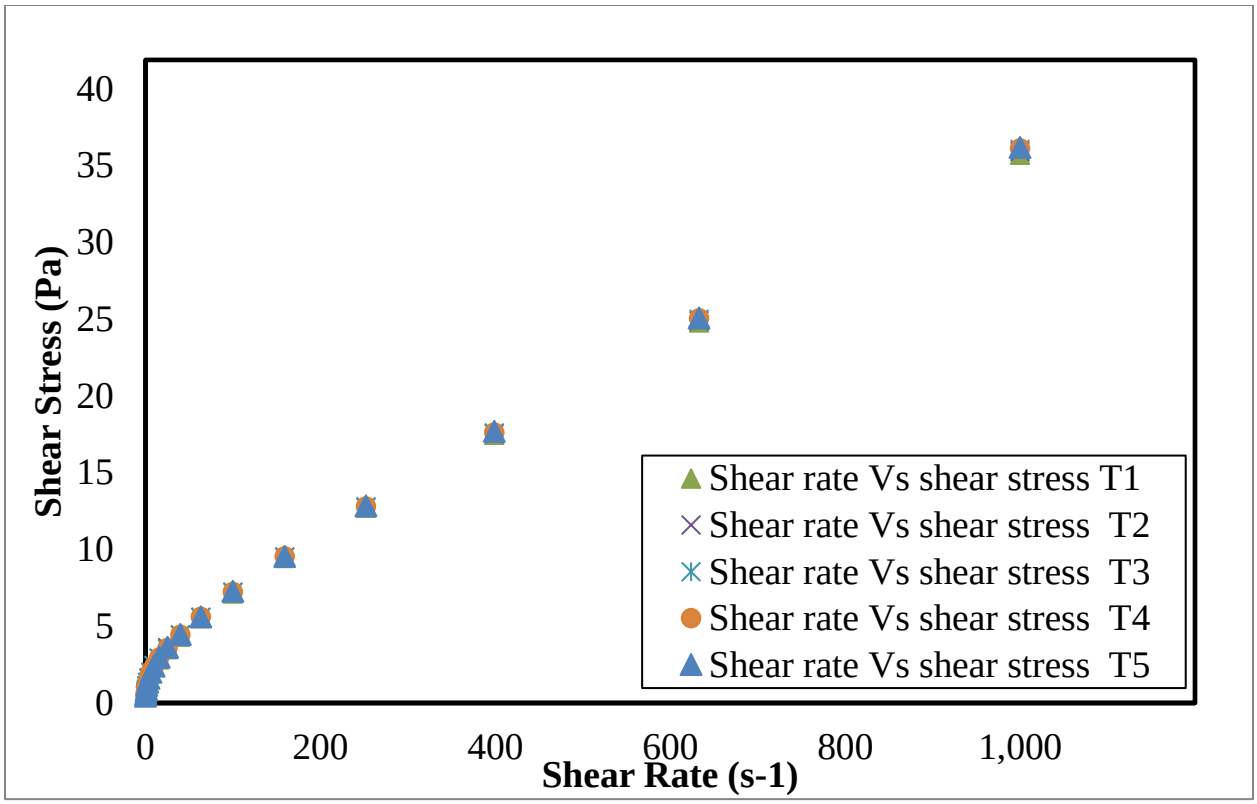

Figure A.22— Reproducibility of the shear curves for the rheometer

The Anton Paar rheometer was tested for reproducibility of the measurements obtained and results are showed in **Fig.A.21** and **A.22.**We see that in our case, the emulsion was not disturbed by the applied shear rate even though such behaviors happen for other emulsions

Table A.12—List of the concentration blend used before finding a stable emulsion

N.	Types and concentration of surfactants	Water cut	HLB of the blend	Separation % in terms of water separated	Total separation
1	1% Span 85	30%	4.3	50%	3%
2	3% Tween 80	30%	15.0	24%	6%
3	3% Tween 80	10%	15.0	30%	6%
4	3% Span 85	30%	4.3	21%	4%
5	2% Span 805	30%	4.3	0%	25%
6	1.8% Span 85	30%	1.8	60%	20%
7	2% Span 85	30%	1.8	44%	15%
8	2.2% Span 85	30%	1.8	12%	6%
9	2% span 80+1%tween80	30%	8.1	0%	9%
10	1% span 80+1%merpol A	30%	5.1	7%	8%
11	1% span 80+1%merpol A+ 2% TX 100	30%	9.4	0%	0%
12	1.5% TX 100	30%	13.5	80%	94%
13	1.5% TX 100 + 1% Span 80	30%	10.0	0%	0%
14	2% TX 100 + 1% Span 80 + 1% merpol A	10%	9.4	0%	0%
15	1.5% tx100+0.5%span80	10%	11.3	20%	2%
16	1.5% tx100+1%span80	10%	10.0	13%	2%
17	2% tx100+1%span80	10%	10.6	33%	10%
18	1.5% tx 100 + 1% span 80	20%	10.0	80%	16%
19	1.5% tx 100 + 1% span 85	20%	10.0	33%	20%
20	1%TX100+ 0.66% Span80	20%	10.0	70%	14%
21	0.5%TX100+ 0.33% Span80	10%	10.0	60%	6%
22	1.5% tx 100 + 1% span 80 300 cc	30%	10.0	0%	0%
23	2.64% tx 100 + 1.64% span 80 150cc	15%	10.0	84%	97%
24	1% Merpol A	15%	6.0	89%	29%
25	1% Merpol A	30%	6.0	96%	29%
26	1.5% TX 100 + 1% Span 80 + 1% merpol A	30%	8.8	7%	15%
27	2.5% TX 100 + 0.5% Span 80 + 1% merpol L A	15%	10.5	5%	25%
28	1.5%TX100+ 1% SPAN 80+ 1% merpol A	30%	8.8	0%	30%
29	1% Tergitol+ 2.5% SPAN 80	30%	7.0	3%	3%
30	1.5% Tergitol+ 1% SPAN 80	30%	9.7	11%	20%

31	**1.5% Tergitol + 1% TX100 +1% SPAN 80**	**30%**	**11.1**	**3%**	**5%**
32	**2.2% SPAN 85**	**30%**	**1.8**	**1%**	**17%**
33	**2.5% SPAN 85 + 1.5% Tergitol**	**30%**	**6.9**	**3%**	**3%**
34	**1.5% Tergitol+ 1% TX100 + 2% SPAN 80**	**30%**	**9.7**	**4%**	**5%**
35	**5% tx 100**	**30%**	**13.5**	**3%**	**35%**
36	**3% SPAN 85**	**30%**	**1.8**	**1%**	**15%**
37	**mixed half 5% tx100 + half 3% span 80**	**30%**	**6.9**	**4%**	**17%**
38	**1.5 % tx 100 + 1% span 80**	**30%**	**10.0**	**0%**	**20%**
39	**1.5 % tx 100 + 1.5 % span 80 + 1% Merpol A**	**30%**	**8.3**	**0%**	**3%**
40	**3% tx100 + 1 % span 80**	**30%**	**11.3**	**100%**	**100%**
41	**3% tx100 + 2.5 % span 80 +2% merpol A**	**30%**	**8.5**	**13%**	**2%**
42	**3% tx100 + 3 % span 80 + 2.5 % merpol A**	**30%**	**8.1**	**24%**	**4%**
43	**3.4% tx100 + 3 % span 80 + 2.5 % merpol A**	**30%**	**8.4**	**33%**	**5%**
44	**3.6% tx100 + 3.5 % span 80 + 1.5% merpol A**	**30%**	**8.6**	**0%**	**0%**
45	**3 % Merpol SE**	**30%**	**10.5**	**2%**	**93%**
46	**3% Merpol SE + 1.5 % span 85 + 3.2% span 80**	**30%**	**6.0**	**0%**	**3%**
47	**3.6 tx100+ 3.5% span 80 mine 2**	**30%**	**9.1**	**0%**	**0%**
48	**3.3 tx100+ 2.8% span 80**	**30%**	**9.4**	**11%**	**7%**
49	**3.3 tx100+ 3.1% span 80**	**30%**	**9.2**	**9%**	**7%**
50	**3.6 tx100+ 3.5% span 80**	**30%**	**9.1**	**38%**	**7%**
51	**4 tx100+ 3.7% span 80**	**30%**	**9.2**	**0%**	**0%**
52	**4 tx100+ 3.9 % span 80**	**30%**	**9.1**	**0%**	**0%**
53	**5.85 tx100+ 3.5% span 80**	**30%**	**10.2**	**0%**	**0%**
54	**4 tx100+ 3.9 % span 80**	**30%**	**9.1**	**24%**	**3%**
55	**5.85 tx100+ 3.5% span 80**	**30%**	**10.2**	**22%**	**4%**
56	**3.6 tx100+ 3.5% span 80**	**30%**	**9.1**	**27%**	**3%**
57	**3.75 tx100+ 3.65% span 80**	**30%**	**9.1**	**27%**	**3%**
58	**3.9 tx100+ 3.8% span 80**	**30%**	**9.1**	**18%**	**2%**
59	**3.9 tx100+ 3.9% span 80**	**30%**	**9.1**	**18%**	**3%**
60	**4 tx100+ 3.9% span 80**	**30%**	**9.1**	**13%**	**4%**
61	**3.80 tx100+ 4% span 80**	**30%**	**8.9**	**16%**	**3%**
62	**3.9 tx100+ 3.85% span**	**30%**	**9.1**	**9%**	**2%**
63	**3.5 tx100+ 3.4% span 80**	**30%**	**9.1**	**0%**	**0%**

64	**4.4% Tx100 + 3.5% Span 80**	**30%**	**9.6**	**0%**	**0%**
65	**3% span 85(failed)**	**30%**	**1.8**	**20%**	**10%**
66	**3% span 85 + 2.5% Tx 100**	**30%**	**8.7**	**18%**	**15%**
67	**3.6% Tx100 + 3.4% Span 80**	**30%**	**9.2**	**0%**	**0%**
68	**3.6% Tx100 + 3.5% Span 8**	**30%**	**9.1**	**0%**	**0%**